Title
The Roles of the Lrig1- and Lgr6-Positive Stem Cells in the Skin and the Functions of the Molecular Markers That Define Them

Author
Huang, Yaohui Phillips

Publication Date
2014

Peer reviewed|Thesis/dissertation

The Roles of the Lrig1- and Lgr6-Positive Stem Cells in the Skin and the Functions of the Molecular Markers That Define Them

by

Phillips Y. Huang

DISSERTATION

Submitted in partial satisfaction of the requirements for the degree of

DOCTOR OF PHILOSOPHY

in

Biomedical Sciences

in the

GRADUATE DIVISION

of the

UNIVERSITY OF CALIFORNIA, SAN FRANCISCO

Dedication

To adapt a J. M. Coetzee quote – for whom, anyway, do we do the things that lead to PhDs if not for our mothers? I fondly dedicate this dissertation to my parents, and to Adam Smith and Friedrich Hayek, the philosophical touchstones and intellectual beacons in my life.

Acknowledgements

First and foremost, I would like to thank my thesis advisor Allan Balmain. Allan is one of the rare breed of principal investigators who are not only first-rate scientists but also genuinely good, honest people. He takes a keen interest in both the scientific and personal developments of his students and serves as a father figure and role model to me. I have benefitted immeasurably from his incredible mentorship, warmth and support.

The Balmain Lab provides a marvellous home away from home. People in the lab are always friendly and ready to help. I appreciate all the scientific comments, suggestions and critiques that they have offered; more than that, I cherish the bonhomie that permeated over dinners and drinks. There are a few people in particular that I have to single out here – Christine E. Wong, who worked very closely with me and contributed equally on the work described in Chapter 2; Atul Kumar and Minh D. To, who are brilliant geneticists / molecular biologists and who gave me a lot of specific advice and help with my benchwork; and Reyno Delrosario, our consummate mouse technician who saved my skin, literally, time and again with his expertise in the animal facility.

My thesis committee has been instrumental in refining the work presented in this dissertation, and I thank them for generously providing their time and for honing my scientific acumen. Ophir Klein, my committee chair, illuminated discussions with his expert knowledge of stem cell biology and has really trained me to question my assumptions with his sharp, careful observations. Shaun Coughlin provided insightful, big picture analysis and has been invaluable in drawing out the relevance of my work to a broader audience by offering an “outsider’s” point of view.

The BMS programme has an outstanding administrative support staff, who make it possible for us students to focus on our research by cutting out all the red tape. I thank the BMS programme coordinators, especially Lisa Magargal and Monique Piazza, for their patient advice and prompt assistance over the years.

Living alone in a foreign land has not always been easy, particularly when the going got tough. I thank all my friends for their companionship and support in the past six years. I relish all the epicurean adventures, nature hikes and sporting fun that we embarked on together, in rare moments spent outside the lab. Of course, I also could not have done it without the support of my family. I thank my parents and sister for their unwavering love and faith in me over three decades.

Finally, countless other people have helped me in ways big and small over the course of my graduate career. I apologise to those I did not specifically name above; if we have shared moments of toil, fun, adversity or joy, know that I appreciate your presence in my life and thank you from the bottom of my heart.

Declarations and contributions

1. Parts of Chapter 1 are adapted from a published book chapter:

Huang P, Balmain A. 2014. Modeling Cutaneous Squamous Carcinoma Development in the Mouse. In *Cold Spring Harb Perspect Med*. doi:10.1101/cshperspect.a013623.

2. Chapter 2 is adapted from a manuscript currently under review for publication. The co-authors are Christine E. Wong, David A. Quigley, Reyno DelRosario, Anne E Powell, Kevin Haigis, Robert J. Coffey and Allan Balmain.

3. Much of the material in Chapter 3 will be submitted for publication. The current co-authors of the manuscript are David A. Quigley, Reyno Delrosario, Jost Seibler, Vincent Beuger and Allan Balmain.

Abstract

The adult mouse skin is made up of many separate cell compartments, each of which contains its own resident stem cell population(s) that acts to maintain it. The hair follicle, in particular, is a rich vein of stem cells – several distinct populations, with different lineage potentials, reside there and these have to communicate with one another to coordinate their actions during normal homeostasis and in times of tissue regeneration.

In this dissertation, I describe the roles of two different stem cell populations in the hair follicle, and the functions of molecular markers that define them. First, Lrig1 is a marker of stem cells in the junctional zone of the hair follicle. By gene expression network analysis of normal mouse skin, we placed *Lrig1* within a network, including *Krt79* and *Efnb2*, involved in homeostasis of the hair follicle infundibulum. Lineage tracing showed that Lrig1$^+$ cells maintain a discrete infundibulum cell compartment, and that single cells from this compartment migrate into the epidermis during normal homeostasis and also downward in anagen follicles. This process is accelerated by treatment with 12-*O*-tetradecanoylphorbol-13-acetate, which stimulates both epidermal proliferation and follicle growth. Activation of mutant *Hras* or *Kras* in Lrig1$^+$ cells leads to distinct phenotypes – the former leads to wavy hair while the latter gives rise to oily skin. Both *Hras* and *Kras* activation can cause wound-dependent papilloma development, but Lrig1$^+$ cells are not common cells-of-origin of chemically induced tumours. Rather than acting as a stem cell reservoir, we propose that Lrig1$^+$ cells may play a facilitating role during tissue regeneration and tumour development.

Second, Lgr6 marks stem cells in the central isthmus of the hair follicle just above the bulge. By expression analysis of a panel of skin cell lines, we demonstrate

that Lgr6, and not Lgr5, is a cutaneous squamous cancer stem cell marker. *In vitro* knockdown of Lgr6 in squamous tumour cell lines leads to increased growth, while *in vivo* Lgr6 knockdown causes elevated proliferation in the epidermis along with increased epidermal lineage tracing from the $Lgr6^{+}$ stem cells. Finally, Lgr6 deficiency results in reduced latency to papilloma development during skin chemical carcinogenesis. We propose that Lgr6 positively regulates Wnt signalling in epidermal cells and acts to restrain commitment of skin stem cell towards the epidermal lineage during normal homeostasis and tumour development.

Table of Contents

List of Tables

Chapter 2

List of Figures

Chapter 1

Chapter 2

Chapter 3

Chapter 1

General Introduction

Skin Compartments and Stem Cells

The adult mouse skin comprises many distinct cell compartments, including the interfollicular epidermis (IFE), dermis, hair follicle (HF), sebaceous gland (SG) and sweat duct and gland. Each of these compartments possesses its own resident stem cell population(s), which is uniquely capable of replenishing the cells within its host compartment.

For instance, the sweat duct and gland have been reported to contain 3 distinct unipotent progenitor populations, which separately maintain the duct, myoepithelial lineage or luminal lineage of the gland epithelium (Lu et al. 2012). The SG, on the other hand, has been variously reported to possess unipotent progenitor cells that are located either in the basal layer (Cui et al. 2003; Petersson et al. 2011; Cottle et al. 2013) or near the bud site, where they are defined by the transcription factor Blimp1 (Horsley et al. 2006).

The dermis connects the epidermis to the underlying subcutaneous layer and is largely composed of mesenchymal fibroblasts that deposit collagen and elastic fibres. Recent work by Driskell *et al.* has unveiled two distinct fibroblast lineages within the dermis – one lineage gives rise to the upper dermis and is required for hair formation, whereas the other lineage gives rise to the lower dermis as well as the preadipocytes and adipocytes of the hypodermis (Driskell et al. 2013). Interestingly, the authors also reported that during wounding, the initial wave of dermal regeneration is driven by the lower fibroblast lineage, with recruitment of the upper fibroblast lineage only later during wound re-epithelialisation, which could explain the

observation that wound repair is often associated with the formation of scar tissue that is devoid of hair.

The Epidermis

The IFE of the mouse skin has a very high turnover rate estimated to be around 7 days (Potten 1981; Ghazizadeh and Taichman 2001). Homeostasis of the IFE is maintained by progenitor cells that reside within the basal layer, which proliferate to generate keratinocytes that terminally differentiate as they rise to surface. The exact nature and hierarchy of epidermal progenitor cells is a hotly debated subject. Classic work by Potten and colleagues suggests that epidermal progenitor cells are slow-cycling stem cells that give rise to around 10 transit amplifying cells each, which further proliferate to form columns of clones known as epidermal proliferative units (EPUs) (Potten 1981; Potten et al. 1982). Later work by Clayton *et al.* involving single cell labelling of epidermal progenitor cells and quantitative analyses of the resulting clone size distributions suggests an alternative model in which the mouse tail IFE is maintained by a single committed progenitor (CP) cell; these CP cells undergo mostly asymmetric cell divisions, but also a smaller proportion of symmetric divisions in which the stochastic cell fate is precisely balanced between self-renewal and loss through differentiation (Clayton et al. 2007).

More recently, work by Mascre *et al.* attempted to reconcile the seeming contradictions between the two models. The authors propose the existence of two distinct progenitor cell populations in mouse tail IFE, arranged in a hierarchy in which slow-cycling stem cells (marked by Keratin 14 expression) give rise to CP cells (marked by Involucrin expression) (Mascré et al. 2012). Further, the authors reported

that only slow-cycling stem cells, and not CP cells, make a substantial contribution to epidermal repair in the wake of an injury.

However, in apparent contrast to this finding, Lim *et al.* recently reported the existence of a single epidermal progenitor cell population in the mouse hindpaw. These progenitor cells express Axin2, contribute robustly to epidermal wound repair and exhibit a probabilistic cell fate reminiscent of CP cells (Lim et al. 2013).

One possible explanation for these divergent conclusions is the different anatomical sites examined – the tail IFE in the Clayton and Mascre studies, and the mouse footpad in the Lim report. In addition, the studies involving tail IFE are further complicated by the existence of two distinct terminal differentiation compartments within the tail IFE, known as the scale and the interscale (Gomez et al. 2013). Involucrin expression is restricted to interscale IFE, so the Involucrin-labelled CP cells in the Mascre study would have been limited to the interscale lineage; moreover, the scale IFE has a higher intrinsic rate of proliferation than the interscale IFE, which would also call into question the conclusion in the Clayton study that epidermal clone size differences are due purely to neutral competition among CP cells (Gomez et al. 2013). Regardless, it remains to be seen if any of these models for epidermal homeostasis may also apply to mouse back skin, which, with its dense coat of hair follicles and thinner epidermis, is physiologically very distinct from either the tail or hindpaw skin.

The Hair Follicle

The mouse HF is home to several distinct stem cell populations (Fig. 1.1). Early studies uncovered the existence of a multipotent stem cell population in the

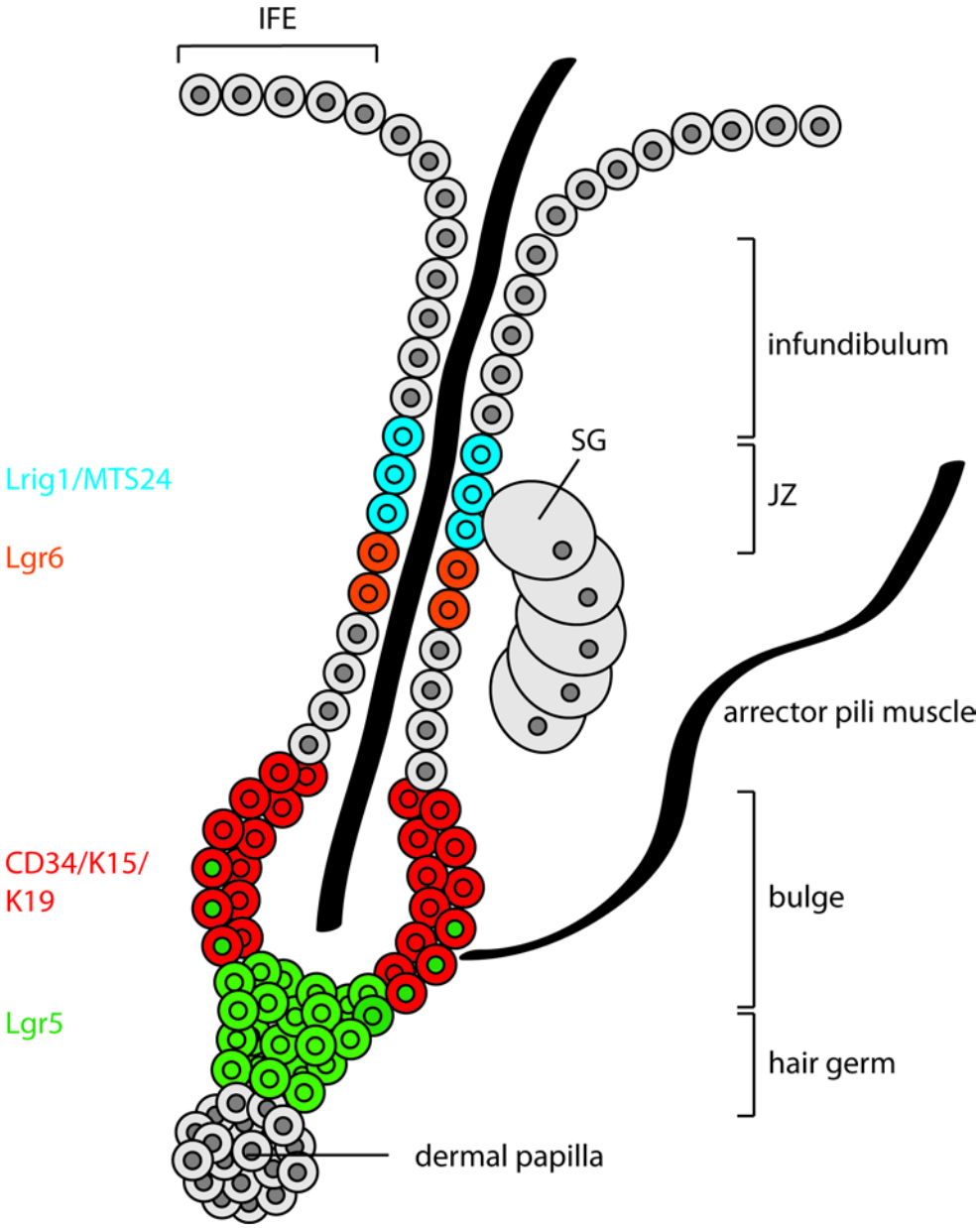

Figure 1.1 Diagram illustrating the different compartments of the mouse HF, and the locations of various stem cell populations therein.

bulge region of the HF (Cotsarelis et al. 1990), defined by markers such as CD34 (Trempus et al. 2003) and Keratin 15 (Liu et al. 2003). While bulge stem cells are capable of regenerating the HF, SG and IFE when orthotopically transplanted onto full-thickness back skin wounds, they are quiescent during normal skin homeostasis and may act more as a reserve stem cell pool that becomes activated in response to wounding (Ito et al. 2005).

Interestingly, the HF bulge also provides a niche for a number of other stem/progenitor cell populations in the skin. For instance, melanocyte stem cells, which give rise to the pigment-producing melanocytes that are responsible for hair pigmentation, reside within the bulge (Nishimura et al. 2002). Here, they adhere directly to bulge stem cells, which supply TGF-β1/2 that maintain the melanocyte stem cells in a quiescent state (Nishimura et al. 2010; Tanimura et al. 2011). At the onset of anagen, Wnt signalling is coordinately activated in both the bulge and melanocyte stem cell populations, which causes the melanocyte stem cells to proliferate and differentiate into mature melanocytes, thus ensuring the production of properly pigmented hair follicles (Rabbani et al. 2011). In newborn mouse skin, bulge stem cells also deposit nephronectin into the basement membrane; adjacent mesenchymal progenitors that express the nephronectin receptor α8 integrin are induced to upregulate smooth muscle markers, ultimately differentiating into the arrector pili muscles that are responsible for raising HFs during piloerection (Fujiwara et al. 2011).

Beyond the bulge, several stem cell populations have also been characterised in the HF. For instance, Leucine-rich repeats and immunoglobulin-like domains 1 (Lrig1) is a cell surface protein that negatively regulates Egfr signalling (Gur et al. 2004; Laederich et al. 2004; Jensen and Watt 2006). In the HF, Lrig1 marks a

distinct population of stem cells that are located at the junctional zone (JZ) between the bulge and the SG. In one study, Lrig1$^+$ cells were reported to be bipotent, contributing to both the IFE and the SG during normal homeostasis (Jensen et al. 2009). A subsequent report, however, demonstrated instead that Lrig1$^+$ cells are involved in maintaining the infundibulum and the SG in the HF, and does not make a contribution to the IFE in the absence of a wound stimulus (Page et al. 2013). Apart from Lrig1, the thymic epithelial progenitor cell marker MTS24 has also been used to localise a stem cell population to the JZ (Nijhof et al. 2006), which appears to largely overlap the Lrig1$^+$ cell population (Page et al. 2013).

Interestingly, the G protein coupled receptors Lgr5/6 mark distinct cell populations in the HF. Lgr5 marks stem cells in the telogen bulge and hair germ that actively cycle to give rise to new follicles (Jaks et al. 2008). Lgr6, on the other hand, marks stem cells just above the bulge that have been reported to preferentially give rise to cells of the IFE and the SG (Snippert et al. 2010). The functions of Lgr5/6 and the stem cell populations they define are discussed in more detail in the next section.

Lgr5/6^{+} Stem Cells and Lineage Tracing

Lgr4-6 are a family of closely related G protein coupled receptors. Until recently, Lgr4-6 were orphan receptors and not much was known about their potential biological functions. By examining the Wnt target gene expression signature of human colorectal cancers and making cross comparisons to the gene expression profile of mouse intestinal crypts, Barker *et al.* derived a list of candidate intestinal crypt stem cell marker genes (Barker et al. 2007). Most of these, however, were expressed in transit amplifying or Paneth cells, except Lgr5, which was uniquely expressed in columnar cells that are intermingled with Paneth cells at the crypt base, as determined by *in situ* hybridisation analysis.

Using Mouse Models to Characterise Stem Cells In Situ

First, to validate the *Lgr5 in situ* hybridisation pattern that they observed in the murine small intestine, Barker *et al.* generated two different strains of mice, using the *Lgr5* promoter to directly drive the expression of either LacZ or EGFP (Barker et al. 2007). Indeed, *Lgr5* promoter activity was detected in crypt base columnar cells in either mouse strain.

Next, to determine if these Lgr5^{+} cells acted as stem cells in the intestine, the authors employed the powerful technique known as lineage tracing. Pioneered by developmental biologists in an attempt to map cell fate during embryogenesis (Conklin 1905; Sulston et al. 1983), lineage tracing has since become an essential tool in stem cell research (for review, see Kretzschmar & Watt, 2012). In this

technique, an individual cell or population of cells is marked with a permanent neutral, heritable label, such that all progeny of that cell(s) can subsequently be identified on the basis of the label.

Early labels used in lineage tracing included dyes such as DiI and DiO that are incorporated into the plasma membrane of target cells (Serbedzija et al. 1989; Eagleson and Harris 1990), and horseradish peroxidase that is injected directly into cells of interest (Weisblat et al. 1978; Balakier and Pedersen 1982). A subsequent advance in the field was the development of genetic markers, which, when stably incorporated into the genome of target cells, are non-leaky and will not be diluted over cell generations. For instance, genetic markers such as the *GFP* and *LacZ* genes have been introduced into chick and mouse embryos via electroporation (Itasaki et al. 1999), and incorporated into the genomes of rat retinal cells and chick embryos via retroviral infection (Price et al. 1987; Fekete and Cepko 1993).

In mice, the development of first transgenic and then knockout/knockin mouse technologies (for reviews, see Jacks, 1996; Palmiter & Brinster, 1986) allowed genetic recombination to be used for lineage tracing and represented a major leap forward for stem cell research. Historically, researchers have relied on *in vitro* clonogenicity assays and limiting dilution transplantation experiments to identify putative stem cell populations (Yann Barrandon 1987; Purton and Scadden 2007). In the latter approach, cells of interest are isolated via flow cytometry and a small number are transplanted into recipient animals to test for a heightened ability to reconstitute all cell lineages of the tissue of origin compared to a control cell population. A major caveat to these assays is that since the cells of interest are not studied *in situ*, the isolation procedure and/or non-native environment into which the

cells are introduced may induce significant genetic/molecular changes that obscure the true endogenous behaviour of the cells.

With the use of genetic recombination to perform lineage tracing in mouse models, researchers are now able to study the activity of putative stem cell populations *in situ*, thus circumventing the issues that plague earlier approaches described above. Typically in this method, a gene of interest that specifically marks the target stem cell population is first identified; a transgenic/knockin mouse strain is then generated where the promoter of the gene of interest is used to drive the expression of Cre recombinase. By crossing this mouse strain to another where a genetic marker flanked by loxP sites is under the control of a universal promoter (for instance, *Rosa26-LSL-LacZ*), researchers are able to selectively activate the genetic marker in a target cell population and observe the location and behaviour of marked cell clones over time. Subsequent development of an inducible form of the Cre recombinase allowed for postnatal activation of the genetic marker at a time of the researcher's choosing.

Lgr5/6 Mark a Variety of Stem Cell Populations in the Mouse

By generating *Lgr5-EGFP-IRES-CreERT2* mice (in which the *Lgr5* promoter drives the expression of Cre recombinase) and performing lineage tracing, Barker *et al.* showed that the $Lgr5^{+}$ crypt base columnar cells act as stem cells that actively cycle to generate all cell lineages of the small intestine and colon epithelium (Barker et al. 2007).

Intriguingly, by performing lineage tracing analysis of other anatomical sites in the same mouse strain, the Clevers lab and others have shown that Lgr5 selectively marks stem cell populations in a wide variety of tissues, including the stomach (Barker et al. 2010), kidney (Barker et al. 2012), breast (Plaks et al. 2013) and ovary (Flesken-Nikitin et al. 2013; Ng et al. 2014). In the liver and pancreas, Lgr5 is not normally expressed but gets turned on upon injury and marks populations of induced stem cells that mediate tissue regeneration (Huch et al. 2013b, 2013a).

Interestingly, in the HF, Lgr4-6 are expressed in distinct cell populations. Lgr5 marks a population of cells in the bulge and hair germ of telogen follicles and the lower outer root sheath of anagen follicles. These cells actively cycle, and are responsible for giving rise to new follicles (Jaks et al. 2008). Lgr6, on other hand, marks a population of cells located in the central isthmus, just above the bulge. By performing lineage tracing in *Lgr6-EGFP-IRES-CreERT2* mice, Snippert *et al.* showed that $Lgr6^+$ cells are capable of giving rise to the IFE and the SG (and less commonly the HF), which indicates that the $Lgr6^+$ cells represent a multipotent stem cell population (Snippert et al. 2010). Subsequent analysis by Page *et al.*, however, indicated a more widespread expression pattern of Lgr6 in the skin – in addition to the central isthmus in the HF, Lgr6 expression was also detected in single cells in the SG, HF bulge and basal layer of the IFE (Page et al. 2013). This observation calls into question the conclusion that the $Lgr6^+$ cells in the isthmus are multipotent – it could be that distinct $Lgr6^+$ cell populations are responsible for the lineage tracings seen in the IFE and the SG. Finally, Lgr4 is broadly expressed in the lower half of the HF, overlapping the expression domains of both Lgr5 and Lgr6 (Snippert et al. 2010).

Lgr4-6 Impinge upon Wnt Signalling

The wide range of stem cell populations in which Lgr5/6 are expressed points to a fundamental role for these genes in adult stem cell biology. By selectively deleting *Lgr4* alone or *Lgr4* in combination with *Lgr5* in murine intestinal crypts, de Lau *et al.* observed proliferation defects and crypt loss, coupled with an impairment of Wnt signalling (de Lau et al. 2011). Indeed, through mass spectrometry analysis, the authors determined that Lgr4-6 bind directly to the Wnt agonists R-spondins, and thus act to enhance Wnt signalling in stem cells. This biochemical finding was subsequently corroborated by two other groups (Carmon et al. 2011; Glinka et al. 2011; Gong et al. 2012), and x-ray crystallography analysis indicates that Lgr4/5 and R-spondin associate in a dimeric 2:2 complex (Peng et al. 2013; Chen et al. 2013; Wang et al. 2013; Xu et al. 2013).

Subsequent work reveals details of the mechanism through which the Lgr4-6/R-spondin complex potentiates Wnt signalling. The E3 ubiquitin ligase zinc and ring finger 3 (Znrf3) and its homologue ring finger 43 (Rnf43) negatively regulate Wnt signalling by physically associating with the Frizzled/Lrp6 Wnt receptor complex and promoting its ubiquitin-mediated endocytosis and turnover (Hao et al. 2012; Koo et al. 2012). R-spondin binds to Znrf3 and induces its association with Lgr4, which results in membrane clearance of Znrf3 and hence relief of Wnt signalling inhibition.

Paradoxically, however, a negative role for Lgr4-6 in Wnt signalling has also been reported in some cases. For instance, in human colorectal cancer cell lines, Lgr5 is reported to negatively regulate Wnt signalling, such that knockdown of Lgr5 enhances growth and invasion (Defossez et al. 2011). In line with these observations, Rspo2 was reported to be downregulated in human colorectal cancers;

overexpression of Rspo2 reduces Wnt signalling and impedes growth of colorectal cancer cell lines, but crucially only in those that express high levels of Lgr5 (Wu et al. 2014). The authors propose the existence of a negative feedback loop in colorectal cancer cells, wherein Rspo2 induces a transient activation of Wnt and hence upregulation of the Wnt target Lgr5; the Rspo2-Lgr5 interaction then acts to suppress Wnt signalling through Lrp6 degradation, with a net growth inhibitory effect on colorectal cancer cells.

Hence, the exact role of Lgr4-6 in Wnt signalling appears to be a highly complex one, with possibly opposing effects depending on the specific Lgr4-6/Rspo1-4 homologues that are expressed and interact in a given cellular environment.

Lgr5 Marks Cancer Stem Cells in Intestinal Adenomas

Normal adult stem cells are sometimes thought to be capable of acting as tumour-initiating cells upon transformation, since both cell populations have a high capacity for self-renewal and clonogenic growth. Moreover, the increased incidence of cancer with age could be explained by an accumulation of mutations in adult stem cells that persist throughout life.

To investigate this hypothesis in the murine small intestine, Barker *et al.* first crossed *Lgr5-EGFP-IRES-CreERT2* mice to *Apc*$^{flox/flox}$ mice. *Apc* is a negative regulator of Wnt signalling and is frequently lost in human colorectal cancers (Kinzler and Vogelstein 1996; Jones et al. 2008). When the authors activated Cre recombinase in their double transgenic mice to selectively delete *Apc* in Lgr5^{+} cells,

intestinal adenomas rapidly arose; in contrast, deletion of *Apc* in a transit amplifying cell population failed to give rise to macroscopic intestinal adenomas (Barker et al. 2009). Consistent with these observations, use of another Cre driver (*CD133-CreERT2*) to aberrantly activate Wnt signalling in the same crypt base columnar cells gave similar results (Zhu et al. 2009). Together, these studies suggest that $Lgr5^+$ crypt stem cells are capable of acting as cells-of-origin of intestinal adenoma.

Nevertheless, whether the $Lgr5^+$ stem cell / progeny hierarchy of the normal intestinal crypt is retained in intestinal adenomas remains unclear. Indeed, the existence of so-called “cancer stem cells” (CSCs) that self-renew and proliferate to fuel the growth of the tumour in which they reside is a subject of intense debate (Quintana et al. 2008; Boiko et al. 2010). By using specific Cre driver mouse strains to perform lineage tracing, three different laboratories, including the Clevers group, reported being the first to observe cancer stem cell activity *in situ* (Schepers et al. 2012; Driessens et al. 2012; Chen et al. 2012). In the Clevers study, $Lgr5^+$ cells were observed at the base of intestinal adenomas, interspersed with Paneth cells in an architecture reminiscent of normal intestinal crypts. When Lgr5 lineage tracing was initiated in established adenomas, the authors saw the emergence of ribbon-like clones from the adenoma base, which grew to take up large parts of the adenomas over time (Schepers et al. 2012). Interestingly, the authors also observed that the numbers of $Lgr5^+$ cells within traced clones increased over time, which suggests that $Lgr5^+$ cells clonally expanded within the adenomas. Hence, $Lgr5^+$ cells in intestinal adenomas appear to act as *bona fide* cancer stem cells.

Given that Lgr5 and its homologue Lgr6 also mark stem cells in the HF, it is tempting to speculate that $Lgr5/6^+$ skin cells may act as tumour-initiating cells and that Lgr5/6 may mark cancer stem cells in skin malignancies, such as cutaneous

squamous cell carcinoma (SCC). Clearly, a vigorous test of these hypotheses will require a robust mouse model of SCC, which is the topic of discussion in the next section.

Modelling Cutaneous Squamous Cell Carcinoma in the Mouse

Non-melanoma skin cancer, comprising SCC and basal cell carcinoma (BCC), is by far the most common cancer among Caucasian people, with a recorded incidence in 2006 of more than 3 million in the US alone (Rogers et al. 2010). Of the two subtypes, SCC is the more aggressive with a significant risk of metastasis, and is associated with greater morbidity and mortality.

SCC most commonly arises on sun-exposed areas of the skin, but is also a feature of several hereditary disorders, including Multiple Self-Healing Squamous Epithelioma (MSSE), which afflicts individuals with mutations in the *TGFBR1* gene coupled with rare variants in an adjacent region of Chromosome 9q22.3 (Goudie et al. 2011; Kang et al. 2013); a form of XX-male sex reversal that is caused by mutations in the *RSPO1* gene (Parma et al. 2006); and a number of diseases characterised by genome instability, such as Dyskeratosis Congenita (DKC), where SCC may arise as a consequence of elevated genome mutation rates.

Recent somatic mutation analyses of sporadic skin SCCs have revealed frequent mutations in *NOTCH1*, *NOTCH2*, *TP53*, *CDKN2A* and *HRAS* (Durinck et al. 2011; Wang et al. 2011; Mauerer et al. 2011). These new studies emphasise the strong similarities among the mutation spectra of human squamous tumours at different anatomical sites, including the skin, head and neck, and lung (Agrawal et al. 2011; Stransky et al. 2011; The Cancer Genome Atlas Research Network 2012). In particular, while *HRAS* mutations are rare in human adenocarcinomas of the lung, colon and pancreas, *HRAS* is the most frequently mutated member of the *RAS* family in squamous cancers generally, underlining the human relevance of mouse

models of skin chemical carcinogenesis (where *Hras* mutations are also predominant).

Although most non-melanoma skin cancer can be successfully treated with surgery and/or chemotherapy, metastatic SCC is associated with an extremely poor long-term prognosis, with a 10-year survival rate of less than 20% (Alam and Ratner 2001). To develop better clinical treatments and chemoprevention strategies for SCC, there is a need to achieve a better understanding of the biology of the disease through animal models.

UV Radiation Carcinogenesis

While the majority of mouse skin cancer models involving carcinogens have used chemical mutagens and promoters, it is nevertheless the case that 90% of non-melanoma skin cancer is estimated to be attributable to excessive exposure to UV radiation (Grossbart and Lew 1996). To examine whether UV radiation can induce SCC in mice, several groups utilised hairless but immunocompetent *SKH-1* mice, which are well-suited for this purpose because they lack the dense, UV-impenetrable hair coat of wild-type mice. Together, these studies showed that UV exposure is capable of inducing SCC in *SKH-1* mice, in a dose-, exposure time- and wavelength-dependent manner (for review, see Van Kranen and De Gruijl 1999). The SCCs that arise commonly have *Trp53* mutations, which closely recapitulate the *TP53* mutations seen in sporadic human SCCs (van Kranen et al. 1995).

However, it remains unclear what other mutations arise in this model to cooperate with *Trp53* mutations in driving tumourigenesis. For instance, while *RAS*

mutations are seen in 3-25% of human SCC cases (Mauerer et al. 2011; Durinck et al. 2011; Khavari 2006), they are extremely rare in this model (van Kranen et al. 1995). Work in this area is hampered by the fact that *SKH-1* mice have a non-functional *Hairless* (*Hr*) gene, and while this confers a practical advantage for experiments involving controlled exposure to UV light on a daily basis, the *Hr* gene plays an important role in skin metabolism (Kumpf et al. 2012) and its absence may influence the pathways by which tumours develop in this model. The remainder of this chapter will focus on chemical/genetic models of SCC development.

Chemical Induction of Skin Tumours

The first links between chemical exposure and development of skin cancers (Pott 1775) prompted early attempts to develop tractable models for the study of chemically induced skin cancers. Chemical carcinogenesis of the skin has since emerged as the workhorse model of SCC, having been used to test hundreds of individual hypotheses across a wide range of topics in cancer biology. It played a pivotal role in the evolution of the concept of multistage carcinogenesis, as commonly applied to both human and mouse cancers, and has given rise to the operational definitions of the key tumour processes of initiation, promotion and malignant progression (for reviews, see Yuspa 2000; Boutwell RK, Verma AK, Ashendel CL 1982).

In the most commonly used model, a typical treatment regimen involves first a single topical dose of the carcinogen dimethylbenzanthracene (DMBA), which introduces the initiating mutation to certain cells in the skin. This is then followed by repeated administration of a proinflammatory phorbol ester such as 12-*O*-

tetradecanoylphorbol-13-acetate (TPA), which promotes the selection and growth of initiated cells into benign tumours known as papillomas (Fig. 1.2). With time, some of the papillomas will progress to malignant SCCs, which can further disseminate to distant sites via metastasis. Some SCCs can also convert to a more aggressive form of tumour known as spindle carcinoma, via epithelial-mesenchymal transition (EMT) (Klein-Szanto et al. 1989). Besides DMBA, other chemical carcinogens that have been used to initiate skin cells include methylnitrosourea (MNU) and 3-methylchol-anthrene (MCA), each of which induces carcinogen-specific mutations in *Hras* (Brown et al. 1990).

While the two-stage DMBA/TPA model does not mimic the precise sequence of events that occur in spontaneous human SCC, it is highly reproducible and can be easily adapted to test various genetic and environmental factors that may affect tumour development. Moreover, it offers the advantage that the distinct tumour stages can be easily discerned and separately studied in the context of multistage carcinogenesis. Accordingly, the DMBA/TPA model has been extensively characterised in terms of the series of biological and genetic events that occur during tumour growth.

For instance, a specific mutation in codon 61 of *Hras* (*Q61L*) was identified as the first example of an initiating mutation in a mouse cancer model *in vivo* (Balmain and Pragnell 1983; Balmain et al. 1984; Quintanilla et al. 1986). Evidence for this includes the demonstration that a viral version of activated *Hras* is sufficient to induce tumours in infected, TPA-promoted skin (Brown et al. 1986), and the observation that different mutagens produce different activating mutations in *Hras* but can all effect tumour initiation (Brown et al. 1990). Interestingly, the recent flurry of whole genome and exome sequencing studies have identified the *Q61L* mutation

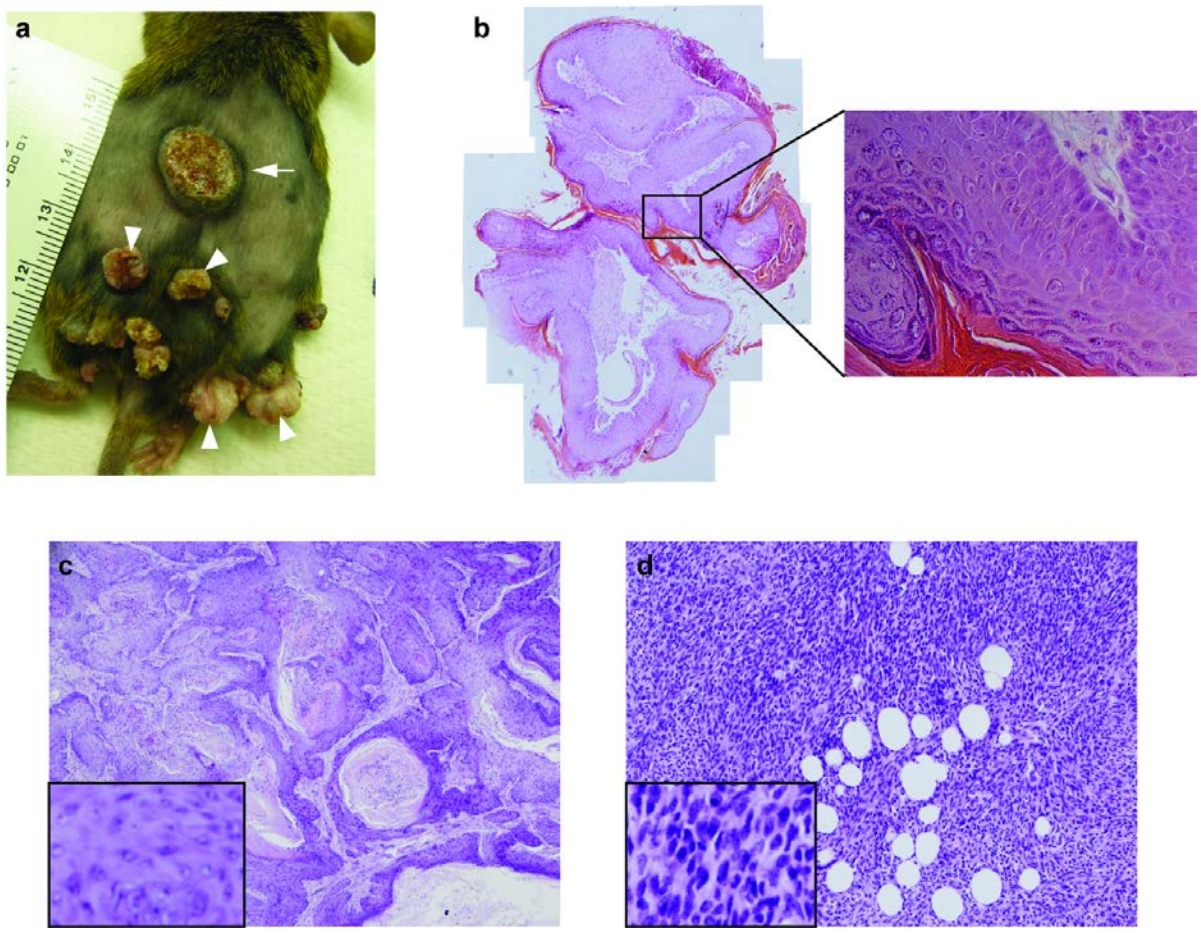

Figure 1.2. Macroscopic and histological views of cutaneous papillomas and SCCs. (**a**) Picture of the back skin of a DMBA/TPA-treated mouse showing papillomas (arrowheads) and an SCC (arrow). Note the exophytic, nodular appearance of the papillomas, and the crater-like architecture of the SCC. (**b**) Papillomas do not breach the underlying epithelial basement membrane and exhibit a high degree of keratinisation. (**c**) Class A tumours include pure squamous cell carcinomas and squamous tumours with a small spindle component. This particular Class A tumour is well-differentiated with heavy keratinisation. (**d**) Class B tumours are mostly pure spindle cell carcinomas, which are poorly differentiated with spindle-shaped cells that resemble fibroblasts. (**c**) and (**d**) are modified from Wong *et al.* 2013.

in *HRAS* as the most common *RAS* mutation generally in squamous cancers of the skin, head and neck, and lung (references above).

During the promotion phase, the papillomas that arise frequently exhibit trisomy of chromosome 7 (Aldaz et al. 1989), where the *Hras* gene is located. Further, the duplicated chromosome is invariably that which bears the mutant *Hras* allele, which thus suggests a strong preference for amplification of the mutant *Hras* allele (Bremner and Balmain 1990). SCCs, on the other hand, often show mutation and loss of heterozygosity (LOH) of the tumour suppressor *Trp53* that are not seen in papillomas, which indicates a role for *Trp53* mutation or loss in malignant progression (Burns et al. 1991; Buchmann et al. 1991).

Apart from the classical route to carcinoma (henceforth Class A carcinoma) formation outlined above, recent work in our laboratory has uncovered an alternative route to invasive carcinoma (henceforth Class B carcinoma) development (Wong et al. 2013). A genetically heterogeneous population of mice was treated with the DMBA/TPA protocol, and unsupervised hierarchical clustering of the gene expression profiles obtained from over 60 carcinomas collected from these mice identified two distinct molecular categories. Class A carcinomas include pure squamous cell carcinomas and squamous tumours with a small spindle component, whereas Class B carcinomas are the most aggressive carcinomas that develop in the DMBA/TPA model, composed primarily of pure spindle cell carcinomas. As expected from their spindle morphology, Class B carcinomas express EMT markers, such as *Snai1*, *Zeb1* and *Vimentin*; however, unlike Class A carcinomas, Class B carcinomas are characterised by loss of the *Ink4/Arf* locus and have, paradoxically, downregulated components of the canonical Hras signalling pathway despite their increased invasiveness (although Mapk and Akt signalling remain elevated). Class B

carcinomas are also less dependent on inflammation for their formation (discussed in detail later), and thus may represent a different category of tumours that diverge from the Class A pathway soon after initiation or arise from a separate target cell altogether (Fig. 1.3).

The vast body of scientific work utilising the DMBA/TPA model gives us the unique opportunity to compare and dissect the influence of many biological and genetic factors on tumour development. Nevertheless, when attempting to interpret the results of various DMBA/TPA studies, one should bear in mind the important caveat that mouse strain background has a considerable influence on tumour susceptibility and outcome. For instance Spretus and C57BL/6 mice are known to be tumour-resistant, while FVB/N mice have been shown to be tumour-susceptible (Hennings et al. 1993). The difference in sensitivity between C57BL/6 and FVB/N mice to Ras-induced skin carcinogenesis, for instance, has been mapped to a polymorphism in the *Ptch* gene, which affects binding to the tumour suppressor Tid1 and consequently Ras-induced apoptosis (Wakabayashi et al. 2007). Hence, without prior knowledge of the mouse genetic backgrounds involved, one should exercise some caution when comparing the effects observed in different studies.

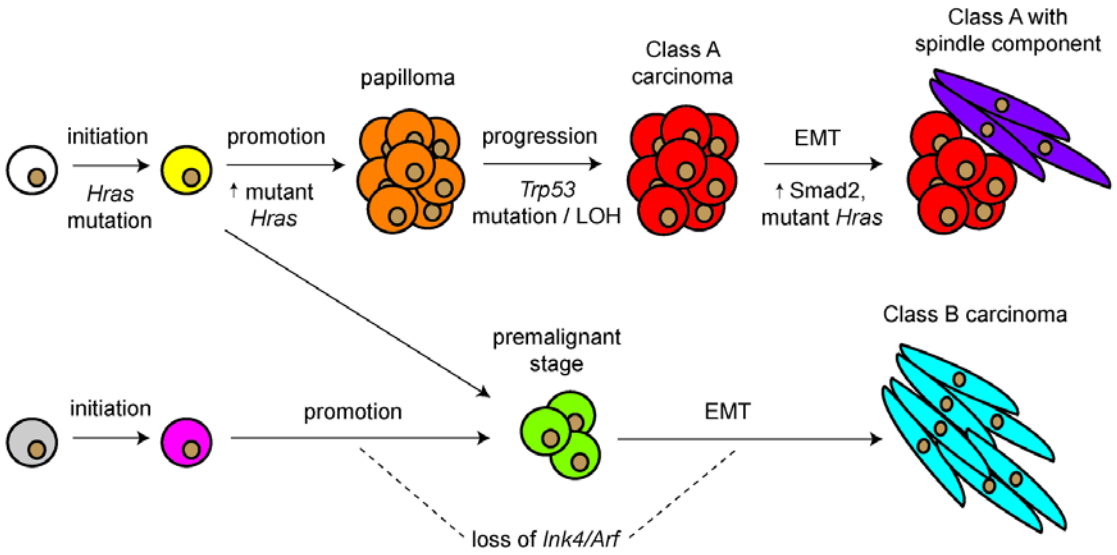

Figure 1.3. Genetic and molecular events during multistage skin carcinogenesis. Class A and Class B carcinomas may arise from the same target cell, but diverge soon after initiation resulting in different premalignant stages. Alternatively, Class A and Class B carcinomas may come from distinct target cells, with possibly different initiating mutations in these cells. Spindle carcinoma formation via the Class A route is thought to involve increased mutant *Hras* levels and nuclear accumulation of Smad2 (Oft et al. 2002); in contrast, in Class B spindle carcinomas, mutant *Hras* levels are downregulated instead.

Use of Transgenic Mice to Investigate Target Cell for Initiation

The identity of the target cell that acquires the first genetic insult leading to initiation is a central question in cancer biology (for review, see Perez-Losada and Balmain 2003). Many tumours contain rare cells that express stem cell markers and are capable of long-term self-renewal; these cells have also been shown to initiate secondary tumours in limiting dilution transplantation assays and even generate large parts of the tumour *in situ* (Schepers et al. 2012; Driessens et al. 2012; Chen et al. 2012; Lapouge et al. 2012). Together, these observations are compatible with the notion of so-called “cancer stem cells,” which act as tumour cells-of-origin and fuel the growth of the tumour (Lapidot et al. 1994). Further, it has been hypothesized that they arise from normal adult stem cells that become transformed during the tumour initiation phase, since both cell populations have a high capacity for self-renewal and clonogenic growth. However, it remains possible that cancer stem cells may actually originate from the initiation of more committed progenitor cells, which only acquire stem cell-like characteristics after undergoing oncogenic insult or exposure to inflammatory stimuli (Schramek et al. 2010; Gonzalez-Suarez et al. 2010; for review, see Gupta et al. 2009).

One of the first studies to shed light on this question of the target cell for initiation in the DMBA/TPA model was performed by Berenblum and Shubik (Berenblum and Shubik 1949). The authors initiated mouse skin tumours with DMBA but allowed one year to elapse before treating the mice repeatedly with croton oil (from which TPA was eventually isolated). They observed that papillomas developed with approximately the same latency and yield as they did in control mice that were

treated immediately with the promoter, indicating that the initiated cells remained in the skin for most of the murine lifespan. This central finding of the “permanence” of the initiating event was subsequently corroborated by other groups, who accounted for confounding factors such as age at time of promotion (Van Duuren et al. 1975) and used intragastric DMBA administration to avoid topical DMBA-induced wound healing, which is thought to possess promoting activity (Loehrke et al. 1983). Importantly, these demonstrations that initiated cells can reside in the skin for long periods of time without giving rise to visible lesions until selection and growth through promotion are consistent with stem cells being the initiated target cells, as only stem cells have the self-renewal potential to allow for such long-term persistence (although, as noted above, it remains possible that stem cell properties may be induced by oncogenic events).

Another early study to address the question of target cell utilises the process of epidermal abrasion, which involves using a tool such as a motorized felt wheel to remove the interfollicular epidermis (IFE) while leaving the hair follicles intact (Argyris 1985). This process will remove all the terminally differentiating cells in the IFE, while sparing the various stem cell populations that have been shown to reside in the hair follicle (for review, see Jaks et al. 2010). One week after initiation with DMBA, mice were either abraded as the experimental group or left unabraded as the control group; TPA treatment was then started four weeks later, when the IFE had regenerated from cells in the hair follicles and returned to normal (Morris et al. 2000). In this study, the authors observed that abraded mice developed far fewer papillomas than unabraded mice; however, the carcinoma responses of the two groups were similar. One interpretation of these data is that benign papillomas arise from initiated cells in the IFE, while malignant SCCs arise from initiated cells in the

hair follicle (including possibly stem cells). Together, the early studies described above point to a role for the identity of the target cell in influencing the course of tumour development.

The next steps taken in the quest for the target cell for initiation were made possible by the advent of transgenic mouse technology (for review, see Palmiter and Brinster 1986). This technology was quickly adopted by the cancer field and putative oncogenes with transforming activity *in vitro* were tested for their capacity to fuel tumour growth *in vivo* (for review, see Hanahan et al. 2007). With the cloning of keratin promoters capable of directing transgene expression to specific skin compartments (Vassar et al. 1989; Byrne and Fuchs 1993; Fuchs et al. 1992), it soon became possible to target oncogenes to subpopulations of cells in the skin, in order to test the ability of these cells to initiate tumour.

Early examples of this approach were the demonstrations that targeting of mutant *Hras* to even terminally differentiating cells in the skin (using the *K10* or *K1* promoter) could give rise to papillomas, which, however, did not progress to malignancy (Bailleul et al. 1990; Greenhalgh et al. 1993). In contrast, when mutant *Hras* was expressed in the outer root sheath (ORS) of the hair follicle (using a truncated version of the *K5* promoter), where stem cells have been shown to reside, malignant SCCs and spindle carcinomas arose (Brown et al. 1998).

One common criticism of these early transgenic mouse studies is that the oncogene of interest was vastly overexpressed in subpopulations of cells. This problem can now be circumvented through knock-in of mutant alleles into their endogenous loci, which allows the mutant alleles to be subsequently activated in subsets of cells via removal of a *Stop* cassette by a tissue-specific Cre recombinase

(Jackson et al. 2001). Using this approach, several groups targeted the expression of an activated form of *Kras* (*KrasG12D*) to different cell populations within the skin (Caulin et al. 2007; White et al. 2011; Lapouge et al. 2011). When oncogenic *Kras* was expressed in terminally differentiating suprabasal cells of the IFE (using *Involucrin-Cre*), or cell populations with stem cell characteristics such as basal keratinocytes (using *K5-Cre*) and hair follicle bulge stem cells (using *K15-Cre* or *K19-Cre*), papillomas developed**.** However, when oncogenic *Kras* was expressed in transit amplifying hair matrix cells (using *Shh-Cre*; White et al. 2011; Lapouge et al. 2011), no papillomas arose. More recently, expression of *KrasG12D* in hair follicle junctional zone stem cells (Jensen et al. 2009) using *Lrig1-Cre* has also been shown to be capable of giving rise to papillomas when combined with full-thickness back wounding (Page et al. 2013). Importantly, while these studies reinforce the idea that the identity of the target cell has a role to play in determining the course of tumour development, they also indicate a certain degree of plasticity among different stem cell populations during tumourigenesis, such that many of them are capable of giving rise to tumours when engineered to express an appropriate oncogene.

An interesting feature of these oncogene-targeting studies is that activation of Ras gives rise to tumours generally in the dorsal skin, but not usually in the tail skin, in spite of the activity of promoters of genes such as *K14* and *Involucrin* in tail epidermis (Gomez et al. 2013; Youssef et al. 2010; White et al. 2011; Lapouge et al. 2011). These data are compatible with previous observations of resistance of tail skin to DMBA/TPA carcinogenesis (Schweizer and Marks 1977). The reasons for this discrepancy between tail skin and back skin may give us additional information about the nature of the target cells for carcinogenesis, particularly as activation of the *Smoothened* (*Smo*) gene using the same *K14* promoter gives rise to basal cell

carcinomas (BCCs) predominantly in tail but not in dorsal epidermis (Youssef et al. 2010).

A final point of contention with the above transgenic mouse studies is that oncogene activation generally occurs in whole populations of cells in the targeted cell compartment, rather than in the clonal fashion that presumably characterises spontaneous or carcinogen-induced tumours. Further, the fact that a particular cell compartment is capable of giving rise to tumours when engineered to express an oncogene is not synonymous with those cells being *bona fide* target cells during carcinogen-induced tumour development. In view of these objections, a better approach to study the target cell for initiation may be to use neutral labelling methods to mark the potential target cell *a priori*, followed by carcinogen treatment and lineage tracing of progeny cells that carry the permanent label during subsequent tumour development.

An early study to use a neutral labelling approach addressed the question of whether chemically induced skin papillomas have a polyclonal origin (Winton et al. 1989). The authors first generated chimeric mice by aggregating embryos of two different strains. These mice demonstrate mosaicism in their tissues, including skin. By subjecting these mice to the DMBA/TPA protocol and performing immunohistochemical analyses, the authors were able to show that about 30% of the papillomas that arose have a mixture of cells from both parent embryos. Hence, they conclude that a significant proportion of papillomas are polyclonal in origin. A similar approach was adopted by Arwert *et al.* to investigate the contribution of terminally differentiating cells to tumorigenesis in *InvEE* mice, which overexpress activated Mek1 in the suprabasal layer of the IFE (Arwert et al. 2010). Here, the authors generated chimeras by aggregating *InvEE* embryos and GFP-positive embryos, and

demonstrated that proliferative, transgene-negative (but GFP-positive) cells are fully incorporated into the tumors that develop upon wounding; these transgene-negative cells thus actively contribute to tumor formation, and are stimulated to do so by non-cell autonomous signals from the Mek1-expressing, terminally differentiating cells.

More recently, a neutral labelling method was also used to determine if bulge stem cells are the cells of origin of chemically induced skin tumours (Li et al. 2012). In this study, the authors initiated *Krt1-15CrePR1;R26R* mice with DMBA, then activated Cre recombinase with the drug RU486 one week later; finally, tumour promotion was performed with biweekly administration of TPA for 20 weeks. When the authors collected tumours from the mice and performed LacZ staining to trace the progeny of the $K15^+$ bulge stem cells, they observed that all papillomas contained a mixture of non-blue and blue cells, with the latter making up, on average, approximately 30% of papilloma cross-section area. This suggests that $K15^+$ stem cells may have the potential to contribute long-term to papillomas in the DMBA/TPA model. However, there are a few caveats to this study. One, there is a significant level of promoter leakiness in the *Krt1-15CrePR1;R26R* mice, which makes it difficult to determine the true contribution of the $K15^+$ stem cells to papillomas. A second caveat is that Cre recombinase was activated only after DMBA treatment, in which case initiated progenitor cells may acquire stem cell properties and start expressing K15 *de novo*.

Another recent study that uses a similar but distinct approach was carried out by Driessens *et al*. They treated *K14CreER/Rosa-YFP* mice with the DMBA/TPA protocol and then initiated lineage tracing in the resulting papillomas and SCCs at clonal density, by administering a low dose of tamoxifen (Driessens et al. 2012). Through 3D reconstruction of whole clones from serial sections, they report the

existence of two proliferative cell compartments in papillomas, mirroring the hierarchy seen in normal tissues – a slower-cycling “progenitor cell” fraction that is shorter-lived and gives rise to smaller clones, and a faster-cycling “stem cell” fraction that persists longer and gives rise to larger clones. In contrast, in SCCs, the authors report the existence of a single proliferative cell population that expands geometrically and has a low probability of terminal differentiation. One caveat to this study is that the lineage tracing results reported are for relatively short periods of time (9 days for SCCs, and up to 7 weeks for papillomas). It remains to be seen if the same tracing patterns will hold up over longer periods of time and qualify the observed proliferative cell compartments as arising from *bona fide* cancer stem cells. Moreover, because lineage tracing is only initiated after tumour formation, several important questions remain outstanding. For example, what is the relationship of the $K14^+$ proliferative cell populations reported in this study to stem cell compartments in normal skin? Also, what is the nature of the target cells that lead to benign or malignant tumours and how may these differ?

Taking into account all the studies described above, a picture emerges of the existence of a continuum of target cells amenable to initiation. Here, the course of tumour development, in terms of cell fate decisions and malignant potential, is likely a function of both the nature of the initiating mutation and the identity of the target cell. Hence, while initiated terminally differentiating cells are capable of giving rise to papillomas, these often lack the propensity to progress to malignancy; ultimately, the promotion of initiated multipotent stem cells may be required to lead to malignant SCCs.

Use of Knockout Mice to Examine Ras Effectors and Tumour Suppressor Pathways

Ras Effectors in Skin Carcinogenesis

As with the development of transgenic mouse technology in the previous decade, the advent of knockout mouse technology in the 90's was a tremendous boon to cancer research (for review, see Jacks 1996). A subsequent major advance in the field was the invention of Cre-Lox technology, which made it possible to target ablation of the gene of interest to subpopulations of cells, by flanking the gene with *LoxP* sites and activating its removal with Cre recombinase specifically in subsets of cells. Further development of an inducible form of the Cre recombinase allowed for postnatal gene deletion at a time of the researcher's choosing.

One use of the knockout mouse technology has been in characterising the roles of downstream Ras effectors. The highly reproducible mutational activation of *Hras* in the DMBA/TPA model, together with the demonstration of the causality of this event in initiating carcinogenesis, has led to the widespread use of this model for testing the functions of a wide variety of components of the Ras signalling pathway. Besides mutant *Hras*, transgenic expression of a number of upstream activators of Ras in the skin has also been reported to be capable of inducing tumours. In particular, mice that overexpress *TGF-α* in their epidermis develop papillomas upon wounding or TPA treatment (Vassar et al. 1992; Dominey et al. 1993). TGF-α is the ligand for the EGF receptor, which activates Ras through the guanine nucleotide exchange factor SOS (Fig. 1.4). Importantly, the papillomas that arise in *TGF-α* transgenic mice do not have a mutation in *Hras*, which suggests that activation of the Ras pathway through *TGF-α* overexpression is sufficient to induce skin tumour

initiation in the absence of *Hras* mutational activation. Consistent with this idea, most sporadic human SCCs exhibit activated Ras signalling, despite *Ras* being mutationally activated in only a small subset of these tumours (references above). Interestingly, the papillomas from the *TGF-α* transgenic mice also have the tendency to regress and were never observed to progress to malignancy. More recently, *K5-SOS-F* transgenic mice that overexpress a dominant form of *SOS* in basal keratinocytes were generated and these develop spontaneous papillomas with 100% penetrance (Sibilia et al. 2000).

The roles of Raf-MAPK and PI3K-Akt signalling downstream of Ras have been extensively characterised. Raf-1 is the first identified and most intensively-studied Ras effector. It activates mitogenic MAPK signalling, leading to induction of the Ets family of transcription factors and Cyclin D1. PI3K-Akt signalling, on the other hand, activates mTOR, with downstream consequences for protein synthesis and cell growth. Apart from Raf-1 and PI3K, Ras has a number of other known effectors (Fig. 1.4) whose *in vivo* functions remain relatively poorly understood. Here, use of the DMBA/TPA model, in conjunction with knockout mouse technology, has been instructive.

For instance, Ras binds and activates PLCε, which produces the second messengers diacylglycerol and inositol 1,4,5-triphosphate. These, in turn, activate Protein Kinase C (PKC) and mobilize intracellular calcium, respectively. PKC is thought to have a role in skin tumour promotion, since TPA is known to bind and regulate PKC (Castagna et al. 1982; Fournier and Murray 1987; Hansen et al. 1990), which in turn suggests a potential role for *PLCε* in tumourigenesis downstream of

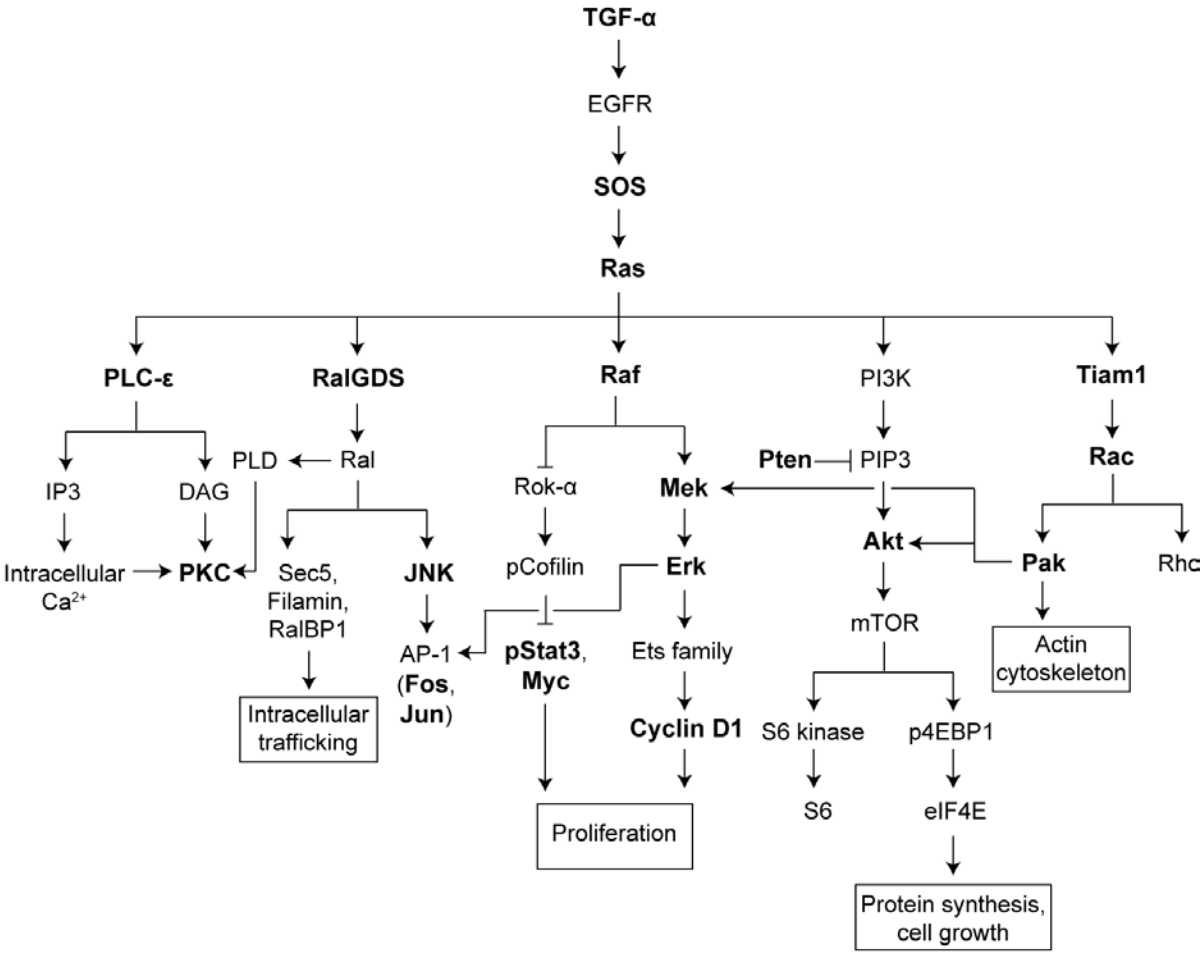

Figure 1.4. Ras effector pathways in skin carcinogenesis.

Signalling components in bold have been directly investigated for their *in vivo* functions during skin tumour development. The roles of TGF-α, SOS, Ras, PLCε, RalGDS, Raf-1, Stat3, Pten and Tiam1 are described in detail in the text.

Ras activation. When treated with the DMBA/TPA protocol, *PLCε*-deficient mice developed papillomas with increased latency, reduced yield and a decreased propensity to undergo malignant conversion (Bai et al. 2004). This indicates that PLCε has far-ranging roles in skin carcinogenesis, impinging upon both the promotion and malignant progression stages.

Ras also binds and activates Tiam1, which is a guanine nucleotide exchange factor that in turn activates Rac GTPases. *In vitro*, Rac GTPases are implicated in cell migration and cell cycle progression (Hordijk et al. 1997; Keely et al. 1997; Olson et al. 1995, 1998). When treated with the DMBA/TPA protocol, *Tiam1*$^{-/-}$ mice were resistant to tumour development, and this was attributed to increased apoptosis during the initiation stage and reduced proliferation during the promotion stage (Malliri et al. 2002). However, *Tiam1*$^{-/-}$ mice also had a higher ratio of malignant to benign tumours, which thus indicates a biphasic role for Tiam1 in skin carcinogenesis. Interestingly, *Tiam1* is downregulated in Class B carcinomas (Wong et al. 2013). Hence, while papilloma formation via the classical route is impeded by *Tiam1* deficiency, the higher percentage of malignant tumours seen in DMBA/TPA-treated *Tiam1*$^{-/-}$ mice could be a reflection of their origin as Class B carcinomas. Indeed, when the authors treated *Tiam1*$^{-/-}$ mice with an alternative carcinogenesis protocol that involved repeated treatment with DMBA in the absence of TPA (known as the complete carcinogenesis protocol), they obtained a higher percentage of high grade, poorly differentiated SCCs, which may represent Class B carcinomas. Another guanine nucleotide exchange factor downstream of Ras is RalGDS, which activates the Ral GTPase. *In vitro*, Ral is involved in intracellular trafficking and regulating gene expression through transcription factors such as AP-1 (Kops et al.

1999; de Ruiter et al. 2000; Nakashima et al. 1999; Moskalenko et al. 2002). DMBA/TPA treated *RalGDS*-deficient mice had reduced tumour incidence, size and malignant progression (González-García et al. 2005). Further, RalGDS was reported to mediate survival through the JNK/SAPK signalling pathway, so that heightened apoptosis was observed in the papillomas that arose in *RalGDS*-deficient mice.

Finally, a novel function of Raf-1 was more recently characterised by studying mice with epidermis-specific *Raf-1* deficiency. These mice exhibit hyperactivity of the Rho effector Rok-α in their skin, while Erk activation is unaffected by *Raf-1* ablation (Ehrenreiter et al. 2005). When treated with the DMBA/TPA protocol, *Raf-1*-deficient mice were resistant to tumour development; further, induction of *Raf-1* ablation only after tumours had already developed resulted in tumour regression (Ehrenreiter et al. 2009). This addiction of SCCs to Raf-1 was attributed to Raf-1's role in binding and inhibiting Rok-α, which prevents Rok-α from phosphorylating and inactivating cofilin; when active, cofilin is able to stimulate Stat3 phosphorylation and Myc expression, leading to proliferation. Hence, when *Raf-1* is ablated in mice, Stat3 phosphorylation and Myc expression will be turned off, so that differentiation predominates over proliferation and tumourigenesis is impeded.

Therefore, apart from its well-documented role in tumour initiation, Ras also has diverse and complex functions that range across multiple stages of skin carcinogenesis. Depending on the particular Ras effector ablated, specific arms of these Ras responses will be abrogated, leading to varied, nuanced consequences for tumour development.

Knockout Mice and Tumour Suppressor Pathways

Another use of knockout mouse technology has been to interrogate the nature and specific functions of tumour suppressor pathways in skin carcinogenesis. *TP53* is frequently mutated in spontaneous human SCC and, as described earlier, is also commonly mutated or lost in SCCs that arise in the DMBA/TPA model. When *Trp53*$^{+/-}$ mice were treated with the DMBA/TPA protocol, papillomas developed with approximately the same latency, yield and size as they did in wild-type mice (Kemp et al. 1993). However, these papillomas progressed more rapidly to SCCs, and malignant conversion was associated with loss of the remaining copy of wild-type *Trp53*; DMBA/TPA-treated *Trp53*$^{-/-}$ mice, on the other hand, had a reduced yield of papillomas but these progressed even more rapidly to malignancy. Hence, *Trp53* does not appear to have a major role in the initiation or promotion phase of tumour development; rather, loss of *Trp53* is associated with malignant progression. In line with these observations, restoration of p53 activity was shown to have no effect on early stage tumours but caused regression of late stage tumours in a mouse model of *KrasG12D*-driven lung adenocarcinoma (Feldser et al. 2010; Junttila et al. 2010). Additionally, in the *KrasG12D*-driven skin tumour mouse models described earlier, oncogenic *Kras* alone can only give rise to papillomas, with no evidence of malignant progression; instead, oncogenic *Kras* driven by *K5*, *K15* or *K19* has to be coupled to *Trp53* deficiency to induce malignant SCCs.

Apart from promoting the malignant conversion of papillomas, *Trp53* loss can have other effects that are also consistent with an increased frequency of malignant tumours. For instance, *Trp53* loss may lead to increased numbers of stem cells, and hence an expansion of the pool of target cells that may specifically give rise to malignant tumours. In support of this hypothesis, *Trp53* loss has been shown to

increase the self-renewal of both mammary and neural stem cells (Cicalese et al. 2009; Meletis et al. 2006). In particular, p53 regulates the polarity of cell division in mammary stem cells, with *Trp53* loss predisposing toward self-renewing symmetric cell divisions. Remarkably, mammary tumour stem cells also exhibit an elevated frequency of symmetric cell divisions, and restoration of p53 activity rescues asymmetric stem cell divisions and results in tumour growth reduction. Importantly, stem cell numbers increase progressively in premalignant *Trp53*$^{-/-}$ murine mammary gland over time. In the context of the epidermis, various models have been proposed to account for how stem cells in the basal layer proliferate and self-renew in maintaining the tissue (Potten 1981; Potten et al. 1982; Clayton et al. 2007; Mascré et al. 2012). Like mammary stem cells, epidermal stem cells are capable of both asymmetric and symmetric cell divisions. If *Trp53* loss in the epidermis similarly favours self-renewing symmetric stem cell divisions at the expense of asymmetric stem cell divisions, then we might also expect stem cell numbers to progressively increase in *Trp53*$^{-/-}$ skins over time.

Yet another area where *Trp53* loss can have an effect is cell competition. This phenomenon was first described in *Drosophila melanogaster*, where cells of two different genotypes within a common developmental niche were shown to compete with each other for tissue occupancy (Morata and Ripoli 1975); at the cell population level then, cell competition can be described as a process of natural selection of the fittest cells. The same principle has since been shown to govern cell-cell interactions in many tissue types and organisms, including mammals. For instance, ionizing radiation (IR)-induced stress has been shown to be capable of eliciting cell competition within the hematopoietic stem cell (HSC) compartment (Bondar and Medzhitov 2010); in particular, by generating mice with a mosaic pattern of p53

deficiency within the HSC compartment, the authors of the study demonstrated that in the presence of IR stress, p53-deficient HSCs have a selective proliferative advantage and induce a senescence-like phenotype in outcompeted HSCs with higher levels of p53 activity. More recently, a genome-wide screen in murine induced pluripotent stem cells similarly identified p53 as a key gene whose downregulation created “cheater” cells that outcompete wild-type cells during pluripotent stem cell differentiation *in vitro* and *in vivo* (Dejosez et al. 2013).

In the context of the skin, UV exposure in both mice and humans gives rise to patches of normal-looking cells that contain mutant p53, which suggests that p53 mutation is an early event in the development of UV-induced SCC (Berg et al. 1996; Jonason et al. 1996; Ren et al. 1996). More recent work by Klein *et al.* indicates that such p53 mutant clones (PMCs) undergo stochastic exponential growth during periods of UV illumination (Klein et al. 2010); such a mode of growth is remarkably consistent with PMCs being derived from mutant CP cells (Clayton et al. 2007; Mascré et al. 2012) that demonstrate a stochastic cell fate tipped in favour of proliferation. Further, once UV exposure ceases, the data suggest that the proliferation and loss of p53 mutant cells become balanced so that the population of preneoplastic cells reaches a steady state. Notably, such a paradigm for the behaviour of p53 mutant cells in the skin is fully compatible with the cell competition model described above – in the presence of UV-induced stress, p53 mutant CP cells have a proliferative/survival advantage over wild-type CP cells, leading to the expansion of PMCs; upon UV cessation, this competitive advantage disappears, so that the stochastic cell fate of p53 mutant CP cells is once again balanced between proliferation and loss. This interpretation is supported by a recent report describing

the effect of p53 deletion on stem cell competition within the intestinal stem cell niche (Vermeulen et al. 2013).

Besides *TP53*, another tumour suppressor gene commonly mutated in tumours is *PTEN* (Li et al. 1997; Steck et al. 1997), which negatively regulates the PI3K-Akt signalling pathway downstream of Ras. Although somatic *PTEN* mutations have not been reported in cutaneous SCC, germline *PTEN* mutations are the cause of Cowden Disease in humans, which is associated with an elevated risk of SCC (Liaw et al. 1997). Mice that are *Pten*-null in their epidermis develop spontaneous papillomas, many of which eventually progress to malignancy (Suzuki et al. 2003). Further, $Pten^{+/-}$ mice treated with the DMBA/TPA protocol have increased papilloma numbers and develop SCCs at a faster rate (Mao et al. 2004). Interestingly, most of the SCCs from these mice do not have an initiating *Hras* mutation; rather, these SCCs have lost their remaining copy of wild-type *Pten*, while the minority of SCCs that do have an *Hras* mutation retain their wild-type *Pten*. Hence, *Hras* activation and *Pten* LOH are mutually exclusive events in the DMBA/TPA model, which may be due to their redundant effects in activating Akt signalling. In support of this hypothesis, *Pten*-null SCCs have downregulated pERK levels but similar pAkt levels compared to *Hras*-mutated SCCs, which suggests that Akt signalling, and not MAPK signalling, may be the critical Ras effector in this particular model of skin carcinogenesis.

Tumour Suppressor and Non Cell-Autonomous Effects of Notch Signalling in SCC Development

Notch signalling has been implicated in controlling the process of keratinocyte differentiation (Rangarajan et al. 2001; Lowell et al. 2000). *In vitro*, activated Notch1

in keratinocytes induces p21 expression, which leads to growth arrest, while *in vivo*, keratinocyte-specific deletion of *Notch1* results in epidermal hyperplasia and deregulated expression of differentiation markers. These observations suggest a role for Notch1 in limiting proliferation in the skin, in contrast to the situation in many other tissues where Notch signalling is involved in preventing differentiation and plays a positive oncogenic role (Jhappan et al. 1992; Zagouras et al. 1995; Capobianco et al. 1997). Indeed, loss-of-function mutations in *NOTCH1* or *NOTCH2* have been reported in 75% of human cutaneous SCCs (Wang et al. 2011), which indicates a tumour suppressor function for Notch signalling in SCC development.

To investigate this, Nicholas *et al.* ablated *Notch1* postnatally in the epidermis of mice (Nicolas et al. 2003). These mice developed spontaneous BCC-like skin tumours, and were more susceptible to tumour development when subjected to the DMBA/TPA protocol. The chemically induced tumours were mostly papillomas, but also included some malignant SCCs and BCC-like tumours. The authors suggest that the increased tumour susceptibility may be due to heightened Gli2 expression and derepressed β-catenin signalling in *Notch1*-deficient epidermis. In line with these observations, mice that overexpress the pan-Notch inhibitor *DNMAML1* in their skin also exhibit enhanced epidermal β-catenin signalling and develop spontaneous skin tumours, although these were histologically characterised as SCCs and not BCCs (Proweller et al. 2006).

More recently, a non-cell autonomous tumour suppressor function has been reported for *Notch1* in the epidermis. Using mice with a chimeric pattern of *Notch1* deletion in the epidermis, Demehri *et al.* showed that both *Notch1*-deleted and *Notch1*-expressing keratinocytes readily formed papillomas in the DMBA/TPA model, which indicates that Notch1 does not suppress tumourigenesis in a cell autonomous

fashion (Demehri et al. 2009). Rather, *Notch1* loss leads to defective skin barrier formation and thus induces wound repair responses; the resulting stromal microenvironment is characterised by inflammation, dermal fibroplasia and increased angiogenesis, which the authors suggest to be responsible for promoting tumour formation in these mice. In support of this hypothesis, deletion of other *Notch* paralogues that also impaired skin barrier formation similarly led to spontaneous skin tumour development.

Further evidence for a non-cell autonomous function for Notch signalling in the epidermis comes from Ambler *et al*. Here, the authors activated Notch signalling aberrantly in the epidermis, by utilising transgenic mice with 4-hydroxy-tamoxifen (4OHT)-inducible, K14-driven expression of the Notch intracellular domain (NICD) (Ambler and Watt 2010). Upon 4OHT application, these mice developed blisters at the epidermal-dermal junction, along with dermal accumulation of T lymphocytes and stromal cells. The authors showed that this phenotype was dependent on upregulation of the Notch ligand Jag1 in the epidermis, which is associated with a concomitant induction of Jag1 in the underlying dermis and activated NF-κB signalling. Hence, the authors concluded that Jag1 is a key mediator of non-cell autonomous epidermal Notch signalling.

Finally, a non-cell autonomous role for Notch signalling in the dermis has also been reported. Hu *et al*. ablated *CSL/RBP-Jκ*, a key Notch effector, specifically in murine mesenchyme, which includes the dermal fibroblasts that underlie the epidermis (Hu et al. 2012). These mice developed dermal atrophy and inflammation, which preceded the spontaneous appearance of multifocal SCCs. *CSL*-deficient dermal fibroblasts were shown to exhibit features of cancer-associated fibroblasts, such as the expression of growth factors and matrix metalloproteases, as well as the

deposition of Periostin and Tenascin C – two extracellular matrix proteins that have been reported to foster cancer stem cell niches (Malanchi et al. 2012; Oskarsson et al. 2011). Importantly, in human skin samples, the stroma underlying premalignant lesions also exhibited reduced Notch signalling; moreover, UVA exposure was shown to be capable of inducing *NOTCH2* silencing by DNA methylation in human skin explants, which provides a potential mechanism for how dermal Notch signalling may be downregulated in response to sun exposure that predisposes to SCC development.

Therefore, in the skin, Notch signalling may have both cell-autonomous and non-cell autonomous tumour suppressor activities, the latter deriving from a crosstalk between the epidermis and the underlying dermis.

Chapter 2

Plasticity of Lrig1^{+} skin infundibulum stem cells during normal homeostasis, wounding and tumourigenesis

Abstract

Lrig1 is known to be a marker of stem cells in the mouse hair follicle infundibulum. By gene expression network analysis of normal mouse skin, we identified *Lrig1* within a network, including *Krt79*, involved in homeostasis of the hair follicle infundibulum. Lineage tracing showed that Lrig1$^+$ cells maintain a discrete infundibulum compartment, and that single cells from this compartment migrate into the epidermis. This process is accelerated by treatment with TPA, which also stimulates downward migration of labelled infundibulum cells in anagen hair follicles. Activation of mutant *Hras* or *Kras* in Lrig1$^+$ cells leads to distinct phenotypes – the former causes wavy hair while the latter gives oily skin. Both *Hras* and *Kras* activation can cause papilloma development, but Lrig1$^+$ cells are not common cells-of-origin of chemically induced tumours. Rather than acting as a stem cell reservoir, Lrig1$^+$ cells may play a facilitating role during tissue damage and tumour development.

Introduction

The adult mouse skin comprises several distinct compartments, each harbouring its own resident stem/progenitor cell population(s). For instance, stem cells in the interfollicular epidermis (IFE) basal layer proliferate to generate keratinocytes that form clones of cells known as epidermal proliferative units (EPUs) (Potten 1981; Mackensie 1970; Ro and Rannala 2004; Mascré et al. 2012). The sebaceous gland (SG), on the other hand, has been variously reported to possess progenitor cells that reside either in the basal layer (Cui et al. 2003; Petersson et al. 2011) or near the bud site, where they are defined by the transcriptional repressor Blimp1 (Horsley et al. 2006).

The mouse hair follicle (HF) is home to several distinct populations of stem cells. In the telogen bulge and hair germ, stem cells marked by the G protein-coupled receptor Lgr5 actively cycle to maintain the HF (Jaks et al. 2008). Further up the follicle, the Lgr5 homologue Lgr6 marks stem cells that have been reported to preferentially give rise to cells of the IFE and the SG (Snippert et al. 2010). Finally, quiescent stem cells, defined by markers such as CD34 (Trempus et al. 2003) and Keratin 15 (Liu et al. 2003), reside in the follicle bulge and may act as a reserve stem cell pool that becomes activated in response to stress situations such as wounding (Ito et al. 2005).

To provide critical barrier functions during normal homeostasis and to effect proper tissue regeneration during wound healing, the various skin compartments have to work effectively together. To achieve this, these compartments have to communicate with one another to coordinate various cellular functions and processes, such as proliferation and turnover. However, it remains unclear what

signals or cell populations might be involved in mediating these inter-compartmental communications.

Leucine-rich repeats and immunoglobulin-like domains 1 (Lrig1) is a transmembrane protein that negatively regulates Egfr signalling (Gur et al. 2004; Laederich et al. 2004; Jensen and Watt 2006). In the mouse HF, Lrig1^{+} cells lie just above the Lgr6^{+} cells and were reported to be bipotent, contributing to both the IFE and the SG during normal homeostasis (Jensen et al. 2009). In a later study, using lineage tracing, Lrig1^{+} cells were reported to maintain the infundibulum and SG, but contribute to neither the HF nor the epidermis (Page et al. 2013) under normal growth conditions.

Lrig1 also has putative roles in tumourigenesis. It has been proposed to act as a tumour suppressor gene based on functional and genetic analysis of human tumours of the lung and other tissues (Lu et al. 2013), and Lrig1-deficient mice develop spontaneous intestinal crypt adenomas (Powell et al. 2012). In apparent contrast with this putative suppressor role, in tumours derived from mouse skin, Lrig1 was specifically enriched in a population of highly invasive undifferentiated tumours that exhibit several features of stem cells (Wong et al. 2013). In addition, *Kras* activation in cells expressing Lrig1-CreERT2 in the skin was shown to drive hyperplasia leading to tumour formation after application of a wound stimulus (Page et al. 2013).

Here, we have used computational network analysis and lineage tracing to examine the role of Lrig1 in normal skin homeostasis, and under conditions of perturbation by acute or chronic treatment of the skin with inflammatory and tumour-promoting agents. We have also addressed the possible role of *Lrig1* as a skin

tumour suppressor, and as a marker of the cell-of-origin of *Ras* mutant skin tumours initiated by the classical DMBA/TPA skin carcinogenesis protocol.

Results

Network analysis of the Lrig1 compartment in normal mouse skin

We have previously used computational tools to develop a network view of normal mouse skin, based on gene expression analysis of skin samples from a genetically heterogeneous backcross population. This approach identified *Lgr5* as a candidate HF stem cell marker within a strong network motif linked to HF morphogenesis (Quigley et al. 2009). Lineage tracing by Jaks *et al.* (Jaks et al. 2008) provided functional evidence that *Lgr5* marks a stem cell that can give rise to all lineages of the HF, but not of the interfollicular epidermis. We used this approach to investigate the network relationships of *Lrig1*, using data derived from mouse tail skin gene expression profiles (Quigley et al. 2009). Correlation analysis using previously published gene expression data showed that *Lrig1* is in the same network as several known stem cell markers, including *Lhx2*, *Gpr125* and *Lgr5* (Supplementary Table 2.1). These data were derived from the tails of tumour-bearing mice that had been subjected to treatment with DMBA/TPA on the dorsal skins for induction of skin tumours (Quigley et al. 2009). We therefore examined the correlations for *Lrig1* in a separate data set of tail skins from normal 8 week-old mice that had not been subjected to these perturbations, and looked for significant correlations that were replicated in both data sets (Supplementary Table 2.2). Figure 2.1a shows the network of genes whose expression levels were strongly correlated with expression of *Lrig1* in both experiments, suggesting a potential functional link to *Lrig1*. Among these genes was the HF keratin *Krt79*, which has previously been shown to play a functional role in maintaining the infundibulum (Veniaminova et al. 2013), and *Efnb2*,

a member of the ephrin family of ligands for receptors EPHB3 and EPHB4 that are implicated in a wide array of developmental and signalling pathways (Xu et al. 2000; Kuijper et al. 2007).

It is possible that significantly correlated genes are expressed in the same cells within a tissue compartment, or interact within the same signalling pathway, or even reflect paracrine relationships between adjacent cell types. Co-staining of mouse skin for Lrig1 and Krt79 demonstrated that while both are indeed expressed in the infundibulum region of the skin, they are in fact expressed at the protein level in adjacent cells rather than in the same population (Fig. 2.1b). While Lrig1 is expressed primarily in the basal cells of the infundibulum, Krt79 is present mainly in the suprabasal population, with very little co-localisation. This suggests that there may be paracrine crosstalk leading to correlated expression of Lrig1 and Krt79 in basal and suprabasal cells. An alternative explanation that cannot be excluded is that both are correlated at the mRNA level in basal cells of the infundibulum, but Krt79 is only translated within the suprabasal layer. Recent studies using the same antibody against Krt79 have demonstrated a functional role for this keratin in hair canal morphogenesis and regeneration (Veniaminova et al. 2013).

We then examined the localisation of Efnb2 in 8 week-old mouse skin by immunohistochemical analysis. Strong expression of Enfb2 was detected in the infundibulum, and in the basal cells of the SG (Fig. 2.1c). To verify the Efnb2 staining pattern using an independent approach, we examined skin from a mouse strain (*Efnb2*^{GFP}) (Davy and Soriano 2007) engineered to express nuclear H2B-GFP under the control of the Efnb2 promoter. Figure 2.1d shows almost complete co-localisation of Efnb2 as detected by both methods within the skin infundibulum and SGs. Additionally, a strong overlap was observed between the staining patterns for Efnb2

and Lrig1 (Fig. 2.1e). The gene expression network and protein localization data are therefore compatible with these genes being expressed in the same cell population. The specific functional role for Efnb2 in the infundibulum remains to be determined, but these data indicate that gene expression analysis of normal skin from genetically heterogeneous mice can lead to predictions of spatial and functional relationships between genes expressed in this tissue.

Lineage tracing of Lrig1$^+$ infundibulum cells

We next used lineage tracing of Lrig1$^+$ cells to evaluate the roles of this putative stem cell population in normal skin homeostasis and under conditions of stress and tumour development. The *Lrig1-CreERT2* mouse carries a tamoxifen inducible Cre recombinase (CreERT2) targeted to the translational initiation site of the endogenous *Lrig1* locus (Powell et al. 2012). *Lrig1-CreERT2* mice crossed to the *R26RLacZ* reporter line (Soriano 1999) received one topical application of 1mg 4-Hydroxytamoxifen (4OHT) at 8-10 weeks of age, and were then sacrificed at different time points ranging from 2 days to 8 months. Figure 2.2a shows that two days after Cre induction, staining of back skin with X-Gal revealed a cell population located in the upper part of the HF isthmus and junctional zone. 100% of follicles were stained, but no staining in the IFE could be detected (Fig. 2.2a inset). 7 days after Cre induction, X-Gal labelling had extended to the whole infundibulum and single blue cells appeared in the IFE (Fig. 2.2b and inset). In contrast, immunofluorescence staining with an antibody against Lrig1 still resembled the X-Gal labelling 2 days after induction (Fig. 2.2c) with no staining in the upper infundibulum or the IFE and only a few positive cells in the basal layer of the SG. Most SGs at this point were either

partially or completely blue. These results suggested that the traced cells in the infundibulum and epidermis seen after one week were derived from the Lrig1^{+} cells of the junctional zone, but no longer expressed Lrig1.

4 weeks after induction, X-Gal labelling remained similar to the 7-day timepoint for follicles in telogen phase (Fig. 2.2d). However, some HFs that had entered anagen phase showed additional blue staining above and sometimes in the bulb region (Fig. 2.2e,f). Staining in the IFE was more extensive (Fig. 2.2d inset), possibly as a consequence of proliferation of the single cells seen 7 days after induction. Lrig1 antibody staining in anagen follicles was again detected in the upper isthmus and JZ, and was extended to a population above the HF bulb (Fig. 2.2g), as previously noted by Jensen *et al.*(Jensen et al. 2009).

3 months after Cre induction, X-Gal labelling in the infundibulum persisted (Fig. 2.2h,i) but labelling below the infundibulum was only detected in rare cases, sometimes with single cells detected along the outer root sheath (ORS) even below the bulge closer to the bulb (Fig. 2.2j). The IFE still showed the presence of groups of blue cells (Fig. 2.2h inset). 5 to 8 months after induction, X-Gal labelling was still found in the infundibulum (Fig. 2.2k-m), and occasionally in basal and suprabasal IFE cells (Fig. 2.2k,m insets).

Control mice at 8 weeks and 6 months of age that were never treated with 4OHT showed no X-Gal labelling, indicating that the *Lrig1* promoter construct is not leaky (Supplementary Fig. 2.1a,b). Our results suggest that under steady state conditions, the progeny of Lrig1^{+} cells repopulate a distinct cell compartment in the infundibulum, but can also contribute cells to the IFE and the SG, as well as to the HF during anagen phase.

Tissue proliferation causes increased migration of infundibulum cells into the IFE and HF

Next, we used lineage tracing to determine the effects of perturbation of normal skin homeostasis on the Lrig1$^+$ cell compartment. We first treated 7-10 week old mice first with 1 topical dose of 4OHT to achieve full infundibulum, JZ and upper isthmus X-Gal labelling (Fig. 2.2b). 7 days after induction, the mice received 1 topical dose of TPA to induce a wave of inflammation and proliferation in the skin. Mice were then sacrificed at different time points after the TPA treatment. 24 h after TPA treatment, X-Gal labelling of the infundibulum and JZ of all follicles was similar to the tracing 7 days after 4OHT treatment without TPA (Fig. 2.3a). However, in the IFE, groups of blue basal and suprabasal cells were detected (Fig. 2.3c), suggesting that the traced single blue cells seen in the epidermis at 7 days post 4OHT induction (Fig. 2.2b inset) had undergone proliferation 24 h after TPA treatment. At 48 h after TPA treatment, proliferation in the skin was more apparent in the increased thickness of the epidermis and the greater lengths of the growing HFs. Infundibulum, junctional zone and upper isthmus of all follicles were stained up to the epidermis (Fig. 2.3b), with blue cells detected in the basal and suprabasal layers of the IFE (Fig. 2.3d). Lrig1 antibody staining was as described previously for the unperturbed skin (Fig. 2.3e).

72 h after TPA treatment, X-Gal labelling in the infundibulum persisted (Fig. 3f), and single blue cells could occasionally be detected migrating down the ORS towards the bulb in anagen follicles (Fig. 2.3g). Long stretches of blue cells in the IFE basal and suprabasal layers pointed to proliferating clones derived from Lrig1$^+$ cells (Fig. 2.3i). Lrig1 antibody staining revealed the familiar Lrig1$^+$ cell population in the junctional zone, and additional positive cells below the bulge and above the bulb

(Fig. 2.3h). 7 days after TPA treatment, skin morphology had almost returned to normal, but some blue cells in the IFE persisted (Fig. 2.3j), along with labelling in the infundibulum and some single cells further down in the ORS (Fig. 2.3k). Lrig1 antibody staining was again detected in the JZ (Fig. 2.3l). Control mice treated with TPA only and sacrificed at the same time as the 4OHT treated group revealed no X-Gal labelling, confirming the non-leakiness of the Lrig1 allele (data not shown). We conclude that TPA treatment and induction of acute inflammation and proliferation accelerates the migration of cells derived from the Lrig1^{+} population into areas that are undergoing active growth, in the IFE and the HF**.**

Chronic TPA treatment leads to depletion of Lrig1-labelled cells in the infundibulum

To investigate the Lrig1 lineage response to an extended period of proliferation and chronic inflammation, Cre expression was induced with one treatment of 4OHT in 7-10 week old mice, as described above. 7 days later, the mice were started on a regimen of biweekly topical TPA treatments, for a total of 3 weeks. X-Gal labelling was detected in the infundibulum of the HFs and in some SGs (Fig. 2.4a), although only 38% of follicles (20 out of 53 follicles) remained labelled compared to 100% of follicles labelled 72 h and 7 days after an acute single TPA dose. Intriguingly, in 60% of labelled follicles from the 3 week chronic TPA treatment experiment (12 out of 20 follicles), the blue cells were confined to only one side of the infundibulum (Fig. 2.4a), while the other side showed no labelling. Rare follicles with blue cells down the whole length of the ORS were also observed (Fig. 2.4b). Long stretches of cells were still labelled in both the basal and suprabasal layers of

the IFE (Fig. 2.4d). Biweekly TPA treatment of mice for 6 weeks after Cre induction showed a similar X-Gal labelling pattern to that seen for the 3 week TPA treatment experiment, with about 33% of follicles (12 out of 38 follicles) labelled and similar tracing in the IFE (data not shown). Lrig1 antibody staining again detected cells at the JZ and the region between the bulge and the bulb (Fig. 2.4c). As control, *Lrig1-CreERT2*$^{+/-}$*/R26RLacZ*$^{+/-}$ mice not exposed to 4OHT were treated biweekly with TPA for 3 or 6 weeks, and no X-Gal labelling could be detected in these mice (data not shown). We conclude that prolonged treatment with TPA to induce chronic inflammation and proliferation leads to a depletion of Lrig1 lineage cells from the infundibulum, as a consequence of increased and continuous migration into the IFE or the anagen HFs.

Lineage tracing of Lrig1^{+} cells in newborn mouse skin

To investigate the behaviour of the Lrig1^{+} cell compartment during early postnatal development, we treated 0-0.5 day old mouse pups topically with 0.25 mg of 4OHT and sacrificed them at different timepoints. At postnatal day 2 (P2), a few blue cells were detected in the infundibulum and in the ORS in the lower part of the developing follicles (Fig. 2.5a,b). The epidermis is also proliferating at this stage, and blue staining in the IFE was seen in very rare single cells in both the basal and suprabasal IFE layers (Fig. 2.5b, arrowheads). Immunostaining revealed cells expressing Lrig1 protein predominantly in the whole infundibulum (Fig. 2.5c). At P10, the follicles have attained their full length and several staining patterns were observed. Blue cells were detected in the infundibulum and in the ORS in stretches along almost the entire length of the follicle, in some instances reaching a blue bulb

(Fig. 2.5d) and in some not (Fig. 2.5e). Some of the follicles showed only labelling in the infundibulum and single cells in the lower part (Fig. 2.5d, follicle on the right). At P17, HFs have reached the first catagen phase and while some showed X-Gal labelling similar to the results seen at P10, with blue cells along the entire length of the follicles and into the bulb (Fig. 2.5g), others showed labelling only in the infundibulum (Fig. 2.5h). At P21, HFs are back in telogen phase and follicles showed the usual infundibulum labelling and some blue cells in the lower part (Fig. 2.5m,n). Labelling in the IFE was restricted to small groups of cells in both the basal and suprabasal layers (Fig. 2.5m, arrowhead). The last timepoint assessed was P35. Some HFs at this stage had a blue infundibulum and single cells migrating to the lower part of the follicle (Fig. 2.5j); in rare cases, the follicle was almost completely blue, including the bulb, with little labelling in the infundibulum (Fig. 2.5k). Lrig1 antibody staining results were similar from P10-P35, with Lrig1$^+$ cells detected in the JZ and upper isthmus (Fig. 2.5f,i,o,l).

We conclude that although the tracing of Lrig1$^+$ cells in newborn mice is more heterogeneous than in the adult, the traced cells eventually are found largely in the infundibulum region after 3-4 weeks, suggesting that the identity of these Lrig1$^+$ progeny is established during development. As was seen with the adult mice, the Lrig1 traced cells migrate to regions undergoing growth and morphogenesis in the interfollicular or follicular regions, but rarely make a permanent contribution to these compartments.

Distinct phenotypes are induced by mutant Hras or Kras in Lrig1^{+} cells

It has previously been suggested that skin papillomas and carcinomas can arise from the infundibulum (Hansen and Tennant 1994; Morris et al. 2000). To test this hypothesis, we first crossed *Lrig1-CreERT2*$^{+/-}$ mice with *Kras*^{LSLG12D} mice, which carry an inducible copy of mutant *Kras* (Jackson et al. 2001). Previous studies using an alternative *Lrig1-CreERT2* allele (Page et al. 2013) also targeted *Kras* to Lrig1^{+} cells, but this gene is only very rarely activated in a small number of papillomas or carcinomas in wild type mice(Brown et al. 1986). We therefore also crossed conditional mutant *Hras* mice into the *Lrig1-CreERT2* background to compare the phenotypes induced by these two *Ras* family members. The *Lrig1-CreERT2*$^{+/-}$*/Hras*$^{LSL-G12V/+}$ mice developed a wavy hair phenotype approximately 2 to 3 weeks after topical 4OHT treatment (Fig. 2.6a). Interestingly, the *Lrig1-CreERT2*$^{+/-}$*/Kras*$^{LSL-G12D/+}$ mice had a distinct oily skin phenotype (Fig. 2.6b), enabling clear distinction between mice carrying these different activated *Ras* isoforms. Both strains exhibited signs of SG hyperplasia, which was much stronger in the *Kras* mutant animals (Fig. 2.6c,d). In agreement with this observation, Efnb2, shown above to be expressed in Lrig1^{+} cells in the SG, was strongly increased in expression in *Kras* mutant skins (Fig. 2.6e).

A wavy hair phenotype has previously been seen in animals with defects in the Egfr signalling pathway (Lee and Threadgill 2009), while an oily skin phenotype was reported in mice over-expressing Epigen, in association with sebaceous hyperplasia (Dahlhoff et al. 2010). These data therefore suggest that distinct signalling pathways induced by mutations in *Hras* or *Kras* may account for these different phenotypes.

Induction of Hras or Kras mutant papillomas by wounding

Although *Hras* and *Kras* mutations induced different phenotypes when expressed in the infundibulum, both oncogenes are known to be capable of giving rise to papillomas in response to a wounding stimulus (Bailleul et al. 1990; Greenhalgh et al. 1993; Page et al. 2013). We therefore challenged the 4OHT-induced *Lrig1-CreERT2*$^{+/-}$*/Hras*$^{LSL\text{-}G12V/+}$ or *Lrig1-CreERT2*$^{+/-}$*/Kras*$^{LSL\text{-}G12D/+}$ mice through application of a back wound stimulus. Most animals in both genotype groups developed papillomas at the wound site by 4 to 6 weeks after wound induction (Fig. 2.6f,g). In all of the above wounding experiments, none of the observed papillomas showed signs of malignant progression. In contrast, control mice that had not been induced with 4OHT did not develop skin papillomas even when aged for one year. We therefore conclude that Lrig1^{+} cells are capable of giving rise to benign tumours when engineered to express mutant Hras or Kras in the context of a promoting wound stimulus.

Functions of Lrig1 in skin tumourigenesis

The function of Lrig1 as a negative regulator of Egfr signalling, coupled with loss of heterozygosity in the *LRIG1* locus in some human cancers have led to speculation regarding its role as a tumour suppressor gene (Lu et al. 2013). This hypothesis is supported by studies of the *Lrig1-CreERT2* mouse, which acts effectively as a knock-out allele –Lrig1 deficiency in the mouse intestine leads to intestinal hyperplasia and adenoma formation (Powell et al. 2012). In mouse skin, complete germline deletion of Lrig1 results in a psoriasis-like proliferative phenotype (Suzuki et

al. 2002), but no data are available on a potential role for Lrig1 as a skin tumour suppressor.

We carried out a 2-stage skin chemical carcinogenesis study using the *Lrig1-CreERT2*$^{+/-}$*/R26RLacZ*$^{+/-}$ mice to address two questions: a) Does functional inactivation of one copy of *Lrig1* lead to an increased incidence of skin tumours, as would be expected if *Lrig1* functions as a tumour suppressor gene in the classical sense? b) Do the Lrig1^{+} cells in the infundibulum act as cells-of-origin for benign or malignant skin tumours induced by DMBA/TPA?

To investigate the effects of heterozygous *Lrig1* loss on skin tumour formation, we treated 15 *Lrig1-CreERT2*$^{+/-}$*/R26RLacZ*$^{+/-}$ mice, containing only one functional *Lrig1* allele, and 14 *R26RLacZ*$^{+/-}$ mice with a single treatment of DMBA followed one week later by biweekly TPA treatments for 20 weeks. The appearance of any tumours was monitored and mice were sacrificed when carcinomas reached 1.5 cm in diameter. All mice in the experiment developed papillomas, with no significant difference in papilloma latency and yield between *Lrig1-CreERT2*$^{+/-}$*/R26RLacZ*$^{+/-}$ and *Lrig1 WT/R26RLacZ*$^{+/-}$ mice. (Supplementary Fig. 2.2a) Carcinoma numbers and survival also did not vary significantly between the two groups of mice (Supplementary Fig. 2.2b,c). We conclude that Lrig1 does not act as a classical tumour suppressor of squamous skin carcinomas induced by the two-stage DMBA carcinogenesis protocol.

To address the question of whether the Lrig1^{+} cells in the infundibulum act as cells-of-origin for benign or malignant skin tumours induced by DMBA/TPA treatment, we treated 26 *Lrig1-CreERT2*$^{+/-}$*/R26RLacZ*$^{+/-}$ mice with 1 mg of 4OHT topically to induce labelling of the cells within the infundibulum, as shown in Fig. 2.2b. One week

later, when virtually all HF infundibulum compartments are fully labelled, we initiated carcinogenesis as described above. Previous studies using *K1-15-CrePR1/R26RLacZ* mice to label Krt15^{+} bulge stem cells, followed by DMBA/TPA treatment, showed that most papillomas taken 20 weeks after starting TPA treatment carried varying numbers of permanently labelled LacZ^{+} cells, and therefore contained a proportion of cells derived from the HF bulge region (Li et al. 2012). We reasoned that if the Lrig1^{+} cells or their progeny in the infundibulum could act as common cells-of-origin of skin tumours, a substantial proportion of any tumours resulting from carcinogen treated *Lrig1-CreERT2*$^{+/-}$*/R26RLacZ*$^{+/-}$ mice would carry the activated *LacZ* allele.

From a total of 46 papillomas analysed by X-Gal staining, 42 showed no evidence for the presence of blue cells. Some harboured blue cells in the epidermis and HFs of attached skin, indicating that recombination had taken place (Fig. 2.7a,b). 2 papillomas showed very few blue cells in small groups or as single cells and 2 papillomas consisted of more than 50% blue cells (Supplementary Fig. 2.3a).

The mice developed a total of 49 skin carcinomas, the majority SCCs. 36 carcinomas were analysed by X-Gal staining and of these 86% had no blue cells except in adjacent skin (Fig. 2.7c,d). Only 5 carcinomas, all SCCs, had small to moderate amounts of blue cells (Supplementary Fig. 2.3b). 2 of the carcinomas analysed were of the aggressive spindle cell type, but X-Gal labelling was absent from these tumours. Similar undifferentiated tumours were previously shown to be enriched in *Lrig1* mRNA and protein expression (Wong et al. 2013) but these new results suggest that these tumours are not derived from Lrig1-expressing cells but acquire Lrig1 expression at a later stage. 19 carcinomas and 35 papillomas derived from control mice not treated with 4OHT but undergoing the same DMBA/TPA

regimen showed only 1 papilloma with small blue patches. Our results suggest that Lrig1^{+} cells do not give rise to skin tumours in this model and are not common target cells for the tumour-initiating *Hras* mutation. These data are in stark contrast to the results of expressing mutant *Hras* or *Kras* (Page et al. 2013) in the Lrig1^{+} cell population, which resulted in wound-dependent papilloma formation (Fig. 2.6f,g). While some Lrig1^{+} cells are therefore capable of giving rise to epithelial lesions when a potent oncogene is coordinately activated in many cells within the infundibulum, clonal initiation of carcinogenesis by mutagen-mediated activation of *Hras* in single cells rarely takes place within this cell compartment.

We further asked whether the Lrig1-expressing cells within tumours could act as cancer "stem cells", capable of giving rise to progeny that could persist for extended periods. A total of 10 *Lrig1-CreERT2*$^{+/-}$*/R26RLacZ*$^{+/-}$ mice were treated with DMBA/TPA until papillomas and carcinomas developed, and the Cre recombinase was then activated by 4OHT to begin tracing of Lrig1^{+} cells within the tumours. Papillomas and carcinomas were harvested at different times after 4OHT treatment, ranging from 2 days to 11 weeks. X-Gal analysis of 27 papillomas and 12 carcinomas showed that although tracing was detected in normal skin adjacent to the lesions, very few cells within tumours showed evidence of being derived from Lrig1^{+} cells (Fig. 2.8a-d). In control experiments using *K14-CreERT2*$^{+/-}$*/R26RLacZ*$^{+/-}$ mice treated in the same way, some labelled clones were detected, both in normal adjacent skin and tumours, which persisted up to 11 weeks after 4OHT treatment (Fig. 2.8e,f). These data are compatible with the results of Driessens *et al.* (Driessens et al. 2012) showing that *K14-CreERT2* tracing can be detected in skin tumours for up to 7 weeks after labelling, although in our studies, staining at 15 weeks was substantially reduced, suggesting that these traced clones may represent

progeny of an intermediate transit amplifying cell rather than a CSC. We conclude that the Lrig1^{+} cells within skin tumours are not capable of acting as CSCs that fuel the growth of the tumours.

Discussion

Several distinct skin cell compartments are derived from specific lineages, each of which has the capacity to regenerate from stem cells that are uniquely capable of replenishing all the cells within that compartment. Tissue regeneration requires that all these compartments communicate with each other, but the mechanisms by which this occurs are unknown. Because of its unique location juxtaposed to the HF, epidermal and sebaceous compartments of the skin, the infundibulum may have evolved as a source of cells that can contribute to regenerative processes in these other skin lineages. We have used gene expression network analysis of normal skin to identify *Lrig1* within a distinct network of genes, some of which are clearly expressed and have functional significance within the infundibulum. The strong correlation between *Lrig1* and *Krt79* at the mRNA level is compatible with an important role for this keratin in the morphogenesis of the infundibulum and hair canal (Veniaminova et al. 2013). Expression correlation between *Lrig1* and *Efnb2* reflects expression of this ligand in the sebaceous gland and infundibulum, which is strongly increased during sebaceous hyperplasia induced by Kras expression. While the annotation of the complete set of genes within this network remains to be carried out, this bioinformatics approach can provide functional information on the location of gene expression within a complex tissue, and/or on the pathways within which genes operate (Quigley et al. 2009; Sjölund et al. 2014).

Our lineage tracing data demonstrate that under normal homeostasis conditions, Lrig1^{+} stem cells can repopulate the infundibulum and the SG. The infundibulum cells give rise to progeny that can migrate into the epidermis and also

into the HF after initiation of anagen growth. These processes are accelerated during increased turnover in early postnatal growth, or after treatment of adult mice with TPA. Similar observations on increased migration after perturbation were observed using an independently-derived Lrig1-EGFP-IRES-CreERT2 mouse strain (Page et al. 2013). This study however did not report migration of infundibulum-derived cells into the epidermis under normal homeostasis, possibly due to differences in the extent of tracing between strains, or to technical differences in the experimental approaches. In our studies, virtually every HF showed infundibulum tracing, possibly accounting for the higher sensitivity using this allele.

It seems unlikely that this migration simply serves to provide cells from the infundibulum that differentiate down the appropriate epidermal or HF lineages. The Lrig1-traced cells found in the epidermis are scattered, and no examples of extensive repopulation of large areas of the epidermis are seen. An alternative hypothesis is that the migrating cells deliver signals that are required to help maintain homeostasis in the normal epidermis, and that this process is accelerated under conditions of increased proliferation after wounding or perturbation by TPA treatment. Such a mechanism is not unprecedented – local insulin signalling can play a critical role in regulation of stem cell behaviour in the fruit fly, where it has been shown that quiescent stem cell activation is dependent on a locally delivered source of insulin-like peptides supplied by neighbouring glial cells (Cheetham and Brand 2013). Similar mechanisms exist in mammalian systems, for example in the rat brain where astrocytes can produce Igf-1 in response to ischaemic damage, promoting the growth of neural progenitor cells in the hippocampus (Ye et al. 2004). In the mouse small intestine, quiescent stem cells can give rise to Paneth cells that in turn contribute to a “stem cell niche” through expression of factors such as Wnt3

(Buczacki et al. 2013; Clevers and Bevins 2013; Sato et al. 2010). Further studies will be required to test this hypothesis in the skin and identify the factors that may be produced by cells migrating from the infundibulum.

Several groups have previously used specific gene promoters to drive expression of activated *Ras* in mouse skin, leading to formation of squamous lesions with differing propensities for malignant progression (Huang and Balmain 2014; Song and Balmain 2014). A number of distinct cell populations in the skin appear to be susceptible to tumour development driven by activated *Ras*, including those expressing Krt5 (Brown et al. 1998; Caulin et al. 2007), Krt10 (Bailleul et al. 1990), Krt1 (Greenhalgh et al. 1993), Krt14, Krt15, Krt19 (White et al. 2011; Lapouge et al. 2011), Lrig1 (Page et al. 2013, this report) and Msx2 (Mukhopadhyay et al. 2011). Direct comparison of these studies is complicated by the fact that the early investigations used these promoters directly to drive expression of activated *Ras* at high levels, whereas later studies used Cre-Lox technology to activate an endogenous *Ras* gene. The latter approaches have all used the same latent allele of *Kras*, although endogenous *Kras* is very rarely activated in mouse skin tumours resulting from classical chemical carcinogenesis protocols (Quintanilla et al. 1986). Page *et al.* have demonstrated that activation of *Kras* in the Lrig1$^+$ infundibulum can give rise to wound-dependent papillomas. We demonstrate here that activation of *Hras* or *Kras* in the same Lrig1$^+$ compartment has a different outcome in terms of the skin phenotypes induced. *Hras* mutation induces a wavy hair phenotype similar to that seen in mice carrying germline mutations in the Egfr pathway (Lee and Threadgill 2009), while *Kras* mutation induces an oily skin phenotype similar to that induced by expression of Epigen in transgenic skin (Dahlhoff et al. 2010). These differences are unlikely to be a consequence of the “signalling strength” of mutant

Hras or *Kras*, as both genotypes give rise to papillomas after wounding, at about the same frequency. We conclude from this and the above-cited studies that no specific cell compartment exists that exclusively harbours cells capable of forming tumours.

One caveat to these engineered mouse models is that they involve synchronous activation of *Ras* oncogenes in multiple cells within each targeted compartment, in contrast to chemical initiation of carcinogenesis by a point mutational event, which is relatively rare and involves clonal activation of mutant Ras in single cells. Single transformed cells can be growth inhibited by surrounding normal cells (Stoker et al. 1966; Bissell and Hines 2011) or may have to out-compete their neighbours (Vermeulen et al. 2013), properties that are not essential after concerted oncogene activation of multiple cells.

We have used an alternative approach based on the premise that prior marking of the Lrig1$^+$ cell population by activation of a neutral marker should, if tumours arise from this cell population, reveal the nature and location of the initiated cells. This approach has previously been used by Morris *et al.* using a *Krt15* promoter known to be expressed within the HF bulge (Li et al. 2012). Activation of the *Lrig1-CreERT2* allele leads to almost 100% labelling of the infundibulum compartment, as detectable by LacZ staining, one week after 4OHT treatment. Initiation of DMBA/TPA carcinogenesis at this stage nevertheless results in the formation of very few tumours carrying LacZ$^+$ cells, suggesting that the vast majority of cells in the Lrig1-traced normal infundibulum compartment are in fact not common targets for initiation. These data also suggest that caution should be exercised in interpreting experiments on identification of the cell-of-origin of tumours using cell compartment-specific promoters to activate endogenous mutant oncogenes. Lrig1$^+$ cells within tumours may still play an accessory role in tumour growth, but do not act

as cancer “stem cells” capable of giving rise to progeny that repopulate tumours over extended time periods. Our results are compatible with the notion that Lrig1^{+} cells in the infundibulum produce signals that help to maintain tissue homeostasis, but do not act as stem cells that are able to regenerate normal epidermal progeny or squamous tumours of the skin.

Materials and Methods

Mouse breeding and lineage tracing in skin

Lrig1-CreERT2 mice were crossed with homozygous *R26RLacZ* mice to obtain *Lrig1-CreERT2*$^{+/-}$*/R26RLacZ*$^{+/-}$ mice, used for all experiments. *Lineage tracing of Lrig1 expressing cells in adult skin*: 8–10 week old mice received one topical application of 4OHT (1 mg in 200 µl of 100% ethanol) (Sigma-Aldrich) onto back skin to induce Cre expression. Mice were sacrificed in triplicate at the following time points after induction: 2 days, 7 days, 4 weeks, 3 months, 5 months and 8 months. Control mice received no treatment. *Lineage tracing of Lrig1 expressing cells in adult skin after acute inflammation*: 8-10 week old mice were treated with 4OHT as described for tracing in adult skin. 7 days after induction they received one topical treatment of TPA (200 µl of a 10^{-4} M solution in acetone) (Sigma-Aldrich) applied to back skin. They were sacrificed 6 h, 24 h, 48 h, 72 h and 7 days after the TPA treatment. Control mice received only the TPA treatment and were sacrificed at the same time points as treated mice. *Lineage tracing of Lrig1 expressing cells in during chronic inflammation*: Cre was induced with 1 topical treatment of 4OHT as described above and after 7 days mice were treated biweekly with TPA for either 3 or 6 weeks, then sacrificed and skin collected. *Lineage tracing of Lrig1 expressing cells in neonatal skin*: newborn to 0.5 day old mice were treated with one topical application of 0.25 mg 4OHT in 50 µl of 100% ethanol onto back skin. Pups were sacrificed in triplicate at P2, P10, P17, P21 and P35. Control mice received no treatment. Mice used for network analysis were generated by breeding [(FVB/N x SPRET/Ei) x FVB/N] backcross mice. Mice were housed in standard conditions, fed

ad libitum, and sacrificed at 8 weeks of age. Animals were housed and treated in accordance with the regulations and protocols stipulated by the UCSF Institutional Animal Care and Use Committee (IACUC).

Lineage tracing in tumour experiments

All *Lrig1-CreERT2*$^{+/-}$*/R26RLacZ*$^{+/-}$ mice used for tumour experiments were bred onto the FVB/N background.

4OHT-DMBA-TPA: 8–12 week old mice received one topical application of 1 mg 4OHT in 100% ethanol onto their back skin. 7 days later they received one topical dose of DMBA (25 mg in acetone). 3 days after initiation with DMBA, tumours were promoted by biweekly topical treatment with TPA (200 µl of a 10^{-4} M solution in acetone) for 20 weeks. Mice were sacrificed when their first carcinoma reached a size of 1.0-1.5 cm in diameter at which point all additional carcinomas and 3 papillomas were collected. As control, mice underwent DMBA-TPA treatment as described above without the initial application of 4OHT.

DMBA-TPA-4OHT: 8–12 week old mice were subjected to the standard DMBA-TPA regimen to induce papillomas and carcinomas. After the TPA treatment was already finished (21-23 weeks after DMBA treatment for *K14-CreERT2*$^{+/-}$*/R26RLacZ*$^{+/-}$ mice, and 26-32 weeks after DMBA treatment for *Lrig1-CreERT2*$^{+/-}$*/R26RLacZ*$^{+/-}$ mice), animals were injected with Tamoxifen (2 mg in peanut oil (Sigma)) in the afternoon of 2 consecutive days. On the second day in the morning they also received one topical dose of 4OHT (1 mg in 100% ethanol). Mice were sacrificed at specific timepoints

after 4OHT treatment. All mouse experiments were approved by the University of California at San Francisco Laboratory Animal Resource Center.

X-Gal staining

Skin: Samples from treated or control *Lrig1-CreERT2*$^{+/-}$*/R26RLacZ*$^{+/-}$ mice were taken and cut into smaller pieces. They were fixed with 4% Formaldehyde in PBS for 10min at RT on a shaker and washed with PBS. After 3 washes samples were incubated overnight at 37 °C with X-Gal staining solution consisting of 1 mg/ml X-Gal, 5 mM $K_3Fe(CN)_6$, 5 mM $K_4Fe(CN)_6$, and 2 mM $MgCl_2$ in PBS. Next day, samples were washed with PBS, transferred to 70% ethanol and processed into paraffin blocks. Sections were cut, counterstained with nuclear fast red (Vector Labs) according to the manufacturer's instructions and analysed under the microscope.

Tumours: Papillomas and carcinomas were collected, directly embedded in OCT and frozen on dry ice. 5 µm sections were cut and stored at -80 °C. For X-Gal labelling, sections were thawed at RT, washed with PBS for 5 min and fixed with 4% Formaldehyde in PBS for 3 min at RT. After 3 washes with PBS, sections were incubated overnight at 37 °C with X-Gal labelling solution. Next day, sections were washed with PBS, counterstained with nuclear fast red and mounted with Citifluor.

Immunofluorescence

5 µm skin sections were deparaffinised and antigen retrieval was performed in 10 mM sodium citrate solution (pH 6) or in Trilogy pretreatment solution (Cell Marque). Sections were blocked for 1h at room temperature with 10% donkey serum (Abcam)

diluted in PBS containing 0.3% Triton X-100 and incubated overnight with primary antibodies against Lrig1 (goat, R&D), Efnb2 (goat, R&D), Krt79 (“Gli2”, rabbit, Abcam) or GFP (rabbit, Santa Cruz) at 4 °C. After washing in PBS, sections were incubated with blocking solution containing an Alexa 555 conjugated donkey anti-goat/rabbit secondary antibody (Molecular Probes) and DAPI for 1 h at room temperature. After another PBS wash slides were mounted using Citifluor.

Statistical analysis

Microarray data published in Quigley *et al.* 2009 were downloaded from GEO (GSE12248). RNA was isolated using TRIzol (Invitrogen) according to the manufacturer’s instructions. Residual genomic DNA was removed by DNase treatment (Ambion). RNA quality was assessed using Bioanalyzer (Agilent). Gene expression was quantified using Affymetrix MoGene ST 1.1 arrays hybridized on an Affymetrix GeneTitan instrument. Gene expression correlation was calculated in the R statistical environment (R Core Team 2012). Gene network diagrams were created using Cytoscape version 2.8 (Shannon et al. 2003).

Figures and Tables

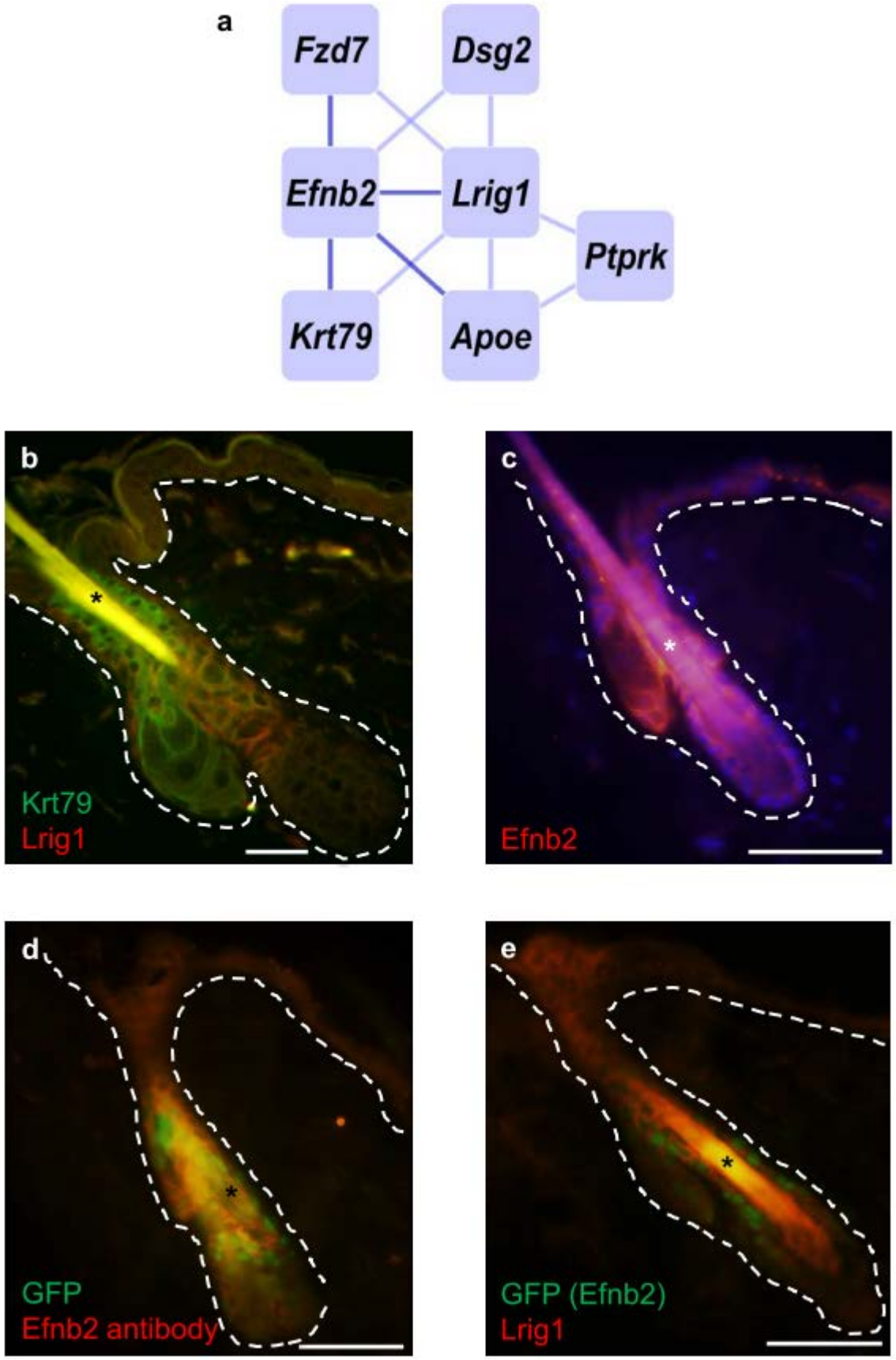

Figure 2.1. ***Gene expression network and immunofluorescence analysis of the Lrig1 compartment in normal mouse skin*****.** (**a**) Correlation network showing genes whose expression is correlated with expression of *Lrig1* in both Quigley *et al.* 2009 and a second population of untreated eight-week-old mouse skin. Genes drawn as nodes with edges connecting genes where expression correlation ≥ 0.6; darker blue lines indicate stronger correlation. (**b**) Representative image showing adult mouse skin co-stained with antibodies against Lrig1 (red) and Krt79 (green). Dotted lines delineate the basement membrane of the epidermis and the outline of the HF. (**c**) Representative image showing immunofluorescence staining using an antibody against Efnb2 in adult mouse skin. (**d**) Representative image showing adult *Efnb2*^{GFP} mouse skin co-stained with antibodies against Efnb2 (red) and GFP (green). (**e**) Representative image showing adult *Efnb2*^{GFP} mouse skin co-stained with antibodies against Lrig1 (red) and GFP (green). Dotted lines delineate the basement membrane of the epidermis and the outline of the HF. Asterisks label the autofluorescent hair shaft. Bars = 50 μm.

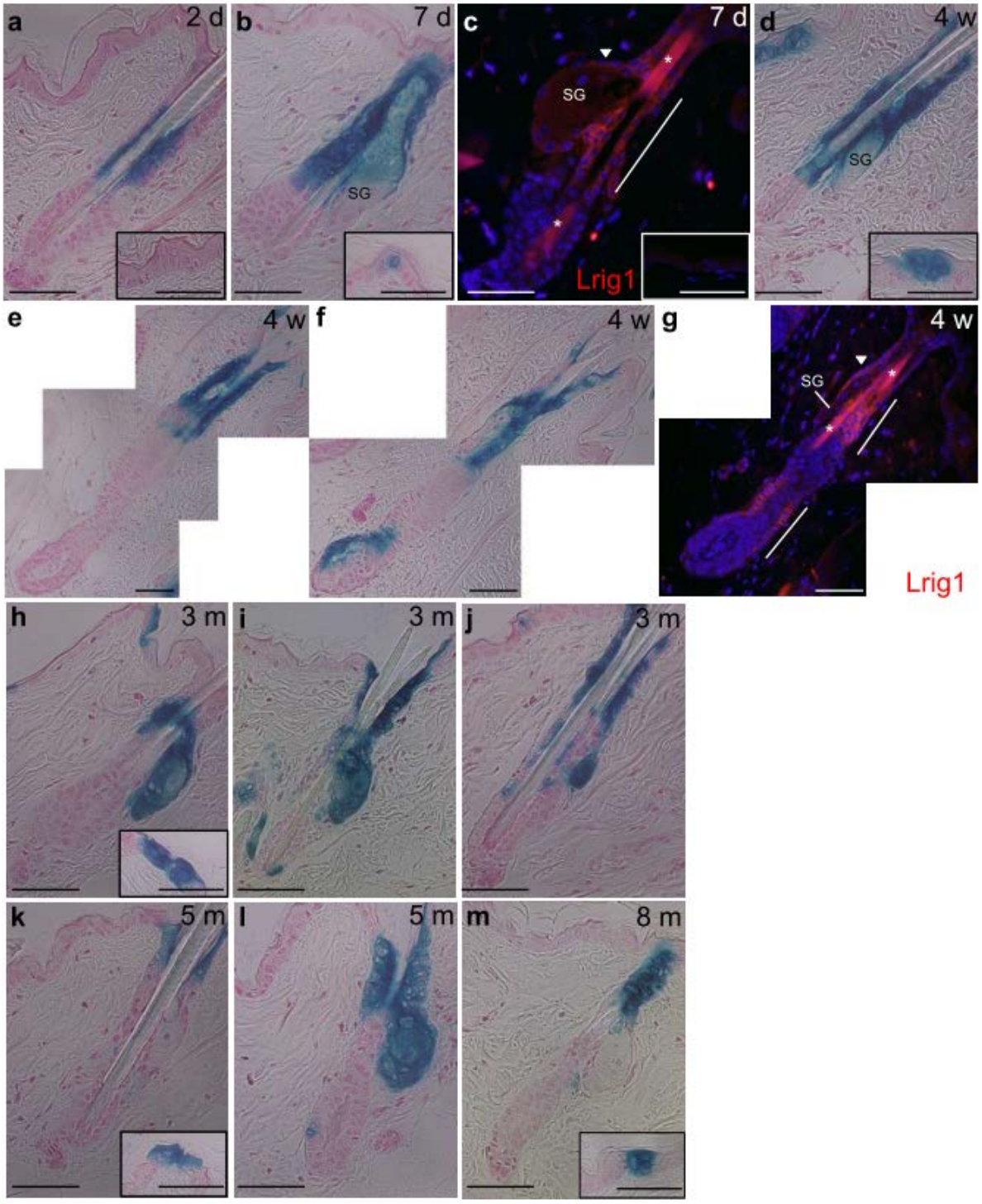

Figure 2.2. Lineage tracing on skin from adult *Lrig1-CreERT2$^{+/-}$/R26RLacZ$^{+/-}$* mice during normal skin homeostasis. Mice were sacrificed at various timepoints after one topical treatment with 4OHT. (**a**,**b**) Representative pictures of HFs stained with X-Gal (**a**) 2 days (**b**) 7 days after 4OHT treatment. (**c**) Immunofluorescence staining on skin from adult mice 7 days after 4OHT treatment using an antibody

against Lrig1. (**d**-**f**) Representative pictures of HFs stained with X-Gal 4 weeks after 4OHT treatment, starting to grow (**d**) and in anagen phase (**e**,**f**). (**g**) Immunofluorescence staining of an anagen follicle 4 weeks after 4OHT treatment using an antibody against Lrig1. (**h**-**m**) Representative pictures of HFs stained with X-Gal 3 months (**h**-**j**), 5 months (**k**,**l**) and 8 months (**m**) after 4OHT treatment. All insets show representative pictures of X-Gal or antibody staining in the IFE at the corresponding timepoints after 4OHT treatment. White lines show the extent of Lrig1 antibody staining in the HFs. White arrowheads show the staining in the SG. Asterisks label the autofluorescent hair shaft. d = days, w = weeks and m = months. Bars = 50 µm.

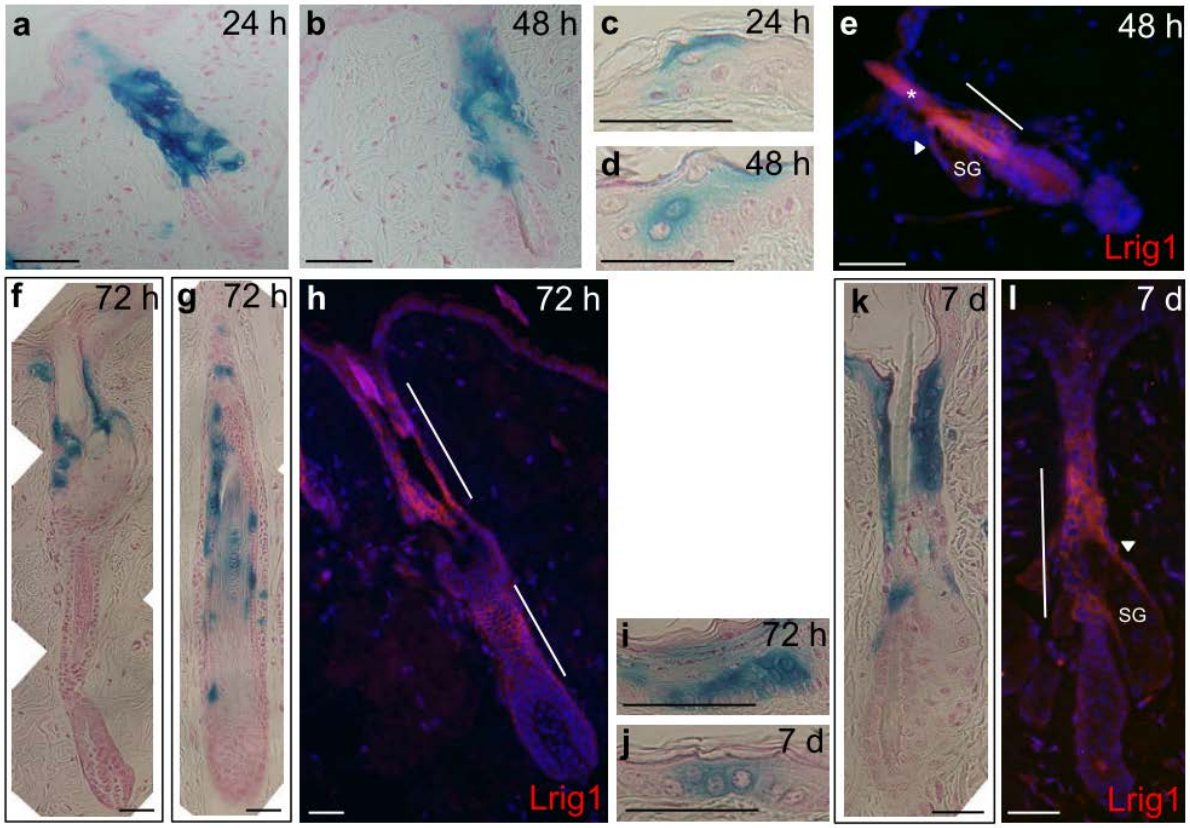

Figure 2.3. Lineage tracing on skin from adult *Lrig1-CreERT2*$^{+/-}$*/R26RLacZ*$^{+/-}$ mice during acute inflammation.

Mice were sacrificed at various timepoints after one topical treatment with 4OHT and a subsequent treatment with TPA. (**a**,**b**) HFs stained with X-Gal 24 h (**a**) and 48 h (**b**) after TPA treatment. (**c**,**d**) X-Gal labelling in the IFE 24 h (**c**) and 48 h (**d**) after TPA treatment. (**e**) Immunofluorescence staining on skin 48 h after TPA treatment using an antibody against Lrig1. (**f**,**g**) 2 examples of HFs stained with X-Gal 72 h after TPA treatment. (**h**) Immunofluorescence staining on skin 72 h after TPA treatment using an antibody against Lrig1. (**i**,**j**) Representative X-Gal labelling in the IFE 72 h (**i**) and 7 days (**j**) after TPA treatment. (**k**) Example of HF stained with X-Gal 7 days after 4OHT treatment. (**l**) Immunofluorescence staining on skin 7 days after TPA treatment using an antibody against Lrig1. White lines show the extent of Lrig1

antibody staining in the HFs. White arrowheads show the staining in the SG. Asterisks label the autofluorescent hair shaft. h = hours, d = days. Bars = 50 µm.

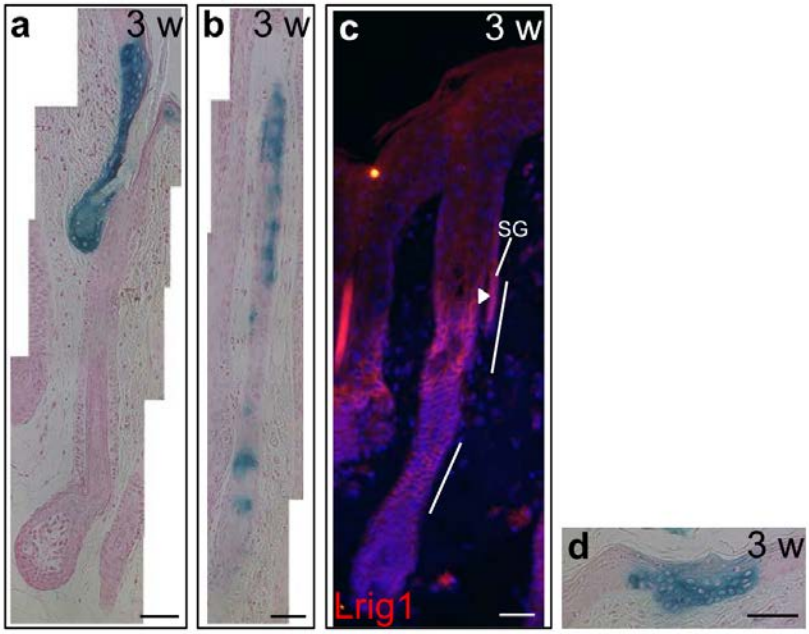

Figure 2.4. Lineage tracing on skin from adult *Lrig1-CreERT2$^{+/-}$/R26RLacZ$^{+/-}$* mice during chronic inflammation.

Mice were sacrificed at various timepoints after one topical treatment with 4OHT and subsequent biweekly treatments with TPA for 3 weeks. (**a**,**b**) Examples of HFs stained with X-Gal after 3 weeks of TPA treatment. (**c**) Immunofluorescence staining on a HF after 3 weeks of TPA treatment using an antibody against Lrig1. (**d**) X-Gal labelling in the IFE after 3 weeks of TPA treatment. White lines show the extent of Lrig1 antibody staining in the HFs. White arrowheads show the staining in the SG. w = weeks. Bars = 50 µm.

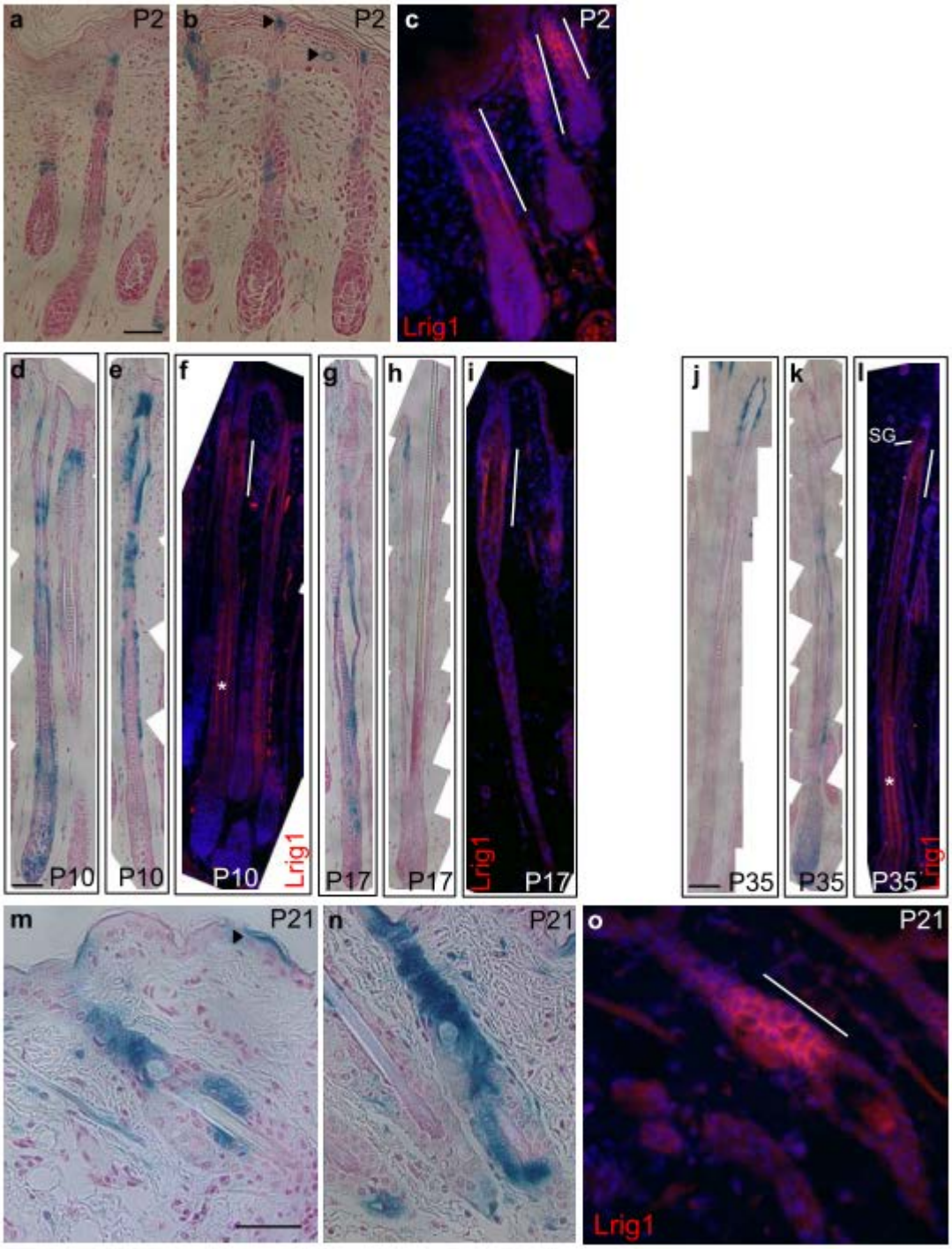

Figure 2.5. Lineage tracing on skin from *Lrig1-CreERT2*$^{+/-}$*/R26RLacZ*$^{+/-}$ mouse pups during skin morphogenesis.

Newborn mice received 1 topical treatment of 4OHT and were sacrificed at various timepoints after induction. (**a**,**b**) Mouse skin stained with X-Gal 2 days after 4OHT treatment (P2) (**c**) Immunofluorescence staining on skin 2 days after 4OHT treatment

using an antibody against Lrig1 (P2). (**d**,**e**) HFs stained with X-Gal 10 days after 4OHT treatment (P10) (**f**) Immunofluorescence staining on skin 10 days after 4OHT treatment using an antibody against Lrig1. (**g**,**h**) HFs stained with X-Gal 17 days after 4OHT treatment (P17) (**i**) Immunofluorescence staining on skin 17 days after 4OHT treatment using an antibody against Lrig1. (**j**,**k**) HFs stained with X-Gal 35 days after 4OHT treatment (P35) (**l**) Immunofluorescence staining on skin 35 days after 4OHT treatment using an antibody against Lrig1. (**m**,**n**) HFs stained with X-Gal 21 days after 4OHT treatment (P21). (**o**) Immunofluorescence staining on skin 21 days after 4OHT treatment using an antibody against Lrig1. White lines show the extent of Lrig1 antibody staining in the HFs. Black arrowheads mark X-Gal staining in the IFE. Asterisks label the autofluorescent hair shaft. P = postnatal day. Bars = 50 µm.

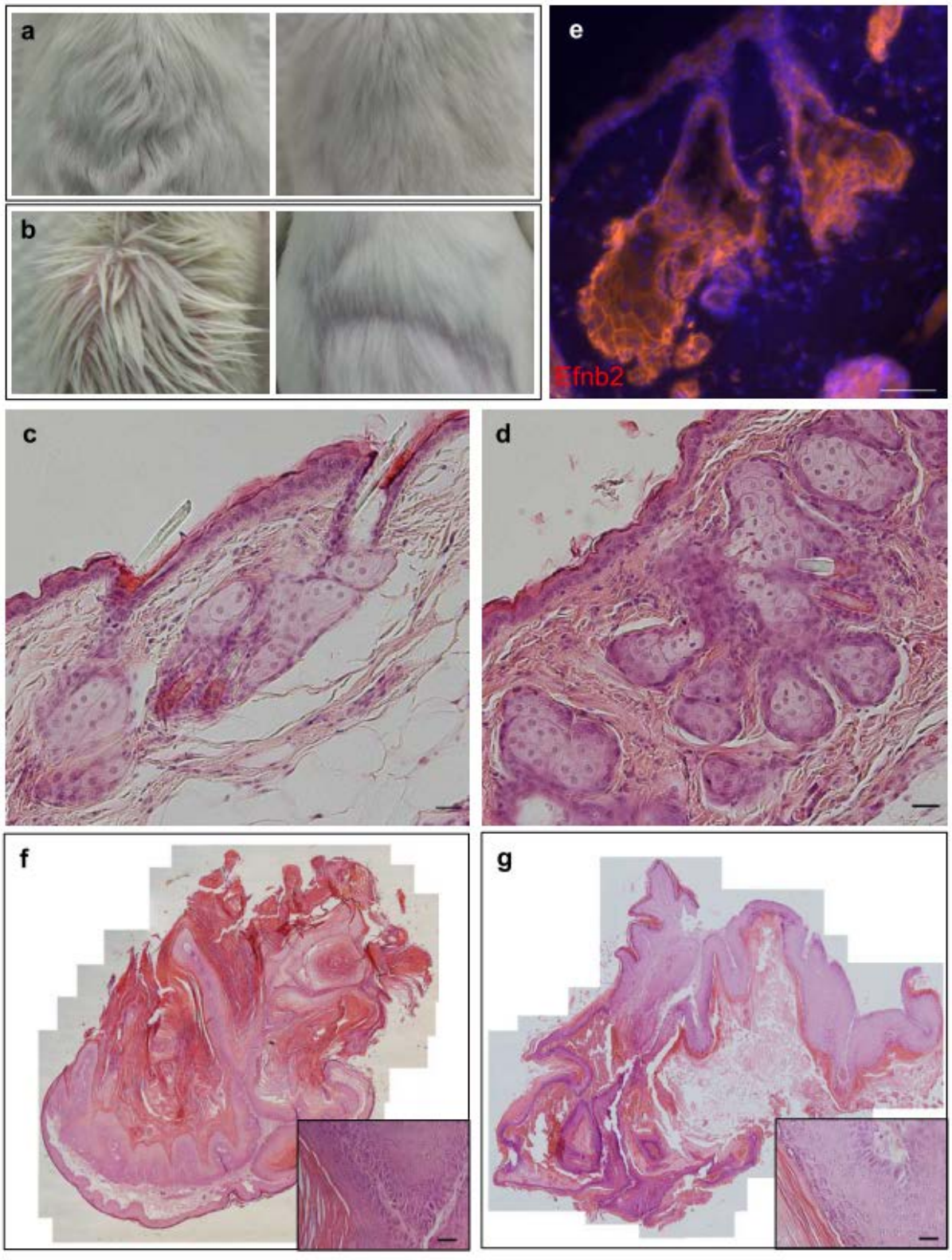
a
b
e
Efnb2
c
d
f
g

Figure 2.6. Expression of mutant *Hras* or *Kras* in Lrig1^{+} cells gives rise to distinct phenotypes, but both are capable of inducing papilloma formation in a wound-dependent manner.

(**a**) 4OHT-treated *Lrig1-CreERT2*$^{+/-}$/*Hras*$^{LSL-G12V/+}$ mouse (left) exhibiting a wavy hair phenotype. Non 4OHT-treated *Lrig1-CreERT2*$^{+/-}$/*Hras*$^{LSL-G12V/+}$ mouse (right) has normal hair. (**b**) 4OHT-treated *Lrig1-CreERT2*$^{+/-}$/*Kras*$^{LSL-G12D/+}$ mouse (left) showing an oily skin phenotype, with hair naturally slicked together into spikes. Non 4OHT-treated *Lrig1-CreERT2*$^{+/-}$/*Kras*$^{LSL-G12D/+}$ mouse (right) has normal skin. The 4OHT-treated *Lrig1-CreERT2*$^{+/-}$/*Kras*$^{LSL-G12D/+}$ mice are slightly smaller due to development of oral papillomas (not shown) that impeded feeding. (**c**) H&E stained back skin section showing SG hyperplasia of *Lrig1-CreERT2*$^{+/-}$/*Hras*$^{LSL-G12V/+}$ mice after 4OHT treatment. (**d**) H&E stained back skin section showing massive SG hyperplasia of *Lrig1-CreERT2*$^{+/-}$/*Kras*$^{LSL-G12D/+}$ mice after 4OHT treatment. (**e**) Representative image showing immunofluorescence staining using an antibody against Efnb2 in the back skin of *Lrig1-CreERT2*$^{+/-}$/*Kras*$^{LSL-G12D/+}$ mice after 4OHT treatment. (**f**) H&E staining of a papilloma that developed in *Lrig1-CreERT2*$^{+/-}$/*Hras*$^{LSL-G12V/+}$ mice after 4OHT treatment and wounding. Inset shows high power view of a section of the papilloma with epithelial morphology. (**g**) H&E staining of a papilloma that developed in *Lrig1-CreERT2*$^{+/-}$/*Kras*$^{LSL-G12D/+}$ mice after 4OHT treatment and wounding. Inset shows high power view of a section of the papilloma with epithelial morphology. Bars = 50 µm.

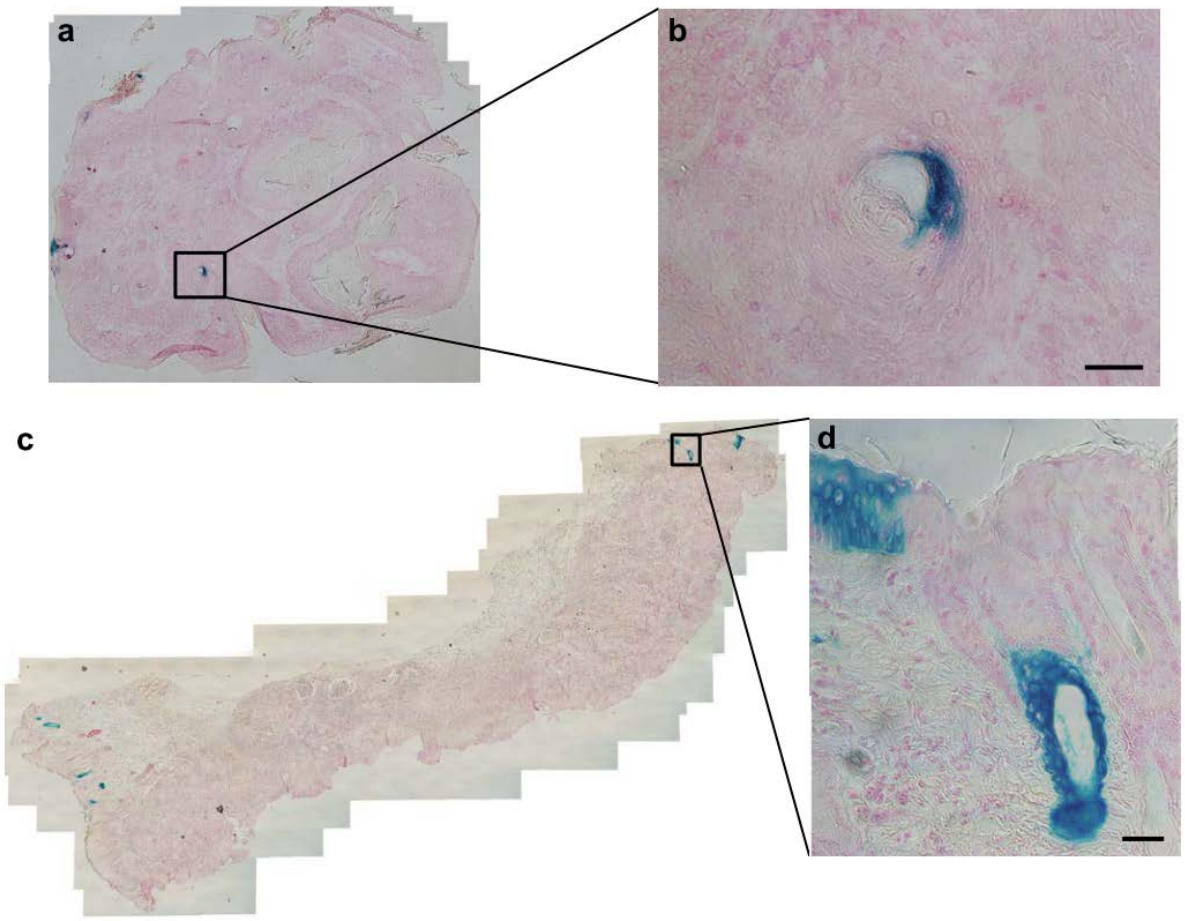

Figure 2.7. Lrig1^{+} cells are not common targets for *Hras* activation by chemical carcinogen treatment.

Lrig1-CreERT2$^{+/-}$*/R26RLacZ*$^{+/-}$ mice were treated topically with 4OHT prior to initiating the standard DMBA-TPA protocol, and sacrificed when their first carcinoma reached a size of 1.0-1.5 cm in diameter. (**a**) Representative lineage tracing in a papilloma harvested from these mice. (**b**) High power view of blue X-Gal labelling in a HF embedded in the papilloma in (**a**). (**c**) Representative lineage tracing in a carcinoma harvested from these mice. (**d**) High power view of blue X-Gal labelling in epidermis and HF of skin attached to the carcinoma in (**c**). Bars = 50 μm.

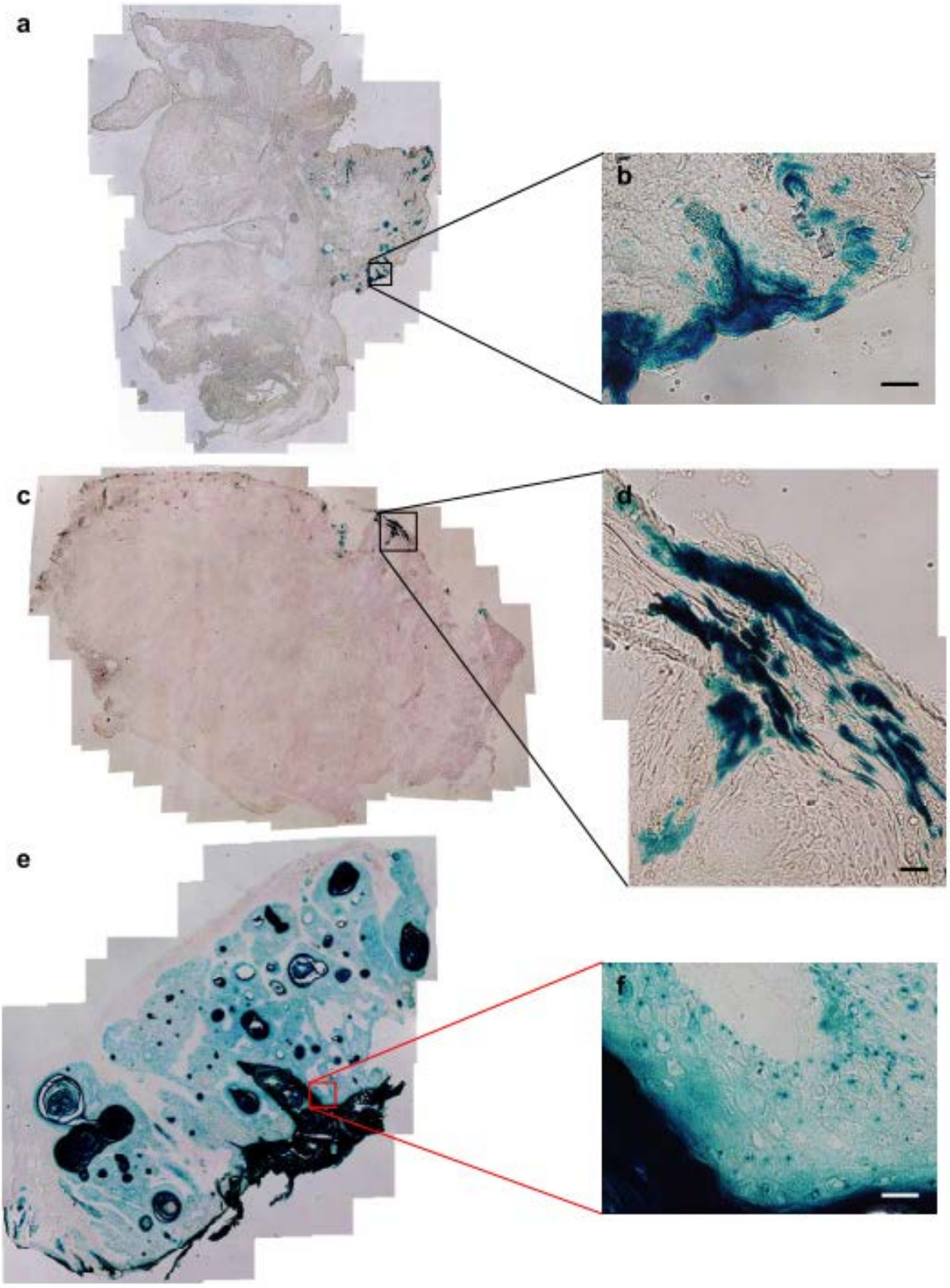
a
b
c
d
e
f

Figure 2.8. Lrig1^{+} cells do not act as CSCs in squamous tumours.

Lrig1-CreERT2$^{+/-}$/R26RLacZ$^{+/-}$ or *K14-CreERT2$^{+/-}$/R26RLacZ$^{+/-}$* mice were first treated with the DMBA-TPA protocol. After tumours have arisen, the mice were treated with 4OHT to initiate lineage tracing in the tumours and subsequently sacrificed at specific timepoints. (**a**) Representative lineage tracing in a papilloma from an *Lrig1-CreERT2$^{+/-}$/R26RLacZ$^{+/-}$* mouse harvested 4 weeks after 4OHT induction. (**b**) High power view of blue X-Gal labelling in HFs and epidermis attached to the papilloma in (**a**). (**c**) Representative lineage tracing in a carcinoma from an *Lrig1-CreERT2$^{+/-}$/R26RLacZ$^{+/-}$* mouse harvested 4 weeks after 4OHT induction (**d**) High power view of blue X-Gal labelling in epidermis and HF of skin attached to the carcinoma in (**c**). (**e**) Representative lineage tracing in a carcinoma from a *K14-CreERT2$^{+/-}$/R26RLacZ$^{+/-}$* mouse harvested 11 weeks after 4OHT induction. (**f**) High power view of blue X-Gal labelling in epithelial cells within the carcinoma in (**e**). Bars = 50 μm.

Supplementary Figures and Tables

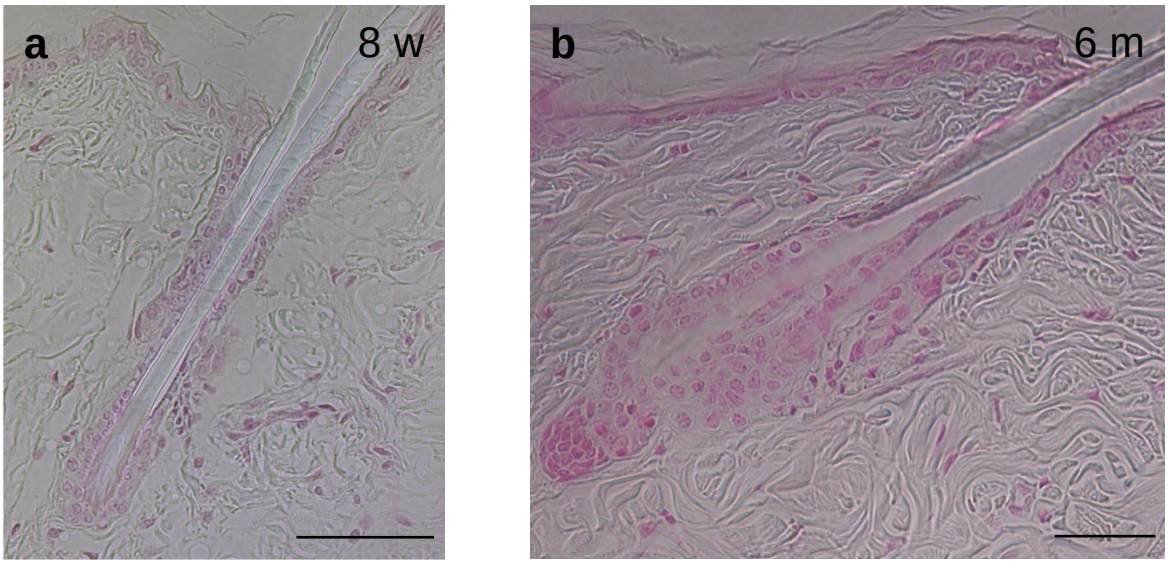

Supplementary Figure 2.1. Non-leakiness of Lrig1 promoter construct.

Lrig1-CreERT2$^{+/-}$R26RLacZ$^{+/-}$ mice that were never treated with 4OHT were sacrificed at different ages. (**a**,**b**) Representative images showing X-Gal staining of skin at (**a**) 8 weeks or (**b**) 6 months of age. w = weeks and m = months. Bars = 50 µm.

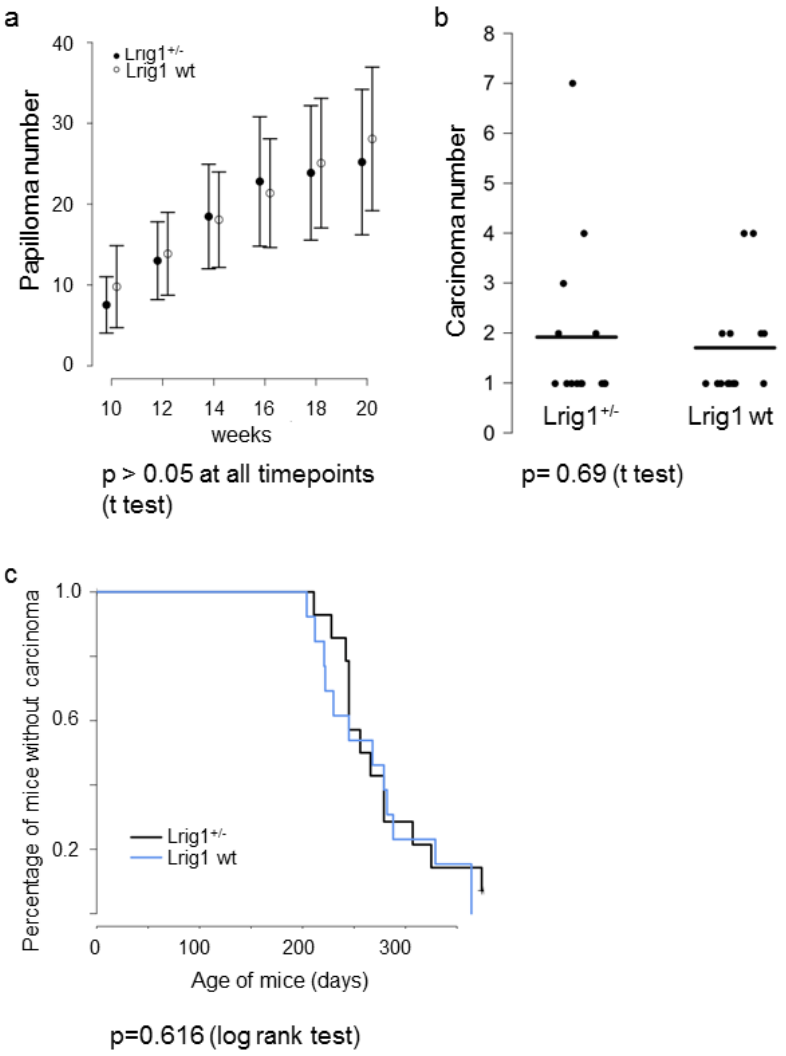

Supplementary Figure 2.2. Loss of one Lrig1 allele does not affect skin tumour number or latency in mice.

(**a**) Graph comparing papilloma numbers of Lrig1-CreERT2$^{+/-}$R26RLacZ$^{+/-}$ and Lrig1-WT mice after 10, 12, 14, 16 and 20 weeks of TPA treatment; p > 0.05 at all timepoints (t test). Data are presented as mean ± s.d. (**b**) Graph comparing the number of carcinomas per mouse developed by Lrig1-CreERT2$^{+/-}$R26RLacZ$^{+/-}$ and Lrig1-WT after a standard DMBA-TPA protocol; p= 0.69 (t test). (**c**) Kaplan-Meier survival curve showing carcinoma incidence of Lrig1-CreERT2$^{+/-}$R26RLacZ$^{+/-}$ mice

(black line) and Lrig1-WT mice (blue line) treated with TPA for 20 weeks; p=0.616 (log rank test).

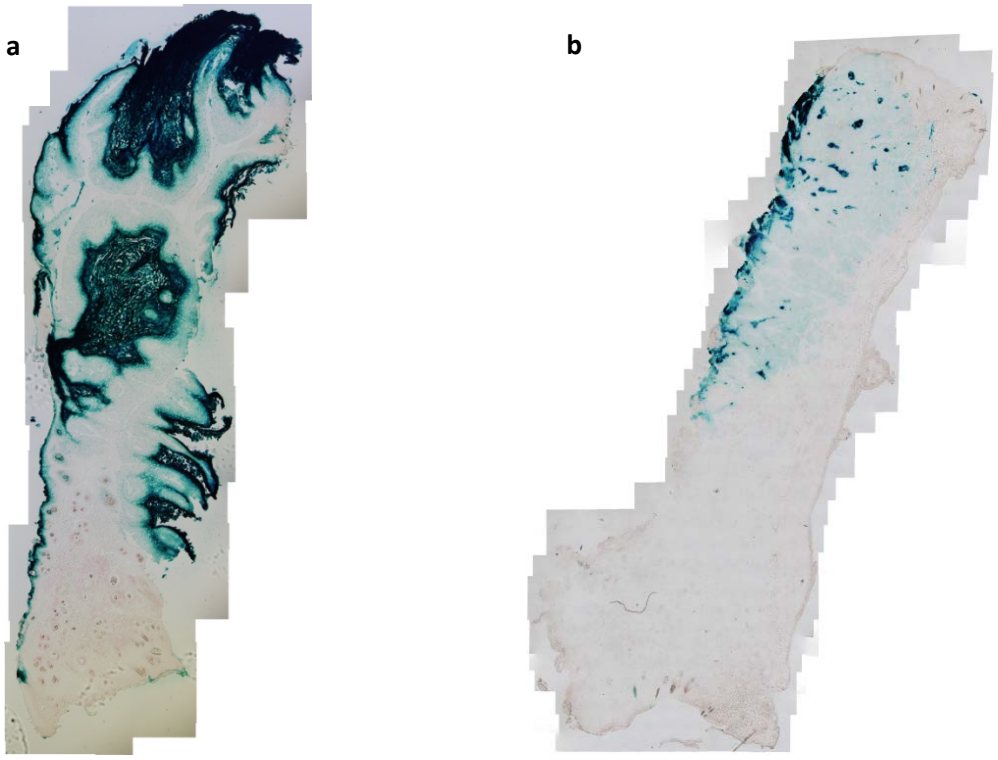

Supplementary Figure 2.3. Rare blue tumours that arose in Lrig1-CreERT2$^{+/-}$ R26RLacZ$^{+/-}$ mice treated with 4OHT prior to the DMBA-TPA protocol.

(**a**) A papilloma that consisted of more than 50% blue cells. (**b**) An SCC that had moderate amounts of blue cells.

Supplementary Table 2.1. Genes most highly correlated with *Lrig1* at the expression level in the microarray dataset published in Quigley *et al.* 2009.

Gene symbol	Affymetrix Probeset	Rho	P value	Corrected P value
Lrig1	*1434210_s_at*	0.87	4.83E-23	8.57E-19
Efnb2	*1419638_at*	0.77	5.01E-15	8.91E-11
Dcbld1	*1418966_a_at*	0.69	2.31E-11	4.10E-07
Gpr125	*1426782_at*	0.69	2.45E-11	4.34E-07
Sertad4	*1454877_at*	0.68	6.43E-11	1.14E-06
Atrn	*1434197_at*	0.68	6.81E-11	1.21E-06
Irx4	*1419539_at*	0.68	9.88E-11	1.75E-06
1190002N15Rik	*1433581_at*	0.67	1.26E-10	2.24E-06
Eya2	*1424127_at*	0.67	1.81E-10	3.21E-06
BB146404	*1424680_at*	0.67	1.99E-10	3.54E-06
Alcam	*1426300_at*	0.67	2.47E-10	4.39E-06
Ptprk	*1423277_at*	0.67	2.53E-10	4.49E-06
Lhx2	*1418317_at*	0.66	3.71E-10	6.59E-06
Sostdc1	*1449340_at*	0.66	4.86E-10	8.62E-06
Sc4mol	*1423078_a_at*	0.65	9.38E-10	1.67E-05
Hoxd11	*1450584_at*	0.65	9.92E-10	1.76E-05
Mgll	*1453836_a_at*	0.65	1.00E-09	1.78E-05
AI646023	*1456878_at*	0.65	1.03E-09	1.82E-05
Cyb5b	*1417767_at*	0.65	1.29E-09	2.29E-05
Tmem46	*1423852_at*	0.64	1.41E-09	2.50E-05
Lass4	*1417781_at*	0.64	1.44E-09	2.56E-05
Gli2	*1459211_at*	0.64	1.64E-09	2.90E-05
Tgoln2	*1423307_s_at*	0.64	2.27E-09	4.02E-05
Rdh11	*1449209_a_at*	0.64	2.28E-09	4.05E-05
Tgoln1	*1418520_at*	0.63	3.69E-09	6.55E-05
Acly	*1425326_at*	0.63	4.41E-09	7.81E-05
Fzd7	*1450044_at*	0.63	4.65E-09	8.25E-05
Gli3	*1455154_at*	0.63	4.76E-09	8.43E-05
Pdzrn3	*1416846_a_at*	0.63	4.91E-09	8.71E-05
Reep5	*1426376_at*	0.62	6.07E-09	1.08E-04
Dsg2	*1425619_s_at*	0.62	6.23E-09	1.11E-04
Dnaja1	*1416288_at*	0.62	6.60E-09	1.17E-04
Arhgap24	1424842_a_at	0.62	6.67E-09	1.18E-04
Rab3ip	1434306_at	0.62	8.90E-09	1.58E-04
Mtus1	1436501_at	0.62	9.29E-09	1.65E-04
2210010C17Rik	1438074_at	-0.62	1.03E-08	1.83E-04
Acaa1a	1416946_a_at	0.62	1.04E-08	1.84E-04
Fhod3	1435551_at	0.62	1.19E-08	2.10E-04
Slc46a2	1423476_at	0.61	1.42E-08	2.51E-04
Dhrs7	1426440_at	0.61	1.55E-08	2.75E-04

Sostdc1	1460250_at	0.61	1.58E-08	2.81E-04
Tmc8	1458372_at	-0.61	1.63E-08	2.89E-04
Sytl2	1421594_a_at	0.61	1.72E-08	3.04E-04
Mod1	1430307_a_at	0.61	1.96E-08	3.48E-04
Apcdd1	1418383_at	0.61	2.00E-08	3.55E-04
Aco1	1423644_at	0.61	2.05E-08	3.64E-04
Fzd2	1418532_at	0.61	2.07E-08	3.66E-04
Krt79	1427352_at	0.61	2.22E-08	3.93E-04
Abhd13	1436516_at	0.61	2.24E-08	3.98E-04
Apoe	1432466_a_at	0.60	2.62E-08	4.64E-04
Hsd17b12	1450010_at	0.60	2.85E-08	5.05E-04
Tspan6	1448501_at	0.60	2.90E-08	5.13E-04
Lrp12	1433864_at	0.60	3.05E-08	5.41E-04
Ccnd2	1430127_a_at	0.60	3.10E-08	5.50E-04

Supplementary Table 2.2. Genes strongly correlated with Lrig1 at the expression level across 2 independent mouse tail skin datasets.

Gene symbol	Affymetrix Probeset	Rho	P value	Corrected P value
Lrig1	1434210_s_at	0.87	4.83E-23	8.57E-19
Efnb2	1419638_at	0.77	5.01E-15	8.91E-11
Ptprk	1423277_at	0.67	2.53E-10	4.49E-06
Fzd7	1450044_at	0.63	4.65E-09	8.25E-05
Dsg2	1425619_s_at	0.62	6.23E-09	1.11E-04
Krt79	1427352_at	0.61	2.22E-08	3.93E-04
Apoe	1432466_a_at	0.60	2.62E-08	4.64E-04

Chapter 3

Lgr6 Restrains Skin Stem Cells from Epidermal Fate Choice and Impedes Squamous Tumour Development

Abstract

Lgr6 has been reported to mark stem cells in the central isthmus of the hair follicle that preferentially give rise to the interfollicular epidermis and the sebaceous gland. By expression and in situ hybridisation analysis of a unique panel of skin cell lines, we demonstrate that Lgr6, and not Lgr5, is a cutaneous squamous cancer stem cell marker. *In vitro* knockdown of *Lgr6* in epidermal cell lines leads to increased growth, while *in vivo Lgr6* knockdown leads to heightened proliferation in the epidermis along with increased epidermal lineage differentiation from the $Lgr6^{+}$ stem cell compartment. Finally, Lgr6 deficiency leads to reduced latency to papilloma development during skin chemical carcinogenesis. We propose that Lgr6 positively regulates Wnt signalling in epidermal stem cells and serves to restrain skin stem cells from selecting the epidermal cell fate during normal homeostasis and tumour development.

Introduction

The mouse skin comprises several distinct cell compartments, each with its own resident stem cell population that acts to maintain it during normal tissue homeostasis. In particular, the hair follicle is home to several disparate stem cell populations. For instance, the Egfr negative regulator Lrig1 marks a progenitor population in the junctional zone that serves to maintain the follicle infundibulum (Jensen et al. 2009; Page et al. 2013; Veniaminova et al. 2013). Further down in the follicle bulge, quiescent stem cells, defined by markers such as CD34 (Trempus et al. 2003) and K15 (Morris et al. 2004), may act as a reserve stem cell pool that becomes activated in response to stress situations such as wounding (Ito et al. 2005).

The G protein-coupled receptors Lgr4-6 are expressed in stem cells in a wide variety of tissues, including the small intestine and colon (Barker et al. 2007), stomach (Barker et al. 2010), kidney (Barker et al. 2012), breast (Plaks et al. 2013) and ovary (Flesken-Nikitin et al. 2013; Ng et al. 2014). Interestingly, in the skin, Lgr4-6 are expressed in distinct cell populations in the follicle. Lgr5 marks stem cells in the telogen bulge and hair germ that actively cycle to give rise to new follicles (Jaks et al. 2008). Lgr6, on the other hand, marks stem cells just above the bulge that have been reported to preferentially give rise to cells of the interfollicular epidermis (IFE) and the sebaceous gland (SG) (Snippert et al. 2010). Finally, Lgr4 marks cells in the lower half of the follicle, which broadly overlaps the expression domains of both Lgr5 and Lgr6 (Snippert et al. 2010).

Lgr4-6 have been reported to bind the Wnt agonists R-spondins, and in this way act to enhance Wnt signalling (de Lau et al. 2011; Carmon et al. 2011; Gong et al. 2012; Glinka et al. 2011). However, several reports have also indicated a

negative role for Lgr5 in Wnt signalling, including in human colorectal cancers (Defossez et al. 2011; Wu et al. 2014). Thus, the exact role of Lgr4-6 in Wnt signalling appears to be a complex one, with possibly different consequences depending on the specific Lgr4-6 and Rspo1-4 family members that are expressed and interact in a given cellular context (Wu et al. 2014). In the skin, it remains unclear how Lgr4-6 may impinge upon Wnt and other signalling pathways, although Wnt signalling is known to be activated in the hair germ and follicle bulge during the transition from telogen to anagen, and is thought to be critical for the formation of new follicles (Van Mater et al. 2003; Lo Celso et al. 2004; Lowry et al. 2005; Greco et al. 2009).

In part because of their high capacity for self-renewal and clonogenic growth, cancer stem cells (CSCs) have often been hypothesised to arise from adult stem cells (Perez-Losada and Balmain 2003). In this connection, it is interesting to note that Lgr5 has also been reported as a CSC marker in intestinal adenoma (Schepers et al. 2012), although it remains unclear if Lgr4-6 may also define CSCs in malignancies that afflict the skin, such as cutaneous squamous cell carcinoma (SCC).

Here, by performing *Lgr4-6* expression and *in situ* hybridisation analyses in a panel of skin cell lines, we address the possible roles of Lgr5 and Lgr6 as cutaneous SCC CSC markers. Using both *in vitro* functional studies and novel *in vivo* mouse models, we examine the functions of Lgr6 in normal and cancer skin stem cells. Finally, we also determine the role of Lgr6 during skin chemical carcinogenesis.

Results

Lgr6, and not Lgr5, is an SCC cancer stem cell marker

Lgr5^{+} cells have been reported to be capable of acting as the cells-of-origin of intestinal and gastric adenoma (Barker et al. 2009, 2010; Zhu et al. 2009), cutaneous basal cell carcinoma (BCC) (Grachtchouk et al. 2011) and SCC (da Silva-Diz et al. 2012). However, the last result was obtained using a papillomavirus-induced SCC mouse model, the physiological relevance of which is unknown since human papillomaviruses are not a common cause of cutaneous SCCs and do not act through inducing known driver mutations in major oncogenes (such as *HRAS*) or tumour suppressors (such as *TP53*). Moreover, the fact that Lgr5^{+} cells are capable of giving rise to SCC is not synonymous with Lgr5 expression being maintained in SCC CSCs, which are the cells within the tumour that self-renew and proliferate to fuel the growth of the tumour (Driessens et al. 2012). Hence, while Lgr5 has been reported as a cancer stem cell marker in intestinal adenoma (Barker et al. 2009; Schepers et al. 2012), it remains unclear whether Lgr5/6 may mark CSCs in other tissues.

Epithelial cancer cell lines can faithfully recapitulate the genomic, transcriptional and biological features of the primary tumours from which they derive (Neve et al. 2006); in particular, the CSC/progeny hierarchy of primary tumours can be preserved in cell lines, which have been documented to contain functional CSCs (Charafe-Jauffret et al. 2009). Indeed, Lgr5 has been shown to mark a CSC subpopulation in several colorectal cancer cell lines (Hirsch et al. 2014; Rao et al. 2013; Rowehl et al. 2014). To address the question of whether Lgr5/6 may mark CSCs in cutaneous SCC, we first examined the expression of *Lgr4-6* in a unique

panel of mouse immortalised keratinocyte and SCC cell lines that are generated in our laboratory (Oft et al. 2002). These cell lines represent various stages of chemically induced tumours, including benign tumours (papillomas), malignant SCCs and aggressive spindle carcinomas that express an EMT, stem cell-like signature (Wong et al. 2013). Remarkably, *Lgr5* is not expressed in any of these cell lines (Fig. 3.1a), while *Lgr4* and *Lgr6* are expressed at varying levels. Generally, *Lgr4* is more highly expressed in immortalised keratinocyte cell lines (C5N and NK) and exhibit lower expression levels in the SCC cell lines, whereas *Lgr6* shows the opposite expression trend, with higher expression in the SCC cell lines and lower expression in the keratinocyte cell lines.

To verify and visualise the *Lgr4-6* expression pattern in the cell lines, we performed *Lgr4-6* multiplex *in situ* hybridisation. As positive control for the *Lgr5* probe, we also included a BCC cell line (Asz001) in the analysis, since Lgr5 has been reported to be expressed in BCCs and to enhance the tumourigenicity of BCC cells (Tanese et al. 2008). Reassuringly, we could detect expression of *Lgr5* in BCC cells. Strikingly, while *Lgr4* is broadly expressed, *Lgr5* and *Lgr6* exhibit a highly restricted expression pattern – they are co-expressed in rare single cells that are relatively large in size (Fig. 3.1b and insets). This observation raises the intriguing possibility that the Lgr5- and Lgr6-double positive cells are BCC CSCs, although further work will be needed to test this hypothesis.

In contrast to the BCC cell line, SCC and keratinocyte cell lines do not show any detectable *Lgr5* expression through *in situ* hybridisation analysis (Fig. 3.2a,b and Supplementary Fig. 3.1). This agrees with our expression data above and thus suggests that Lgr5 is not an SCC CSC marker. *Lgr4* and *Lgr6*, on the other hand, are expressed in the SCC and keratinocyte cell lines in a pattern that is consistent

with our prior observations, with higher *Lgr4* / lower *Lgr6* expression in the keratinocyte cell lines and lower *Lgr4* / higher *Lgr6* expression in the SCC cell lines (Fig 3.2a,b and Supplementary Fig. 3.1).

Notably, in some cell lines, such as C5N, *Lgr6* is not uniformly expressed across all cells but is instead expressed at high levels in small numbers of cells. We entertained the possibility that these cells represent a stem cell subpopulation. To test this, we utilised the Aldefluor assay, which has been widely used to isolate normal and cancer stem cell fractions both *in vitro* and *in vivo* (Cheung et al. 2007; Corti et al. 2006; Ginestier et al. 2007; Charafe-Jauffret et al. 2009). We purified Aldefluor^{+} and Aldefluor^{-} subpopulations from C5N and performed expression analysis on these. Strikingly, *Lgr6* expression is highly elevated in the Aldefluor^{+} fraction compared to the Lgr6^{-} fraction (Fig. 3.2c); as expected, *Lgr5* is not expressed in either the Aldefluor^{-} or Aldefluor^{+} fraction. Coupled with our *in situ* hybridisation data, this observation indicates that the small numbers of cells with high levels of *Lgr6* expression in C5N represents a stem cell subpopulation. We conclude that Lgr6, and not Lgr5, acts as an SCC CSC marker.

Lgr6 suppresses epidermal cell growth

To determine the cellular functions of Lgr6 in normal and SCC CSCs, we first generated a panel of keratinocyte and SCC cell lines in which Lgr6 overexpression can be induced through doxycycline administration. Strikingly, Lgr6 overexpression consistently led to reduced growth in C5N (Fig. 3.3a). To further validate the effects of Lgr6 on cellular growth, we generated an additional set of cell lines in which the expression of Lgr6 can be inducibly donwregulated through doxycycline

administration. Consistent with a growth suppressive role for Lgr6 in epidermal cell lines, Lgr6 knockdown in an SCC cell line (E4) leads to increased growth (Figure 3.3b).

To test the *in vivo* growth effects of Lgr6, we generated *Lgr6 KD* mice, in which Lgr6 expression can be inducibly and efficiently knocked down through doxycycline treatment (Fig. 3.4a). When adult *Lgr6 KD* mice were kept on doxycycline water for 10 days, we observed an approximately 75% reduction in *Lgr6* expression levels in the back skin (Fig. 3.4b). BrDU analysis in the back skins of these animals indicates an increase in proliferation in the epidermis (Fig. 3.4c). We conclude that Lgr6 suppresses epidermal cell growth both *in vitro* and *in vivo*.

Lgr6 restrains skin stem cells from selecting the epidermal cell fate

$Lgr6^{+}$ stem cells have been reported to be capable of generating all skin lineages, although they preferentially contribute to the epidermal and sebaceous gland lineages over the hair follicle lineage (Snippert et al. 2010).

To investigate the effects of Lgr6 deficiency on the lineage potential of $Lgr6^{+}$ stem cells, we generated *Lgr6 KD*$^{+/-}$*/Lgr6-EGFP-IRES-CreERT2*$^{+/-}$*/R26RLacZ*$^{+/-}$ triple transgenic mice. We first administered doxycycline water to 8-week-old triple transgenic animals to achieve *Lgr6* knockdown. As control, we administered vehicle to a separate group of triple transgenic mice. After 10 days, we activated Cre recombinase in these mice with topical 4OHT treatment and collected skin samples 7 days thereafter for X-Gal analysis. Interestingly, we observed a striking increase in Lgr6 epidermal lineage tracing in doxycycline-treated mice compared to vehicle-

treated mice (Fig. 3.5). We also saw some evidence for Lgr6 lineage tracing in the dermis, particularly in the doxycycline-treated animals, which has not been previously reported. The increased epidermal lineage tracing is consistent with the increased proliferation that we saw in the epidermis upon Lgr6 downregulation (Fig. 3.4c). Together, these observations suggest that during normal homeostasis, Lgr6 negatively regulates epidermal lineage differentiation from the $Lgr6^{+}$ stem cell compartment.

Lgr6 impedes papilloma development

Activating Wnt mutations have been reported in a wide range of solid tumours (Clevers and Nusse 2012). Given the documented role of Lgr4-6 in enhancing Wnt signalling, they have often been hypothesised to play a positive oncogenic role (Leushacke and Barker 2012). Indeed, Lgr5 has been reported to be overexpressed in a number of human cancers, including hepatocellular (Yamamoto et al. 2003), colon and ovarian cancers (McClanahan et al. 2006), and has also been demonstrated to promote the proliferation of BCC cells and enhance BCC tumourigenicity *in vivo* (Tanese et al. 2008). Paradoxically, however, Lgr5 has also been shown to reduce the invasion and tumourigenicity of colorectal cancer cells (Defossez et al. 2011; Wu et al. 2014); additionally, tumour suppressive roles have been suggested for Lgr4 (Styrkarsdottir et al. 2013) and Lgr6 (Gong et al. 2012).

Given our results that Lgr6 suppresses the growth of SCC cells, we hypothesised that Lgr6 may play a tumour suppressive function in squamous tumour development. To test this, we subjected *Lgr6 KO* and *WT* mice to the DMBA/TPA chemical carcinogenesis protocol and sacrificed the animals when their first

carcinomas reached 1-1.5 cm in diameter. Here, we observed a decrease in latency to papilloma development in the *Lgr6*$^{-/-}$ mice, which have approximately twice as many papillomas as *Lgr6*$^{+/+}$ mice at 12 weeks post-DMBA treatment (Fig. 3.6a). Interestingly, this effect appears to be haploinsufficient, as *Lgr6*$^{+/-}$ mice also have about twice as many papillomas as *Lgr6*$^{+/+}$ mice at the same timepoint (Fig. 3.6a). However, the papilloma yield of *Lgr6 WT* mice eventually catches up with that of *Lgr6 KO* mice (Fig. 3.6b), and progression to malignancy does not appear to be significantly affected by Lgr6 deficiency as overall survival is similar for the different groups of mice (Supplementary Fig. 3.2). Hence, we conclude that Lgr6 has a haploinsufficient, tumour inhibitory effect during the early stages of SCC development, impinging upon the latency to papilloma development without affecting overall papilloma yield or progression to malignancy.

Discussion

Lgr4-6 are expressed in distinct cell populations in the mouse hair follicle. Of these, Lgr5 and Lgr6 have been reported to mark *bona fide* stem cells, with the former defining a population that maintains all hair follicle lineages (Jaks et al. 2008) and the latter expressed in multipotent stem cells that preferentially give rise to the IFE and the SG (Snippert et al. 2010).

Given the ability of $Lgr5^+$ crypt base columnar stem cells to give rise to intestinal adenomas that maintain an $Lgr5^+$ CSC/progeny hierarchy (Barker et al. 2009; Zhu et al. 2009; Schepers et al. 2012), it is tempting to speculate that a similar phenomenon may occur in other tissues in which Lgr5/6 also define stem cell populations, such as in the skin. To partly address this question, White *et al.* generated *Lgr5-CreERT2;KrasG12D;Pten*$^{f/f}$ and *Lgr6-CreERT2;KrasG12D;Pten*$^{f/f}$ mice, to allow for simultaneous activation of oncogenic *Kras* and deletion of *Pten* in either $Lgr5^+$ or $Lgr6^+$ cells upon tamoxifen treatment (White et al. 2013). Using hyperplasia as a readout for nascent tumourigenesis, the authors reported that $Lgr6^+$ cells, but not $Lgr5^+$ cells, are capable of initiating tumours in this context.

In our laboratory, we have also crossed the *Lgr5-CreERT2* and *Lgr6-CreERT2* mouse strains separately to *KrasG12D* mice. Interestingly, we saw that in the context of a wound stimulus, both Cre drivers are capable of giving rise to papillomas (data not shown), reminiscent of the results obtained when *Lrig1-CreERT2* mice are crossed to *KrasG12D* mice (Page et al. 2013; our unpublished data). Indeed, a number of other cell populations in the skin have been reported to be capable of giving rise to tumours driven by activated *Ras*, including those expressing Krt5 (Brown et al. 1998; Caulin et al. 2007), Krt10 (Bailleul et al.

1990), Krt1 (Greenhalgh et al. 1993), Krt14, Krt15, Krt19 (Lapouge et al. 2011; White et al. 2011) and Msx2 (Mukhopadhyay et al. 2011). Direct comparison of these studies is complicated by the fact that the earlier transgenic mouse models used these promoters to directly drive massive overexpression of mutant *Ras*, whereas later knockin mouse models used Cre-Lox technology to inducibly activate an endogenous *Ras* oncogene. An additional caveat to these mouse models is that they involve the simultaneous activation of oncogenic *Ras* in multiple cells within the targeted cell population, which is vastly different from the clonal activation of mutant *Ras* in single cells that presumably occurs during the initiation phase of skin chemical carcinogenesis. Single transformed cells may have to outcompete (Bondar and Medzhitov 2010; Vermeulen et al. 2013), or could be growth-inhibited by (Stoker et al. 1966; Bissell and Hines 2011), neighbouring cells, and these phenomena are rendered irrelevant in the case of synchronous oncogene activation in multiple cells. Moreover, the fact that a particular stem cell population is capable of giving rise to tumours is not synonymous with that stem cell/progeny hierarchy being maintained in tumours.

Here, we have employed an alternative strategy to demonstrate that Lgr6, and not Lgr5, marks CSCs in cutaneous SCC. Cancer cell lines have been reported to possess functional cancer stem cell subpopulations (Charafe-Jauffret et al. 2009; Hirsch et al. 2014). We performed expression and *in situ* hybridisation analyses of *Lgr4-6* in a unique panel of immortalised keratinocyte and SCC cell lines generated in our laboratory (Oft et al. 2002), which represent various stages of chemically induced skin tumours. Strikingly, *Lgr5* is not expressed in any of the SCC cell lines, but in contrast is expressed in rare single BCC cells; *Lgr6*, on the other hand, is expressed at varying levels in these keratinocyte and SCC cell lines, where it is

sometimes elevated in expression in subpopulations that are enriched for Aldefluor (stem cell) activity.

Using *in vitro* functional studies and novel *in vivo* mouse models, we address the role of Lgr6 in normal and cancer skin stem cells. We demonstrate that Lgr6 negatively regulates the proliferation of epidermal cells and restrains $Lgr6^+$ stem cells from selecting the epidermal cell fate. Such a role for a gene that is specifically expressed in a stem cell population is not unprecedented. For instance, NFATc1/CDK4 signalling is known to regulate the proliferation of bulge stem cells, with loss of NFATc1 activity causing premature stem cell activation and aberrant follicle growth (Horsley et al. 2008). In addition, LRIG1 has been reported to negatively regulate keratinocyte proliferation and differentiation from epidermal stem cells, in part through influencing EGFR signalling and MYC levels (Jensen and Watt 2006). Furthermore, Notch signalling has been shown to suppress the epidermal fate choice in several stem cell populations, including the $K15^+$ bulge stem cells (Demehri and Kopan 2009) and the $Lrig1^+$ junctional zone stem cells (Veniaminova et al. 2013). It remains unclear if Lgr6 may functionally interact with some of these signalling pathways, but the phenotypes we observed with *Lgr6 in vivo* knockdown and *Lgr6* heterozygosity in the DMBA/TPA chemical carcinogenesis model suggest that Lgr6 function in the skin is highly sensitive to gene dosage levels. These observations therefore indicate that caution should be exercised in the interpretation of lineage tracing experiments performed with the knockin *Lgr6-CreERT2* mouse model, which only possesses a single functional copy of the *Lgr6* gene and thus may not fully recapitulate the true behaviour of non-perturbed $Lgr6^+$ stem cells.

Consistent with a negative role for Lgr6 in regulating epidermal lineage differentiation and proliferation, we also found that Lgr6 deficiency leads to a

reduction in latency to papilloma development in the DMBA/TPA chemical carcinogenesis model. We believe the model that best explains our results is shown in Figure 3.7a. $Lgr6^+$ stem cells are capable of giving rise to cells of both the IFE and the hair follicle. In this stem cell compartment, Lgr6 functions as a brake towards epidermal fate choice, so that loss of Lgr6 leads to increased epidermal lineage differentiation and proliferation, ultimately lowering the barrier towards SCC development. In line with this model, we observed that Lgr6 overexpression in a range of SCC cell lines leads to an increase in Wnt signalling (Fig. 3.7b); and since Wnt signalling is known to be required for the formation of new follicles (Gat et al. 1998; Van Mater et al. 2003; Lo Celso et al. 2004; Lowry et al. 2005), this result could indicate a positive role for Lgr6 in specifying hair follicle lineage commitment from skin stem cells. Furthermore, in humans, loss of function mutations in *LGR4* (Styrkarsdottir et al. 2013) and its interacting partner *RSPO1* (Parma et al. 2006) have been shown to predispose individuals towards cutaneous SCC development, which again suggests an inhibitory role for Lgr4-6/R-spondins (and Wnt signalling) towards epidermal lineage differentiation and SCC development. An intriguing question raised by our results is why *Lgr6*-deficient mice do not show a greater susceptibility to development of malignant tumours. One possible explanation is that there is some redundancy among the Lgr4-6 family members, so that the concerted ablation of both Lgr6 and Lgr4 in the skin is necessary for a stronger phenotype to arise. Clearly, further mouse models will have to be developed to address this question definitively, but our results are nevertheless consistent with the notion that Lgr6 positively regulates Wnt signalling in the skin, thus restraining multipotent stem cells from commitment towards the epidermal lineage and in this way providing an impediment towards the development of SCC.

Materials and Methods

Mouse treatments, chemical carcinogenesis and lineage tracing in skin

Doxycycline water was prepared by dissolving 2 g of doxycycyline (RPI) in 1 l of water containing 50 g of sucrose (Affymetrix). For BrDU studies, mice were injected intraperitoneally with BrDU labelling reagent (Life Technologies) at a concentration of 10 uL/g of body weight and sacrificed 3 hours post-injection. For chemical carcinogenesis experiments, 8- to 12-week-old mice received one dose of DMBA (25 mg per mouse in acetone) applied to back skin. One week later, the mice were administered biweekly topical treatments of TPA (200 mL of a 10^{-4} M solution in acetone) for 20 weeks. The animals were then monitored for tumour development and were sacrificed when their first carcinoma reached 1-1.5 cm in diameter. For lineage tracing experiments, 8- to 10-week-old *Lgr6 KD*$^{+/-}$*/Lgr6-EGFP-IRES-CreERT2*$^{+/-}$*/R26RLacZ*$^{+/-}$ mice were administered either doxycycline water or vehicle for 10 days, and then given one topical dose of 4OHT (1 mg in 200 µl of 100% ethanol) (Sigma-Aldrich) on back skin to induce Cre expression. Mice were sacrificed in triplicates 7 days after induction. Animals were housed in standard conditions, fed *ad libitum* and treated in accordance with the regulations and protocols stipulated by the UCSF Institutional Animal Care and Use Committee (IACUC). All mouse experiments were approved by the University of California at San Francisco Laboratory Animal Resource Center.

X-Gal staining

Samples from 4OHT- or vehicle-treated *Lgr6 KD*$^{+/-}$*/Lgr6-EGFP-IRES-CreERT2*$^{+/-}$*/R26RLacZ*$^{+/-}$ mice were taken and cut into smaller pieces. They were fixed with 4% Formaldehyde in PBS for 10 min at RT on a shaker and washed with PBS. After 3 washes, samples were incubated overnight at 37 °C with X-Gal staining solution consisting of 1 mg/ml X-Gal, 5 mM $K_3Fe(CN)_6$, 5 mM $K_4Fe(CN)_6$, and 2 mM $MgCl_2$ in PBS. The next day, samples were washed with PBS, transferred to 70% ethanol and processed into paraffin blocks. Sections were cut, counterstained with nuclear fast red (Vector Laboratories) according to the manufacturer's protocol and analysed under the microscope.

Immunofluorescence

6 µm skin sections were deparaffinised and antigen retrieval was performed in Trilogy pretreatment solution (Cell Marque). Sections were blocked for 1 h at room temperature with 10% donkey serum (Abcam) diluted in PBS containing 0.3% Triton X-100 and incubated overnight with primary antibodies against Ki67 (rabbit, Lab Vision) or BrDU (rat, Abcam) at 4 °C. After washing in PBS, sections were incubated with the appropriate Alexa 488/555 conjugated secondary antibody (Molecular Probes) for 1 h at room temperature. After another PBS wash, the samples were mounted in Vectorshield hardset mounting medium with DAPI (Vector Laboratories).

Cell culture treatments, Aldefluor assay and multiplex in situ hybridisation

Doxycycline was administered, where appropriate, at a concentration of 1 ug/mL of culture medium. For the Aldefluor assay, cells were stained with Aldefluor reagent (and DEAB reagent) (Stem Cell Technologies) according to the manufacturer's instructions. The cells were then sorted on the BD FACSAria III in the UCSF Laboratory for Cell Analysis. RNA was extracted using TRIzol (Invitrogen) and reverse transcription was performed using the High Capacity Reverse Transcription Kit (Life Technologies). qPCR analysis was subsequently carried out using Taqman gene expression assays and master mix (Life Technologies) in the AB7900HT system. For multiplex *in situ* hybridisation, ViewRNA ISH Cell Assay probes for murine *Lgr4-6* were obtained from Panomics and *in situ* hybridisation was performed according to the manufacturer's protocol on cells grown in poly-lysine coated, glass-bottom 96-well plates (In Vitro Scientific). Images were acquired on the 6D high throughput microscope in the UCSF Nikon Imaging Center and analysed using the NIS Elements and ImageJ software packages.

Statistical analysis

Microarray expression analysis was carried out on a panel of cell lines generated in our laboratory (Oft et al. 2002). RNA was isolated using TRIzol (Invitrogen), according to the manufacturer's instructions. Residual genomic DNA was removed by DNase treatment (Ambion). RNA quality was assessed using Bioanalyzer (Agilent). Gene expression was quantified using Affymetrix MoGene ST 1.1 arrays hybridised on an Affymetrix GeneTitan instrument. Statistical analyses were carried out using Prism (Graphpad). Significance of difference between two groups was

determined using the unpaired, two-tailed Student’s t test and labelled as follows: * for $p < 0.05$; ** for $p < 0.01$; and *** for $p < 0.001$.

Figures and Tables

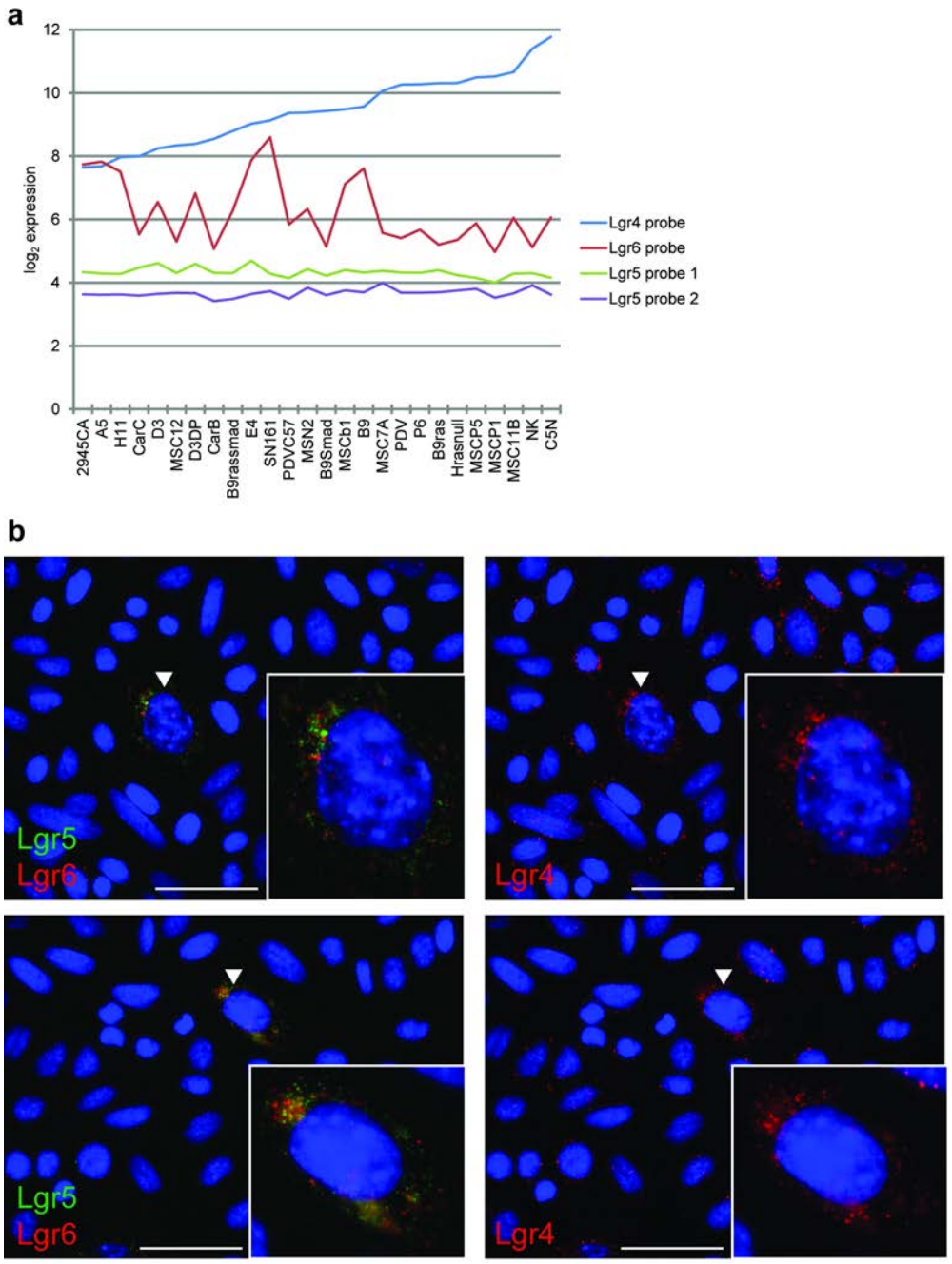

Figure 3.1. ***Lgr5 is expressed in rare single BCC cells but not in SCC cell lines*****.**

(**a**) Expression analysis was performed on a panel of immortalised keratinocyte (NK and C5N) and SCC cell lines. Log2 expression of 4 and below indicates background expression level. (**b**) Top and bottom, 2 different representative fields of a BCC cell line (Asz001) showing Lgr5 (green) and Lgr6 (red) expression patterns in the left

panels and Lgr4 (red) expression patterns in the right panel. White arrowheads point to cells enlarged in the insets. Bars = 50 um.

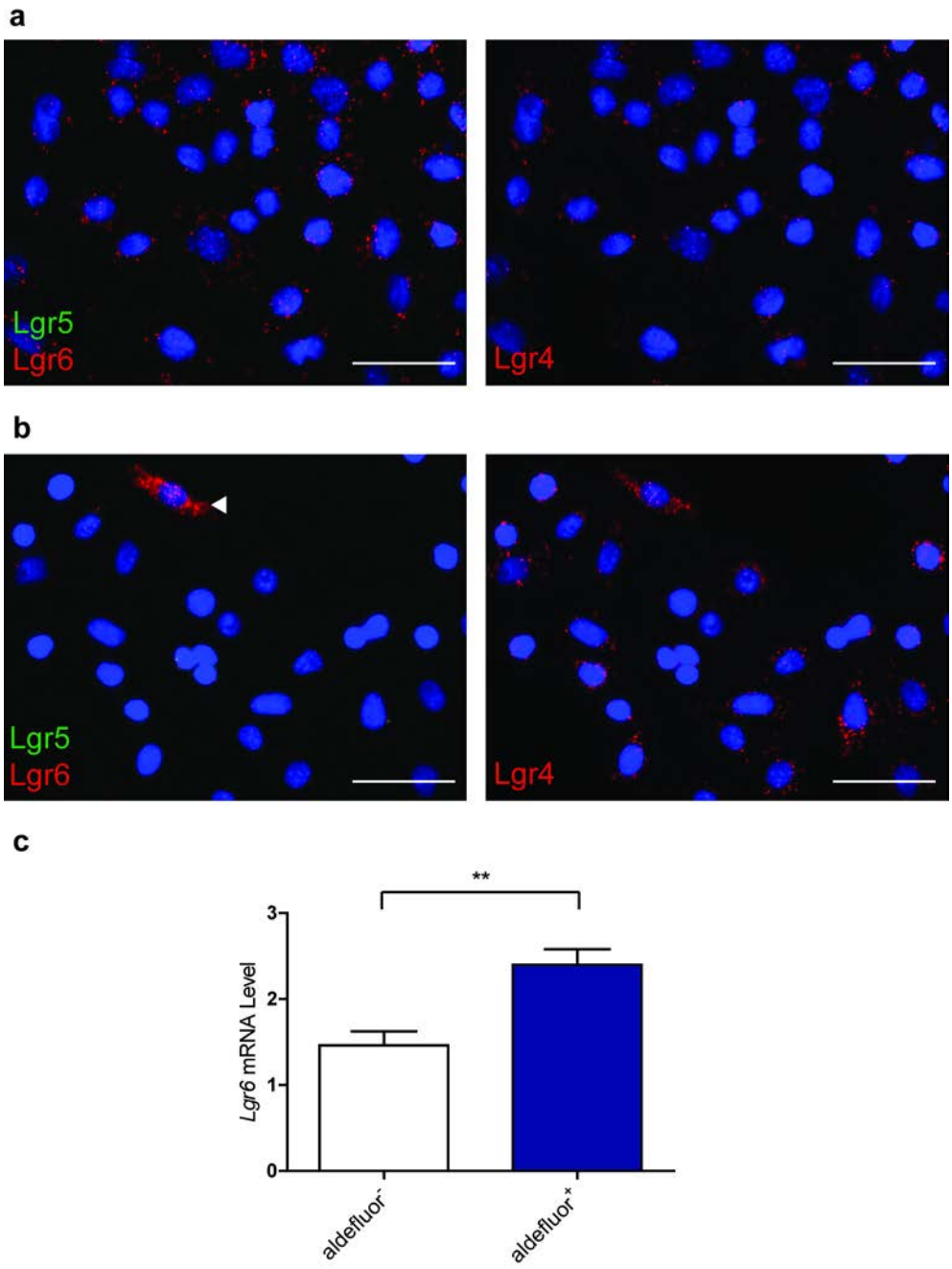

Figure 3.2. Lgr6, and not Lgr5, is an SCC CSC marker.

(a,b) *Lgr4-6* multiplex *in situ* hybridisation was performed in an SCC cell line E4 (**a**) and C5N (**b**). The *Lgr5* (green) and *Lgr6* (red) expression patterns are shown in the left panels, while the *Lgr4* (red) expression patterns are shown in the right panels. White arrowhead points to rare single C5N cell expressing *Lgr6*. (**c**) The aldefluor assay was performed on C5N cells, which were then sorted based on Aldefluor

activity. *Lgr6* expression level was determined in the sorted Aldefluor^{+} and Aldefluor^{-} populations using qrt-PCR. Bars = 50 um.

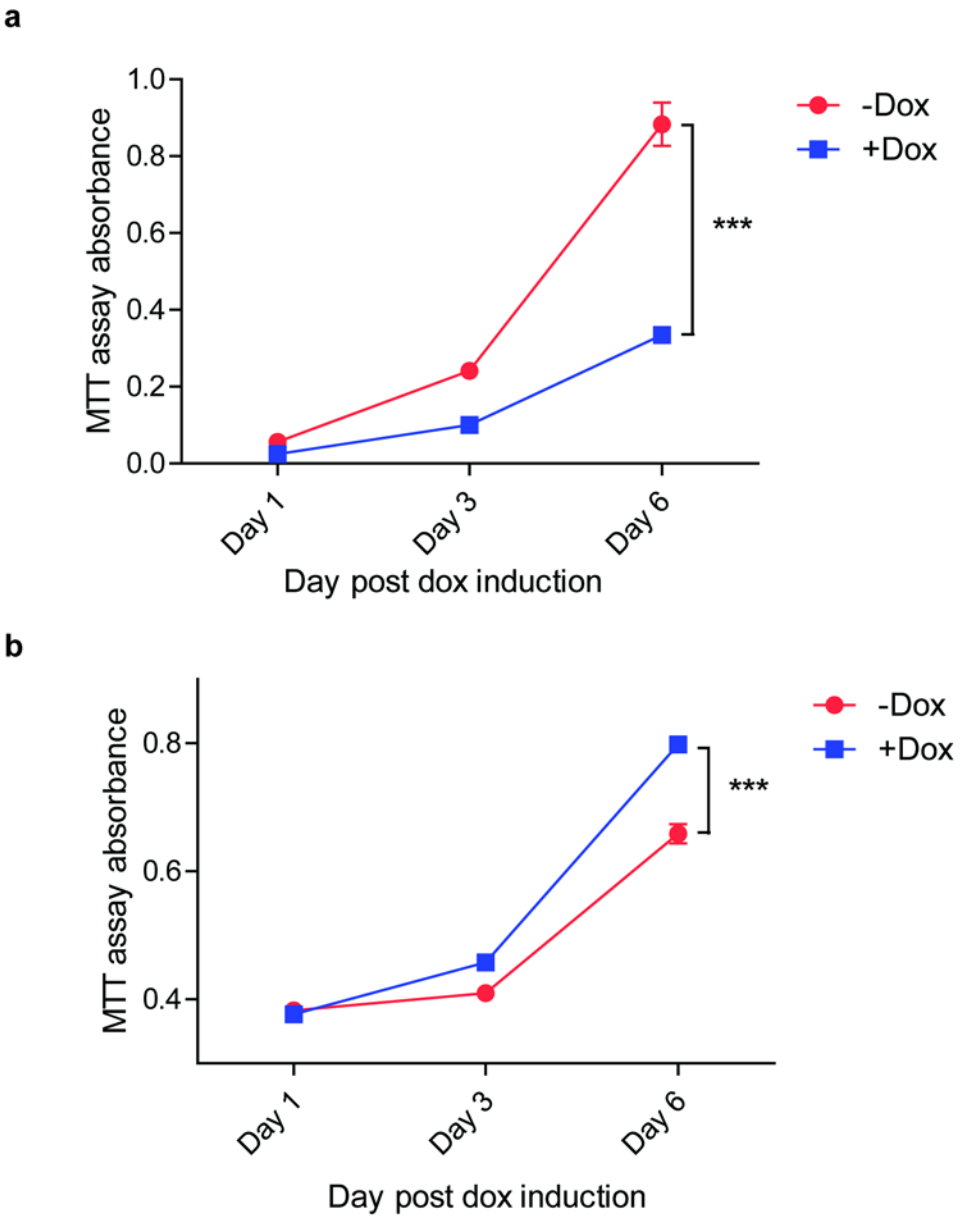

Figure 3.3. ***Lgr6 has growth inhibitory effects in keratinocyte and SCC cell lines*.**

(**a**) A keratinocyte cell line (NK) carrying an inducible Lgr6 overexpression construct was treated either with doxycycline or vehicle and growth was monitored at various timepoints using the MTT assay. (**b**) An SCC cell line (E4) carrying an inducible *Lgr6 shRNA* construct was treated either with doxycycline or vehicle and growth was monitored at various timepoints using the MTT assay. Data are presented as mean ± s.e. ***$p < 0.001$.

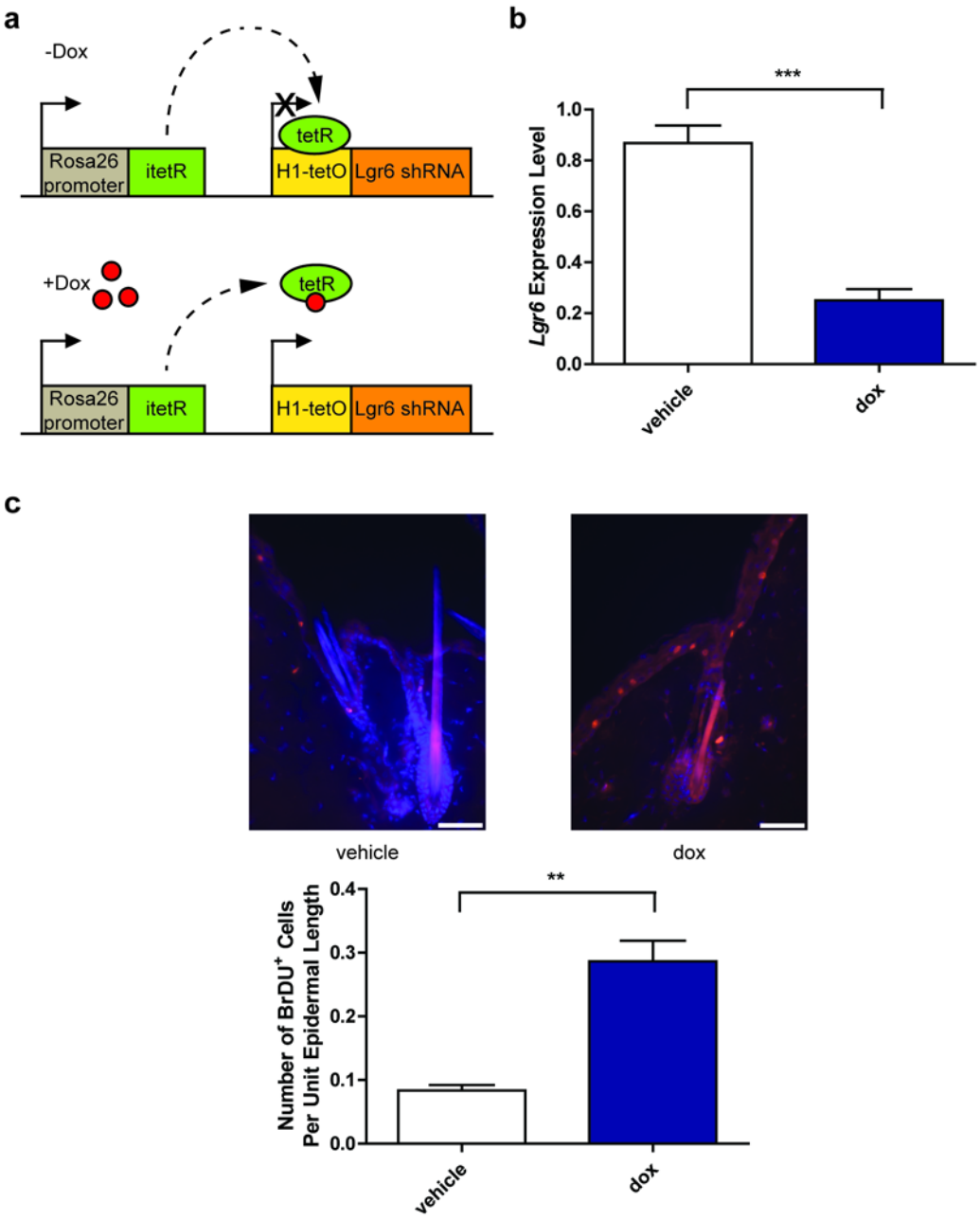

Figure 3.4. *Lgr6 knockdown in vivo increases proliferation in the epidermis*.

Adult *Lgr6 KD*$^{+/-}$ mice were administered doxycycline water or vehicle for 10 days. The animals were then intraperitoneally injected with BrDU and skin samples were harvested 3 h later. (**a**) Cartoon depicting mechanism of *Lgr6* knockdown induced by doxycycline treatment of *Lgr6 KD*$^{+/-}$ mice. (**b**) *Lgr6* levels In back skin samples were determined for the two groups of animals through qrt-PCR. (**c**) Top, representative sections showing BrDU staining in the back skin of *Lgr6 KD*$^{+/-}$ mice administered

either vehicle (left) or doxycycline water (right). Bottom, quantitation of BrDU staining in vehicle- or doxycycline-treated *Lgr6 KD*$^{+/-}$ mice. At least 3 animals were examined in each treatment group. Data are presented as mean ± s.e. **p < 0.01; ***p < 0.001. Bars = 50 um.

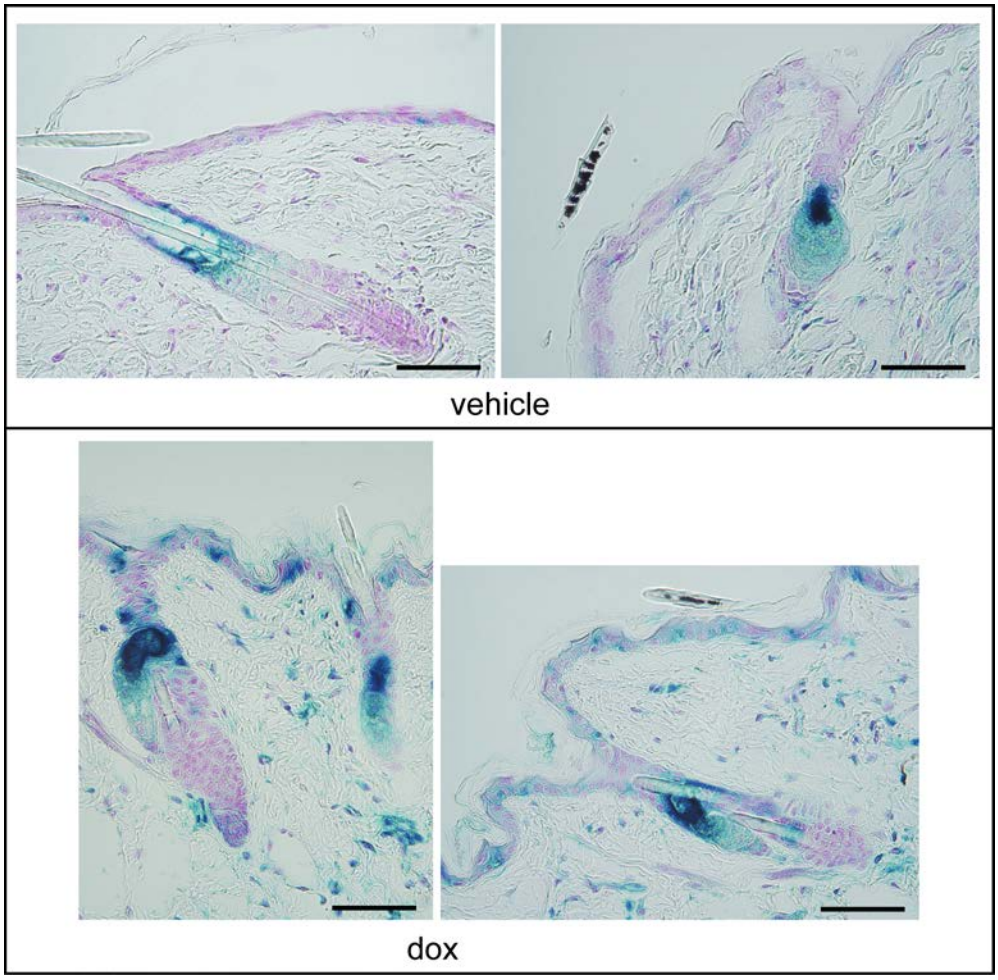

Figure 3.5. ***Lgr6 knockdown in vivo leads to expanded Lgr6 lineage tracing in the epidermis*****.**

Adult *Lgr6 KD*$^{+/-}$*/Lgr6-EGFP-IRES-CreERT2*$^{+/-}$*/R26RLacZ*$^{+/-}$ mice were administered either doxycycline water or vehicle. 10 days later, lineage tracing was induced with a topical dose of 4OHT and skin samples were harvested 7 days later. Top, 2 different representative sections showing X-Gal staining of skins from vehicle-treated mice. Bottom, 2 different representative sections showing X-Gal staining of skins from doxycycline-treated mice. Bars = 50 um.

a

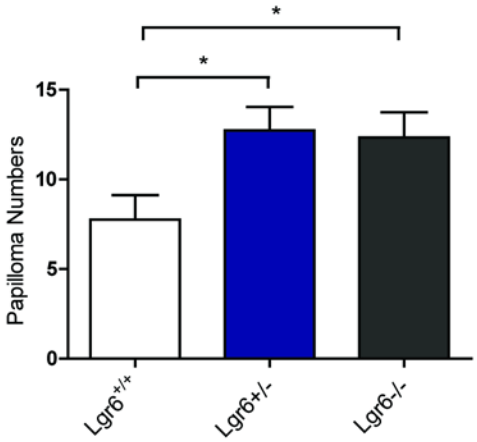

b

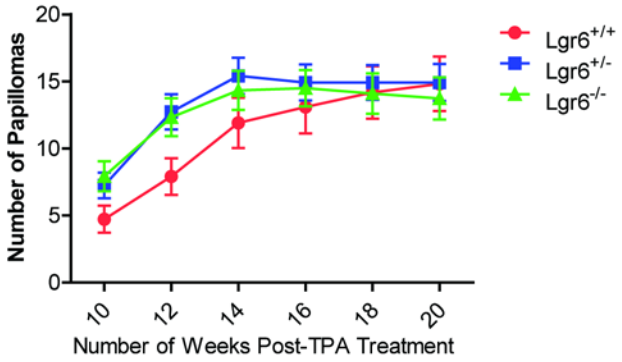

Figure 3.6. ***Lgr6-deficient mice have a reduced latency to papilloma development.*** Adult *Lgr6*$^{+/+}$, *Lgr6*$^{+/-}$ and *Lgr6*$^{-/-}$ mice were initiated with a single dose of DMBA, followed by biweekly treatments of TPA for 20 weeks. The animals were monitored for tumour development and sacrificed when their first carcinomas reached 1-1.5 cm in diameter. (**a**) Papilloma numbers in the various groups of mice at 12 weeks post-DMBA treatment. (**b**) Papilloma numbers in the various groups of mice from 10-20 weeks post-DMBA treatment. Data are presented as mean ± s.e. *p < 0.05.

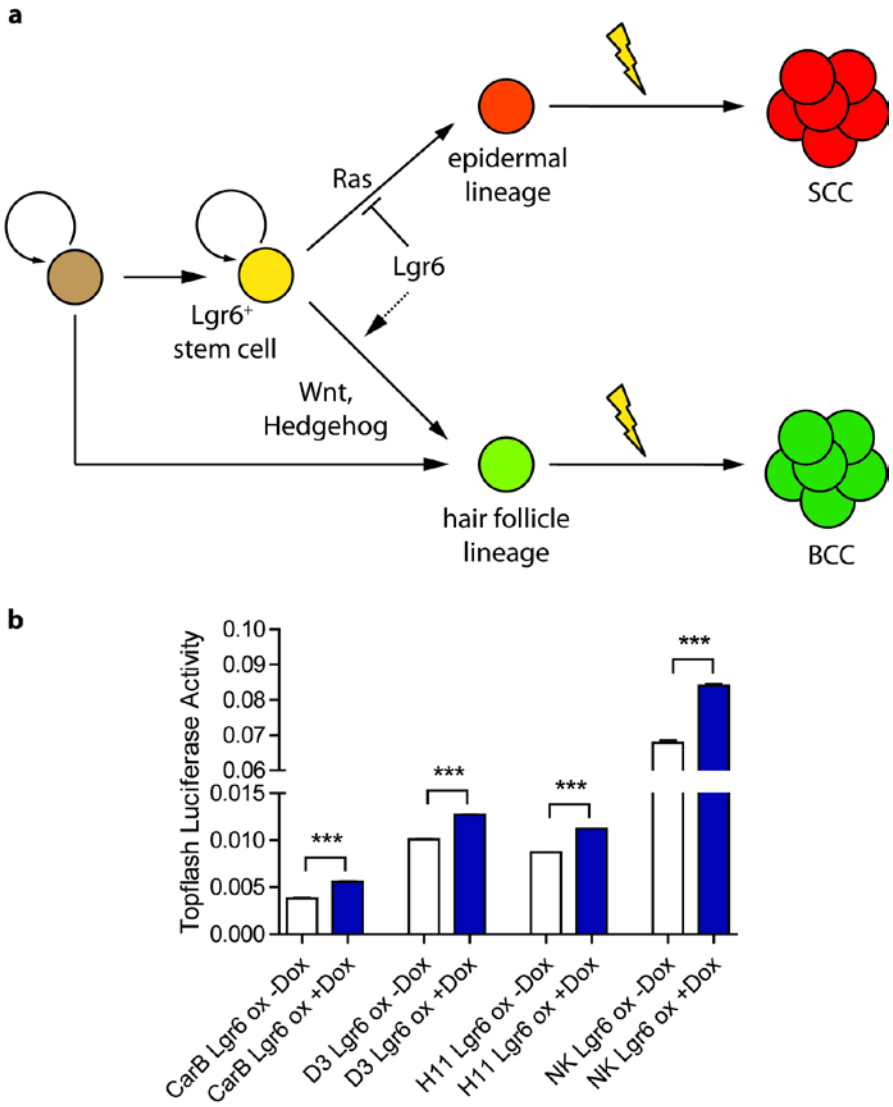

Figure 3.7. ***Model for role of Lgr6 in tumour cell fate decision*.**

(**a**) Lgr6^{+} stem cells in the skin are capable of giving rise to progeny that differentiate down either the epidermal or hair follicle lineage. Within these stem cells, Lgr6 positively regulates Wnt signalling and helps to restrain commitment down the epidermal lineage. (**b**) Lgr6 expression was either induced or left unchanged in a panel of SCC cell lines through administering doxycycline or vehicle. After 2 days, Wnt activity was assessed using the Topflash luciferase reporter assay. Data are presented as mean ± s.d. ***p<0.001.

Supplementary Figures and Tables

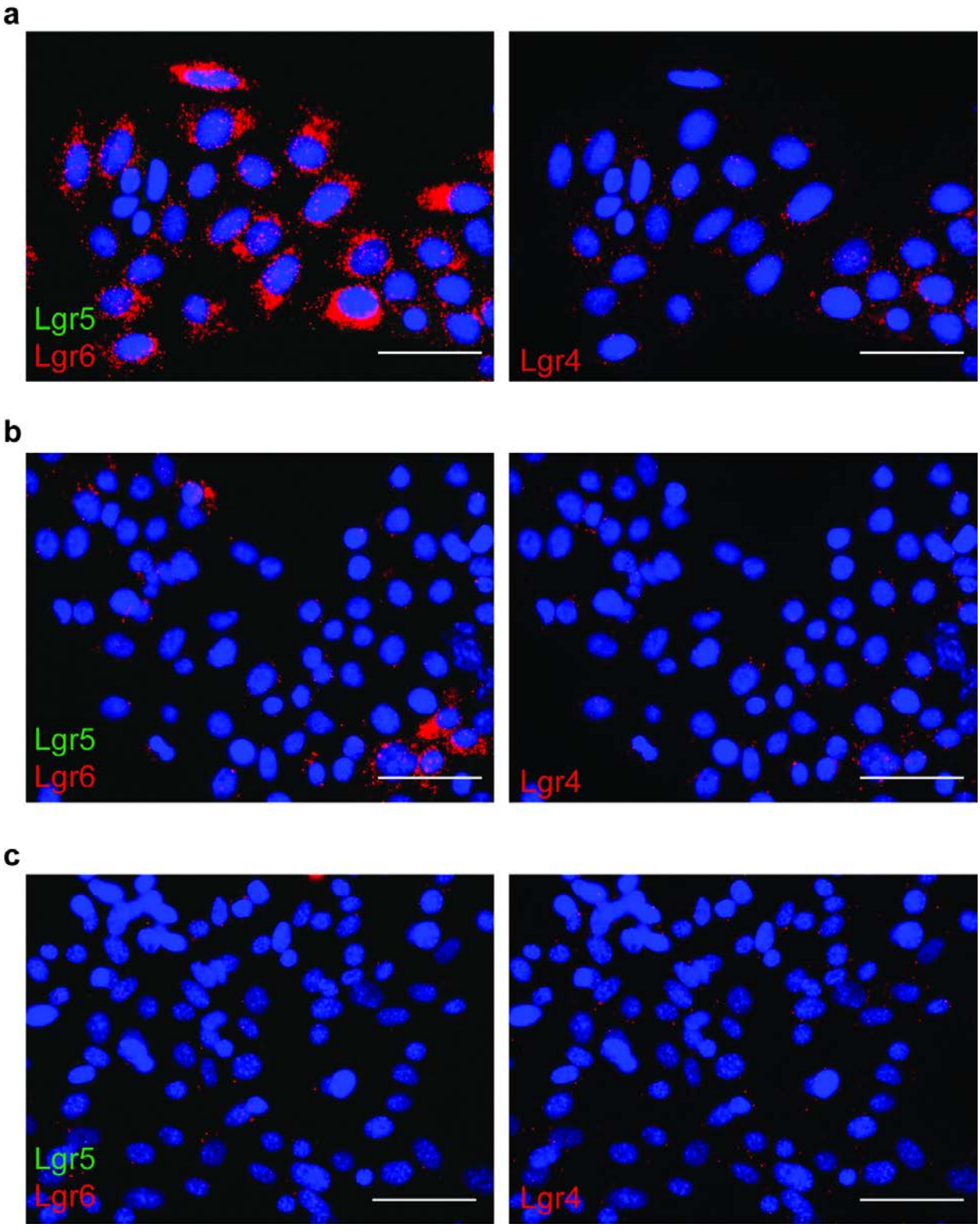

Supplementary Figure 3.1. Lgr5 is not an SCC CSC marker.

Lgr4-6 multiplex *in situ* hybridisation was performed in a selection of skin cell lines – the papilloma cell line P6 (**a**), the SCC cell line B9 (**b**) and the spindle carcinoma cell line CarB (**c**). The *Lgr5* (green) and *Lgr6* (red) expression patterns are shown in the left panels, while the *Lgr4* (red) expression patterns are shown in the right panels. Bars = 50 um.

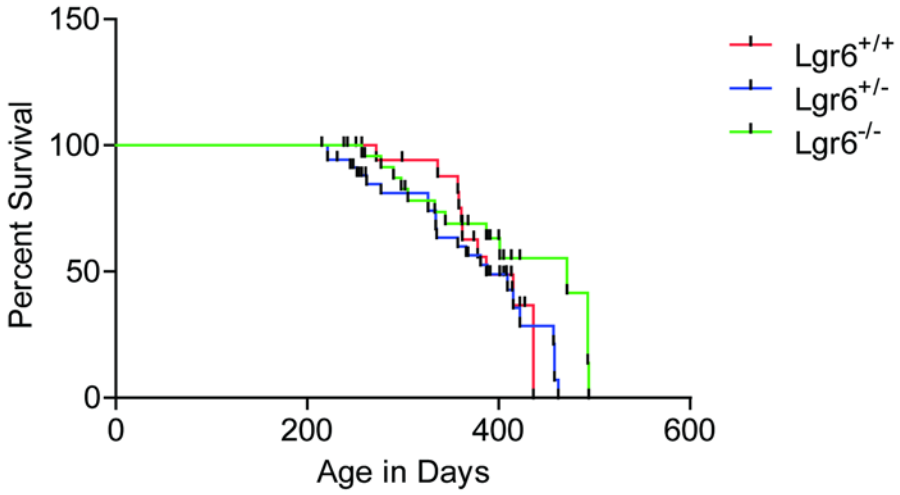

Supplementary Figure 3.2. Lgr6 deficiency does not affect progression to malignancy in the chemical carcinogenesis model.

Adult *Lgr6*$^{+/+}$, *Lgr6*$^{+/-}$ and *Lgr6*$^{-/-}$ mice were subjected to the DMBA/TPA protocol. The animals were sacrificed when their first carcinomas reached 1-1.5 cm in diameter, and overall survival in the different groups of animals are depicted in the Kaplan-Meier curves above.

Concluding Remarks

In this dissertation, I have described the roles of two different stem cell populations in the mouse hair follicle, and discussed the functions of the molecular markers that define them. Our observations have a number of important implications and raise several intriguing questions, which I enumerate below by way of concluding:

One, gene expression network analysis is a powerful tool for predicting the functions of genes in a given tissue. Without microdissection of the component parts, we have used computational network analysis of gene expression in normal skin to place *Lrig1* within a network, including *Krt79*, involved in the homeostasis of the hair follicle infundibulum, which demonstrates the utility of this approach.

Two, the various cell compartments in the skin have to communicate in order to coordinate their activities and functions during normal homeostasis and tissue regeneration. The signals and cell populations involved in such inter-compartmental communications, however, remain elusive. We provide evidence to show that Lrig1 progeny cells, which migrate into the epidermis and downward in anagen follicles, may serve such a function, but precisely how they do this (for instance, the identity of the signals they may provide) remains to be determined.

Three, the nature and identity of the cells-of-origin of cutaneous BCC and SCC remain unclear. While many Cre drivers are capable of giving rise to tumours when engineered to drive the expression of oncogenic *Kras* or *SmoM2*, they do not faithfully recapitulate the process of initiation in skin chemical or radiation

carcinogenesis models. Our results indicate that Lrig1^{+} cells are not common cells-of-origin of chemically induced tumours; Lgr6^{+} cells, however, remain a good candidate given our finding that Lgr6 marks SCC CSCs. In addition, our observation that BCC CSCs may be marked by selective expression of both Lgr5 and Lgr6 raises a number of interesting questions. For instance, do BCCs arise from a subpopulation of Lgr6^{+} stem cells that co-express Lgr5? Indeed, single Lgr6^{+} cells have been detected in the hair follicle bulge, where Lgr5 is also expressed. Related to this, can Lgr5 expression be used as a specific marker for BCCs? Given the prevalence of cutaneous BCC and SCC in Caucasian populations, answers to these questions will not only help to advance our understanding of a fundamental aspect of stem cell biology, but could also provide valuable contributions to the development of clinical treatments and diagnostic tools.

References

Agrawal N, Frederick MJ, Pickering CR, Bettegowda C, Chang K, Li RJ, Fakhry C, Xie T-X, Zhang J, Wang J, et al. 2011. Exome sequencing of head and neck squamous cell carcinoma reveals inactivating mutations in NOTCH1. *Science* **333**: 1154–7.

Alam M, Ratner D. 2001. Cutaneous Squamous-Cell Carcinoma. *NEJM* **344**: 975–983.

Aldaz CM, Trono D, Larcher F, Slaga TJ, Conti CJ. 1989. Sequential trisomization of chromosomes 6 and 7 in mouse skin premalignant lesions. *Mol Carcinog* **2**: 22–6.

Ambler C a, Watt FM. 2010. Adult epidermal Notch activity induces dermal accumulation of T cells and neural crest derivatives through upregulation of jagged 1. *Development* **137**: 3569–79.

Argyris TS. 1985. Promotion of epidermal carcinogenesis by repeated damage to mouse skin. *Am J Ind Med* **8**: 329–37.

Bai Y, Edamatsu H, Maeda S, Saito H, Suzuki N, Satoh T, Kataoka T. 2004. Crucial Role of Phospholipase Cε in Chemical Carcinogen-Induced Skin Tumor Development. *Cancer Res* **64**: 8808–10.

Bailleul B, Surani MA, White S, Barton SC, Brown K, Blessing M, Jorcano J, Balmain A. 1990. Skin hyperkeratosis and papilloma formation in transgenic mice expressing a ras oncogene from a suprabasal keratin promoter. *Cell* **62**: 697–708.

Balakier H, Pedersen R. 1982. Allocation of cells to inner cell mass and trophectoderm lineages in preimplantation mouse embryos. *Dev Biol* **90**: 352–362.

Balmain A, Pragnell I. 1983. Mouse skin carcinomas induced in vivo by chemical carcinogens have a transforming Harvey-ras oncogene. *Nature* **303**: 72–74.

Balmain A, Ramsden M, Bowden G, Smith J. 1984. Activation of the mouse cellular Harvey-ras gene in chemically induced benign skin papillomas. *Nature* **307**: 658–660.

Barker N, van Es JH, Kuipers J, Kujala P, van den Born M, Cozijnsen M, Haegebarth A, Korving J, Begthel H, Peters PJ, et al. 2007. Identification of stem cells in small intestine and colon by marker gene Lgr5. *Nature* **449**: 1003–7.

Barker N, Huch M, Kujala P, van de Wetering M, Snippert HJ, van Es JH, Sato T, Stange DE, Begthel H, van den Born M, et al. 2010. Lgr5(+ve) stem cells drive self-renewal in the stomach and build long-lived gastric units in vitro. *Cell Stem Cell* **6**: 25–36.

Barker N, Ridgway RA, van Es JH, van de Wetering M, Begthel H, van den Born M, Danenberg E, Clarke AR, Sansom OJ, Clevers H. 2009. Crypt stem cells as the cells-of-origin of intestinal cancer. *Nature* **457**: 608–11.

Barker N, Rookmaaker MB, Kujala P, Ng A, Leushacke M, Snippert H, van de Wetering M, Tan S, Van Es JH, Huch M, et al. 2012. Lgr5(+ve) stem/progenitor cells contribute to nephron formation during kidney development. *Cell Rep* **2**: 540–52.

Berenblum I, Shubik P. 1949. The Persistence of Latent Tumour Cells Induced in the Mouse's Skin by a Single Application of. *Br J Cancer* **3**: 384–386.

Berg RJ, van Kranen HJ, Rebel HG, de Vries A, van Vloten WA, van Kreijl CF, van der Leun JC, de Gruijl FR. 1996. Early p53 alterations in mouse skin carcinogenesis by UVB radiation: immunohistochemical detection of mutant p53 protein in clusters of preneoplastic epidermal cells. *Proc Natl Acad Sci U S A* **93**: 274–8.

Bissell MJ, Hines WC. 2011. Why don't we get more cancer? A proposed role of the microenvironment in restraining cancer progression. *Nat Med* **17**: 320–9.

Boiko A, Razorenova O, van de Rijn M, Swetter S, Johnson D, Ly D, Butler P, Yang G, Joshua B, Kaplan M, et al. 2010. Human melanoma-initiating cells express neural crest nerve growth factor receptor CD271. *Nature* **466**: 133–137.

Bondar T, Medzhitov R. 2010. p53-Mediated Hematopoietic Stem and Progenitor Cell Competition. *Cell Stem Cell* **6**: 309–322.

Boutwell RK, Verma AK, Ashendel CL AE. 1982. Mouse skin: a useful model system for studying the mechanism of chemical carcinogenesis. *Carcinog Compr Surv* **7**: 1–12.

Bremner F, Balmain A. 1990. Genetic Changes in Skin Tumor Progression : Correlation between Presence of a Mutant ras Gene and Loss of Heterozygosity on Mouse Chromosome 7. *Cell* **61**: 407–417.

Brown K, Buchmann A, Balmain A. 1990. Carcinogen-induced mutations in the mouse c-Ha-ras gene provide evidence of multiple pathways for tumor progression. *Proc Natl Acad Sci U S A* **87**: 538–42.

Brown K, Quintanilla M, Ramsden M, Kerr IB, Young S, Balmain A. 1986. v-ras genes from Harvey and BALB murine sarcoma viruses can act as initiators of two-stage mouse skin carcinogenesis. *Cell* **46**: 447–56.

Brown K, Strathdee D, Bryson S, Lambie W, Balmain A. 1998. The malignant capacity of skin tumours induced by expression of a mutant H-ras transgene depends on the cell type targeted. *Curr Biol* **8**: 516–24.

Buchmann A, RuggerI B, Klein-Szanto A, Balmain A. 1991. Progression of Squamous Carcinoma Cells to Spindle Carcinomas of Mouse Skin Is Associated

With An Imbalance of H-ras Alleles on Chromosome 7. *Cancer Res* **51**: 4097–4101.

Buczacki SJ a., Zecchini HI, Nicholson AM, Russell R, Vermeulen L, Kemp R, Winton DJ. 2013. Intestinal label-retaining cells are secretory precursors expressing Lgr5. *Nature* **495**: 65–69.

Burns P, Kemp C, Gannon J, Lane D, Bremner R, Balmain A. 1991. Loss of heterozygosity and mutational alterations of the p53 gene in skin tumours of interspecific hybrid mice. *Oncogene* **6**: 2363–2369.

Byrne C, Fuchs E. 1993. Probing Keratinocyte and Differentiation Specificity of the Human K5 Promoter In Vitro and in Transgenic Mice. *Mol Cell Biol* **13**: 3176–3190.

Capobianco A, Zagouras P, Blaumueller C, Artavanis-Tsakonas S, Bishop J. 1997. Neoplastic transformation by truncated alleles of human NOTCH1/TAN1 and NOTCH2. *Mol Cell Biol* **17**: 6265–6273.

Carmon KS, Gong X, Lin Q, Thomas A, Liu Q. 2011. R-spondins function as ligands of the orphan receptors LGR4 and LGR5 to regulate Wnt/ -catenin signaling. *Proc Natl Acad Sci* **108**: 11452–7.

Castagna M, Takai Y, Kaibuchi K, Sano K, Kikkawa U, Nishizuka Y. 1982. Direct activation of calcium-activated, phospholipid-dependent protein kinase by tumor-promoting phorbol esters. *J Biol Chem* **257**: 7847–7851.

Caulin C, Nguyen T, Lang GA, Goepfert TM, Brinkley BR, Cai W, Lozano G, Roop DR. 2007. An inducible mouse model for skin cancer reveals distinct roles for gain- and loss-of-function p53 mutations. *J Clin Invest* **117**: 1893–1901.

Lo Celso C, Prowse D, Watt F. 2004. Transient activation of beta-catenin signalling in adult mouse epidermis is sufficient to induce new hair follicles but continuous activation is required to maintain hair follicle tumours. *Development* **131**: 1787–1799.

Charafe-Jauffret E, Ginestier C, Iovino F, Wicinski J, Cervera N, Finetti P, Hur MH, Diebel ME, Monville F, Dutcher J, et al. 2009. Breast Cancer Cell Lines Contain Functional Cancer Stem Cells with Metastatic Capacity and a Distinct Molecular Signature. *Cancer Res* **69**: 1302–1313.

Cheetham S, Brand A. 2013. Cell biology. Insulin finds its niche. *Science* **340**: 817–818.

Chen J, Li Y, Yu T-S, McKay RM, Burns DK, Kernie SG, Parada LF. 2012. A restricted cell population propagates glioblastoma growth after chemotherapy. *Nature* **488**: 522–6.

Chen P-H, Chen X, Lin Z, Fang D, He X. 2013. The structural basis of R-spondin recognition by LGR5 and RNF43. *Genes Dev* **27**: 1345–50.

Cheung a MS, Wan TSK, Leung JCK, Chan LYY, Huang H, Kwong YL, Liang R, Leung a YH. 2007. Aldehyde dehydrogenase activity in leukemic blasts defines a subgroup of acute myeloid leukemia with adverse prognosis and superior NOD/SCID engrafting potential. *Leukemia* **21**: 1423–30.

Cicalese A, Bonizzi G, Pasi CE, Faretta M, Ronzoni S, Giulini B, Brisken C, Minucci S, Di Fiore PP, Pelicci PG. 2009. The Tumor Suppressor p53 Regulates Polarity of Self-Renewing Divisions in Mammary Stem Cells. *Cell* **138**: 1083–1095.

Clayton E, Doupé DP, Klein AM, Winton DJ, Simons BD, Jones PH. 2007. A single type of progenitor cell maintains normal epidermis. *Nature* **446**: 185–9.

Clevers H, Bevins C. 2013. Paneth cells: maestros of the small intestinal crypts. *Annu Rev Physiol* **75**: 289–311.

Clevers H, Nusse R. 2012. Wnt/β-Catenin Signaling and Disease. *Cell* **149**: 1192–205.

Conklin E. 1905. The organization and cell lineage of the ascidian egg. *J Acad Nat Sci Phila* **12**: 1–19.

Corti S, Locatelli F, Papadimitriou D, Donadoni C, Salani S, Del Bo R, Strazzer S, Bresolin N, Comi GP. 2006. Identification of a primitive brain-derived neural stem cell population based on aldehyde dehydrogenase activity. *Stem Cells* **24**: 975–85.

Cotsarelis G, Sun T, Lavker R. 1990. Label-retaining cells reside in the bulge area of pilosebaceous unit: implications for follicular stem cells, hair cycle, and skin carcinogenesis. *Cell* **61**: 1329–1337.

Cottle DL, Kretzschmar K, Schweiger PJ, Quist SR, Gollnick HP, Natsuga K, Aoyagi S, Watt FM. 2013. c-MYC-Induced Sebaceous Gland Differentiation Is Controlled by an Androgen Receptor/p53 Axis. *Cell Rep* 1–15.

Cui C, Durmowicz M, Ottolenghi C, Hashimoto T, Griggs B, Srivastava A, Schlessinger D. 2003. Inducible mEDA-A1 transgene mediates sebaceous gland hyperplasia and differential formation of two types of mouse hair follicles. *Hum Mol Genet* **12**: 2931–2940.

Dahlhoff M, Müller A-K, Wolf E, Werner S, Schneider MR. 2010. Epigen transgenic mice develop enlarged sebaceous glands. *J Invest Dermatol* **130**: 623–6.

Davy A, Soriano P. 2007. Ephrin-B2 forward signaling regulates somite patterning and neural crest cell development. *Dev Biol* **304**: 182–93.

Defossez P-A, Walker F, Zhang H-H, Odorizzi A, Burgess AW. 2011. LGR5 Is a Negative Regulator of Tumourigenicity, Antagonizes Wnt Signalling and Regulates Cell Adhesion in Colorectal Cancer Cell Lines. *PLoS One* **6**: e22733.

Dejosez M, Ura H, Brandt VL, Zwaka TP. 2013. Safeguards for cell cooperation in mouse embryogenesis shown by genome-wide cheater screen. *Science* **341**: 1511–4.

Demehri S, Kopan R. 2009. Notch signaling in bulge stem cells is not required for selection of hair follicle fate. *Development* **136**: 891–6.

Demehri S, Turkoz A, Kopan R. 2009. Epidermal Notch1 loss promotes skin tumorigenesis by impacting the stromal microenvironment. *Cancer Cell* **16**: 55–66.

Dominey AM, Wang X, King LE, Nanney LB, Gagne TA, Sellheyer K, Bundman DS, Longley MA, Rothnagel JA, Greenhalgh DA, et al. 1993. Targeted Overexpression of Transforming Growth Factor a in the Epidermis of Transgenic Mice Elicits Hyperplasia, Hyperkeratosis, and Spontaneous, Squamous Papillomas. *Cell Growth Differ* **4**: 1071–1082.

Driessens G, Beck B, Caauwe A, Simons BD, Blanpain C. 2012. Defining the mode of tumour growth by clonal analysis. *Nature* **488**: 527–530.

Driskell RR, Lichtenberger BM, Hoste E, Kretzschmar K, Simons BD, Charalambous M, Ferron SR, Herault Y, Pavlovic G, Ferguson-Smith AC, et al. 2013. Distinct fibroblast lineages determine dermal architecture in skin development and repair. *Nature* **504**: 277–81.

Durinck S, Ho C, Wang NJ, Liao W, Jakkula LR, Collisson EA, Pons J, Chan S-W, Lam ET, Chu C, et al. 2011. Temporal dissection of tumorigenesis in primary cancers. *Cancer Discov* **1**: 137–43.

Van Duuren BL, Sivak A, Katz C, Seidman K, Melchionne S. 1975. The Effect of Aging and Interval between Primary and Secondary Treatment in Two-Stage Carcinogenesis on Mouse Skin. *Cancer Res* **35**: 502–505.

Eagleson G, Harris W. 1990. Mapping of the presumptive brain regions in the neural plate of Xenopus laevis. *J Neurobiol* **21**: 427–440.

Ehrenreiter K, Kern F, Velamoor V, Meissl K, Galabova-Kovacs G, Sibilia M, Baccarini M. 2009. Raf-1 Addiction in Ras-Induced Skin Carcinogenesis. *Cancer Cell* **16**: 149–160.

Ehrenreiter K, Piazzolla D, Velamoor V, Sobczak I, Small JV, Takeda J, Leung T, Baccarini M. 2005. Raf-1 regulates Rho signaling and cell migration. *J Cell Biol* **168**: 955–64.

Fekete D, Cepko C. 1993. Retroviral infection coupled with tissue transplantation limits gene transfer in the chicken embryo. *Proc Natl Acad Sci* **90**: 2350–2354.

Feldser DM, Kostova KK, Winslow MM, Taylor SE, Cashman C, Whittaker C a, Sanchez-Rivera FJ, Resnick R, Bronson R, Hemann MT, et al. 2010. Stage-

specific sensitivity to p53 restoration during lung cancer progression. *Nature* **468**: 572–5.

Flesken-Nikitin A, Hwang C-I, Cheng C-Y, Michurina T V., Enikolopov G, Nikitin AY. 2013. Ovarian surface epithelium at the junction area contains a cancer-prone stem cell niche. *Nature* **495**: 241–245.

Fournier A, Murray A. 1987. Application of phorbol ester to mouse skin causes a rapid and sustained loss of protein kinase C. *Nature* **330**: 767–769.

Fuchs E, Esteves R, Coulombe P. 1992. Transgenic mice expressing a mutant keratin 10 gene reveal the likely genetic basis for epidermolytic hyperkeratosis. *Proc Natl Acad Sci U S A* **89**: 6906–10.

Fujiwara H, Ferreira M, Donati G, Marciano DK, Linton JM, Sato Y, Hartner A, Sekiguchi K, Reichardt LF, Watt FM. 2011. The Basement Membrane of Hair Follicle Stem Cells Is a Muscle Cell Niche. *Cell* **144**: 577–589.

Gat U, DasGupta R, Degenstein L, Fuchs E. 1998. De Novo hair follicle morphogenesis and hair tumors in mice expressing a truncated beta-catenin in skin. *Cell* **95**: 605–14.

Ghazizadeh S, Taichman L. 2001. Multiple classes of stem cells in cutaneous epithelium: a lineage analysis of adult mouse skin. *EMBO J* **20**: 1215–1222.

Ginestier C, Hur MH, Charafe-Jauffret E, Monville F, Dutcher J, Brown M, Jacquemier J, Viens P, Kleer CG, Liu S, et al. 2007. ALDH1 Is a Marker of Normal and Malignant Human Mammary Stem Cells and a Predictor of Poor Clinical Outcome. *Cell Stem Cell* **1**: 555–567.

Glinka A, Dolde C, Kirsch N, Huang Y-L, Kazanskaya O, Ingelfinger D, Boutros M, Cruciat C-M, Niehrs C. 2011. LGR4 and LGR5 are R-spondin receptors mediating Wnt/β-catenin and Wnt/PCP signalling. *EMBO Rep*.

Gomez C, Chua W, Miremadi A, Quist S, Headon DJ, Watt FM. 2013. The Interfollicular Epidermis of Adult Mouse Tail Comprises Two Distinct Cell Lineages that Are Differentially Regulated by Wnt, Edaradd, and Lrig1. *Stem Cell Reports* **1**: 19–27.

Gong X, Carmon KS, Lin Q, Thomas A, Yi J, Liu Q. 2012. LGR6 Is a High Affinity Receptor of R-Spondins and Potentially Functions as a Tumor Suppressor. *PLoS One* **7**: e37137.

González-García A, Pritchard CA, Paterson HF, Mavria G, Stamp G, Marshall CJ. 2005. RalGDS is required for tumor formation in a model of skin carcinogenesis. *Cancer Cell* **7**: 219–26.

Gonzalez-Suarez E, Jacob AP, Jones J, Miller R, Roudier-Meyer MP, Erwert R, Pinkas J, Branstetter D, Dougall WC. 2010. RANK ligand mediates progestin-

induced mammary epithelial proliferation and carcinogenesis. *Nature* **468**: 103–7.

Goudie DR, D'Alessandro M, Merriman B, Lee H, Szeverényi I, Avery S, O'Connor BD, Nelson SF, Coats SE, Stewart A, et al. 2011. Multiple self-healing squamous epithelioma is caused by a disease-specific spectrum of mutations in TGFBR1. *Nat Genet* **43**: 365–9.

Grachtchouk M, Pero J, Yang S, Ermilov A, Michael L, Wang A, Wilbert D, Patel R, Ferris J, Diener J, et al. 2011. Basal cell carcinomas in mice arise from hair follicle stem cells and multiple epithelial progenitor populations. *J Clin Invest* 1768–1781.

Greco V, Chen T, Rendl M, Schober M, Pasolli HA, Stokes N, dela Cruz-Racelis J, Fuchs E. 2009. A Two-Step Mechanism for Stem Cell Activation during Hair Regeneration. *Cell Stem Cell* **4**: 155–169.

Greenhalgh D, Rothnagel J, Quintanilla M, Orengo C, Gagne T, Bundman D, Longley M, Roop D. 1993. Induction of epidermal hyperplasia, hyperkeratosis, and papillomas in transgenic mice by a targeted v-Ha-ras oncogene. *Mol Carcinog* **7**: 99–110.

Grossbart TA, Lew RA. 1996. Prevention and Early Detection Strategies for Melanoma and Skin Cancer. Current Status. *Arch Dermatol* **132**: 436–443.

Gupta PB, Chaffer CL, Weinberg RA. 2009. Cancer stem cells: mirage or reality? *Nat Med* **15**: 1010–2.

Gur G, Rubin C, Katz M, Amit I, Citri A, Nilsson J, Amariglio N, Henriksson R, Rechavi G, Hedman H, et al. 2004. LRIG1 restricts growth factor signaling by enhancing receptor ubiquitylation and degradation. *EMBO J* **23**: 3270–3281.

Hanahan D, Wagner EF, Palmiter RD. 2007. The origins of oncomice: a history of the first transgenic mice genetically engineered to develop cancer. *Genes Dev* **21**: 2258–70.

Hansen L a, Tennant RW. 1994. Follicular origin of epidermal papillomas in v-Ha-ras transgenic TG.AC mouse skin. *Proc Natl Acad Sci U S A* **91**: 7822–6.

Hansen LA, Monteiro-riviere NA, Smart RC. 1990. Differential Down-Regulation of Epidermal Protein Kinase C by 12- O -Tetradecanoylphorbol-13-acetate and Diacylglycerol : Association with Epidermal Hyperplasia and Tumor Promotion. *Cancer Res* **50**: 5740–5745.

Hao H-X, Xie Y, Zhang Y, Charlat O, Oster E, Avello M, Lei H, Mickanin C, Liu D, Ruffner H, et al. 2012. ZNRF3 promotes Wnt receptor turnover in an R-spondin-sensitive manner. *Nature*.

Hennings H, Glick a B, Lowry DT, Krsmanovic LS, Sly LM, Yuspa SH. 1993. FVB/N mice: an inbred strain sensitive to the chemical induction of squamous cell carcinomas in the skin. *Carcinogenesis* **14**: 2353–8.

Hirsch D, Barker N, McNeil N, Hu Y, Camps J, McKinnon K, Clevers H, Ried T, Gaiser T. 2014. LGR5 positivity defines stem-like cells in colorectal cancer. *Carcinogenesis* **35**: 849–58.

Hordijk P, ten Klooster J, van der Kammen R, Michiels F, Oomen L, Collard J. 1997. Inhibition of invasion of epithelial cells by Tiam1-Rac signalling. *Science* **278**: 1464–1466.

Horsley V, Aliprantis AO, Polak L, Glimcher LH, Fuchs E. 2008. NFATc1 balances quiescence and proliferation of skin stem cells. *Cell* **132**: 299–310.

Horsley V, O'Carroll D, Tooze R, Ohinata Y, Saitou M, Obukhanych T, Nussenzweig M, Tarakhovsky A, Fuchs E. 2006. Blimp1 defines a progenitor population that governs cellular input to the sebaceous gland. *Cell* **126**: 597–609.

Hu B, Castillo E, Harewood L, Ostano P, Reymond A, Dummer R, Raffoul W, Hoetzenecker W, Hofbauer GFL, Dotto GP. 2012. Multifocal epithelial tumors and field cancerization from loss of mesenchymal CSL signaling. *Cell* **149**: 1207–20.

Huang P, Balmain A. 2014. Modeling Cutaneous Squamous Carcinoma Development in the Mouse. In *Cold Spring Harb Perspect Med*.

Huch M, Bonfanti P, Boj SF, Sato T, Loomans CJM, van de Wetering M, Sojoodi M, Li VSW, Schuijers J, Gracanin A, et al. 2013a. Unlimited in vitro expansion of adult bi-potent pancreas progenitors through the Lgr5/R-spondin axis. *EMBO J* **32**: 2708–21.

Huch M, Dorrell C, Boj SF, van Es JH, Li VSW, van de Wetering M, Sato T, Hamer K, Sasaki N, Finegold MJ, et al. 2013b. In vitro expansion of single Lgr5+ liver stem cells induced by Wnt-driven regeneration. *Nature* **494**: 247–50.

Itasaki N, Bel-Vialar S, Krumlauf R. 1999. "Shocking" developments in chick embryology: electroporation and in ovo gene expression. *Nat Cell Biol* **1**: E203–E207.

Ito M, Liu Y, Yang Z, Nguyen J, Liang F, Morris RJ, Cotsarelis G. 2005. Stem cells in the hair follicle bulge contribute to wound repair but not to homeostasis of the epidermis. *Nat Med* **11**: 1351–4.

Jacks T. 1996. Tumor Suppressor Gene Mutations in Mice. *Annu Rev Genet* **30**: 603–36.

Jackson EL, Willis N, Mercer K, Bronson RT, Crowley D, Montoya R, Jacks T, Tuveson D a. 2001. Analysis of lung tumor initiation and progression using conditional expression of oncogenic K-ras. *Genes Dev* **15**: 3243–8.

Jaks V, Kasper M, Es JH van, Snippert HJ, Clevers H, Barker N, Toftgard R. 2008. Lgr5 marks cycling, yet long-lived, hair follicle stem cells. *Nat Genet* **40**: 1291–1299.

Jaks V, Kasper M, Toftgård R. 2010. The hair follicle-a stem cell zoo. *Exp Cell Res* **316**: 1422–8.

Jensen KB, Collins CA, Nascimento E, Tan DW, Frye M, Itami S, Watt FM. 2009. Lrig1 Expression Defines a Distinct Multipotent Stem Cell Population in Mammalian Epidermis. *Cell Stem Cell* **4**: 427–439.

Jensen KB, Watt FM. 2006. Single-cell expression profiling of human epidermal stem and transit-amplifying cells: Lrig1 is a regulator of stem cell quiescence. *Proc Natl Acad Sci* **103**: 11958–11963.

Jhappan C, Gallahan D, Stahle C, Chu E, Smith G, Merlino G, Callahan R. 1992. Expression of an activated Notch-related int-3 transgene interferes with cell differentiation and induces neoplastic transformation in mammary and salivary glands. *Genes Dev* **6**: 345–355.

Jonason A, Kunala S, Price G, Restifo R, Spinelli H, Persing J, Leffell D, Tarone R, Brash D. 1996. Frequent clones of p53-mutated keratinocytes in normal human skin. *Proc Natl Acad Sci* **93**: 14025–14029.

Jones S, Chen W, Parmigiani G, Diehl F, Beerenwinkel N, Antal T, Traulsen A, Nowak M, Siegel C, Velculescu V, et al. 2008. Comparative lesion sequencing provides insights into tumor evolution. *Proc Natl Acad Sci* **105**: 4283–4288.

Junttila MR, Karnezis AN, Garcia D, Madriles F, Kortlever RM, Rostker F, Brown Swigart L, Pham DM, Seo Y, Evan GI, et al. 2010. Selective activation of p53-mediated tumour suppression in high-grade tumours. *Nature* **468**: 567–71.

Kang HC, Quigley D, Kim I-J, Wakabayashi Y, Ferguson-Smith M a, D'Alessandro M, Lane EB, Akhurst RJ, Goudie DR, Balmain A. 2013. Multiple Self-Healing Squamous Epithelioma (MSSE): Rare Variants in an Adjacent Region of Chromosome 9q22.3 to known TGFBR1 Mutations Suggest a Digenic or Multilocus Etiology. *J Invest Dermatol*.

Keely P, Westwick J, Whitehead I, Der C, Parise L. 1997. Cdc42 and Rac1 induce integrin- mediated cell motility and invasiveness through PI(3)K. *Nature* **390**: 632–636.

Kemp CJ, Donehower LA, Bradley A, Balmain A. 1993. Reduction of p53 gene dosage does not increase initiation or promotion but enhances malignant progression of chemically induced skin tumors. *Cell* **74**: 813–22.

Khavari P. 2006. Modelling cancer in human skin tissue. *Nat Rev Cancer* **6**: 270–80.

Kinzler K, Vogelstein B. 1996. Lessons from hereditary colorectal cancer. *Cell* **87**: 159–170.

Klein AM, Brash DE, Jones PH, Simons BD. 2010. Stochastic fate of p53-mutant epidermal progenitor cells is tilted toward proliferation by UV B during preneoplasia. *Proc Natl Acad Sci U S A* **107**: 270–5.

Klein-Szanto APJ, Larcher F, Bonfil RD, Conti CJ. 1989. Multistage chemical carcinogenesis protocols produce spindle cell carcinomas of the mouse skin. *Carcinogenesis* **10**: 2169–72.

Koo B-K, Spit M, Jordens I, Low TY, Stange DE, van de Wetering M, van Es JH, Mohammed S, Heck AJR, Maurice MM, et al. 2012. Tumour suppressor RNF43 is a stem-cell E3 ligase that induces endocytosis of Wnt receptors. *Nature* 1–6.

Kops G, de Ruiter N, De Vries-Smits A, Powell D, Bos J, Burgering B. 1999. Direct control of the Forkhead transcription factor AFX by protein kinase B. *Nature* **398**: 630–634.

Van Kranen HJ, De Gruijl FR. 1999. Mutations in Cancer Genes of UV-Induced Skin Tumors of Hairless Mice. *J Epidemiol* **9**: 58–65.

Van Kranen HJ, de Gruijl FR, de Vries A, Sontag Y, Wester PW, Senden HC, Rozemuller E, van Kreijl CF. 1995. Frequent p53 alterations but low incidence of ras mutations in UV-B-induced skin tumors of hairless mice. *Carcinogenesis* **16**: 1141–7.

Kretzschmar K, Watt FM. 2012. Lineage Tracing. *Cell* **148**: 33–45.

Kuijper S, Turner C, Adams R. 2007. Regulation of angiogenesis by Eph-ephrin interactions. *Trends Cardiovasc Med* **17**: 145–151.

Kumpf S, Mihlan M, Goginashvili A, Grandl G, Gehart H, Godel A, Schmidt J, Müller J, Bezzi M, Ittner A, et al. 2012. Hairless promotes PPARγ expression and is required for white adipogenesis. *EMBO Rep* **13**: 1012–1020.

Laederich M, Funes-Duran M, Yen L, Ingalla E, Wu X, L. Carraway III K, Sweeney C. 2004. The Leucine-rich Repeat Protein LRIG1 Is a Negative Regulator of ErbB Receptor Family Tyrosine Kinases. *J Biol Chem* **279**: 47050–47056.

Lapidot T, Sirard C, Vormoor J, Mrudoch B, Hoang T, Caceres-Cortes J, Minden M, Paterson B, Caligiuri M, Dick J. 1994. A cell initiating human acute myeloid leukaemia after transplantation into SCID mice. *Nature* **367**: 645–648.

Lapouge G, Beck B, Nassar D, Dubois C, Dekoninck S, Blanpain C. 2012. Skin squamous cell carcinoma propagating cells increase with tumour progression and invasiveness. *EMBO J* **31**: 4563–75.

Lapouge G, Youssef KK, Vokaer B, Achouri Y, Michaux C, Sotiropoulou PA, Blanpain C. 2011. Identifying the cellular origin of squamous skin tumors. *Proc Natl Acad Sci* **108**: 7431–7436.

De Lau W, Barker N, Low TY, Koo B-K, Li VSW, Teunissen H, Kujala P, Haegebarth A, Peters PJ, van de Wetering M, et al. 2011. Lgr5 homologues associate with Wnt receptors and mediate R-spondin signalling. *Nature* **476**: 293–7.

Lee T-C, Threadgill DW. 2009. Generation and validation of mice carrying a conditional allele of the epidermal growth factor receptor. *Genesis* **47**: 85–92.

Leushacke M, Barker N. 2012. Lgr5 and Lgr6 as markers to study adult stem cell roles in self-renewal and cancer. *Oncogene* **31**: 3009–22.

Li J, Yen C, Liaw D, Podsypanina K, Bose S, Wang S, Puc J, Miliaresis C, Rodgers L, McCombie R, et al. 1997. PTEN, a Putative Protein Tyrosine Phosphatase Gene Mutated in Human Brain, Breast, and Prostate Cancer. *Science* **275**: 1943–1947.

Li S, Park H, Trempus CS, Gordon D, Liu Y, Cotsarelis G, Morris RJ. 2012. A keratin 15 containing stem cell population from the hair follicle contributes to squamous papilloma development in the mouse. *Mol Carcinog* **52**: 751–759.

Liaw D, Marsh D, Li J, Dahia P, Wang S, Zheng Z, Bose S, Call K, Tsou H, Peacocke M, et al. 1997. Germline mutations of the PTEN gene in Cowden disease, an inherited breast and thyroid cancer syndrome. *Nat Genet* **16**: 64–67.

Lim X, Tan SH, Koh WLC, Chau RMW, Yan KS, Kuo CJ, van Amerongen R, Klein AM, Nusse R. 2013. Interfollicular epidermal stem cells self-renew via autocrine Wnt signaling. *Science* **342**: 1226–30.

Liu Y, Lyle S, Yang Z, Cotsarelis G. 2003. Keratin 15 promoter targets putative epithelial stem cells in the hair follicle bulge. *J Invest Dermatol* **121**: 963–968.

Loehrke H, Schweizer J, Dederer E, Hesse B, Rosenkranz G, Goerttler K. 1983. On the persistence of tumor initiation in two-stage carcinogenesis on mouse skin. *Carcinogenesis* **4**: 771–775.

Lowell S, Jones P, Le Roux I, Dunne J, Watt FM. 2000. Stimulation of human epidermal differentiation by delta-notch signalling at the boundaries of stem-cell clusters. *Curr Biol* **10**: 491–500.

Lowry WE, Blanpain C, Nowak JA, Guasch G, Lewis L, Fuchs E. 2005. Defining the impact of beta-catenin/Tcf transactivation on epithelial stem cells. *Genes Dev* **19**: 1596–1611.

Lu CP, Polak L, Rocha AS, Pasolli HA, Chen S-C, Sharma N, Blanpain C, Fuchs E. 2012. Identification of stem cell populations in sweat glands and ducts reveals roles in homeostasis and wound repair. *Cell* **150**: 136–50.

Lu L, Teixeira V, Yuan Z, Graham T, Endesfelder D, Kolluri K, Al-Juffali N, Hamilton N, Nicholson A, Falzon M, et al. 2013. LRIG1 regulates cadherin-dependent contact inhibition directing epithelial homeostasis and pre-invasive squamous cell carcinoma development. *J Pathol* **229**: 608–620.

Mackensie I. 1970. Relationship between mitosis and the ordered structure of the stratum corneum in mouse epidermis. *Nature* **226**: 653–655.

Malanchi I, Santamaria-Martínez A, Susanto E, Peng H, Lehr H-A, Delaloye J-F, Huelsken J. 2012. Interactions between cancer stem cells and their niche govern metastatic colonization. *Nature* **481**: 85–9.

Malliri A, van der Kammen R a, Clark K, van der Valk M, Michiels F, Collard JG. 2002. Mice deficient in the Rac activator Tiam1 are resistant to Ras-induced skin tumours. *Nature* **417**: 867–71.

Mao J-H, To MD, Perez-Losada J, Wu D, Del Rosario R, Balmain A. 2004. Mutually exclusive mutations of the Pten and ras pathways in skin tumor progression. *Genes Dev* **18**: 1800–5.

Mascré G, Dekoninck S, Drogat B, Youssef KK, Brohée S, Sotiropoulou P a., Simons BD, Blanpain C. 2012. Distinct contribution of stem and progenitor cells to epidermal maintenance. *Nature* **489**: 257–262.

Van Mater D, Kolligs FT, Dlugosz AA, Fearon E. 2003. Transient activation of beta - catenin signaling in cutaneous keratinocytes is sufficient to trigger the active growth phase of the hair cycle in mice. *Genes Dev* **15**: 1219–1224.

Mauerer A, Herschberger E, Dietmaier W, Landthaler M, Hafner C. 2011. Low incidence of EGFR and HRAS mutations in cutaneous squamous cell carcinomas of a German cohort. *Exp Dermatol* **20**: 848–50.

McClanahan T, Koseoglu S, Smith K, Grein J, Gustafson E, Black S, Kirschmeier P, Samatar A. 2006. Identification of Overexpression of Orphan G Protein-Coupled Receptor GPR49 in Human Colon and Ovarian Primary Tumor. *Cancer Biol Ther* **5**: 419–426.

Meletis K, Wirta V, Hede S-M, Nistér M, Lundeberg J, Frisén J. 2006. P53 Suppresses the Self-Renewal of Adult Neural Stem Cells. *Development* **133**: 363–9.

Morata G, Ripoli P. 1975. Minutes : Mutants of Drosophila Cell Division Autonomously Affecting Cell Division Rate. *Dev Biol* **42**: 211–221.

Morris RJ, Liu Y, Marles L, Yang Z, Trempus C, Li S, Lin JS, Sawicki JA, Cotsarelis G. 2004. Capturing and profiling adult hair follicle stem cells. *Nat Biotechnol* **22**: 411–417.

Morris RJ, Tryson KA, Wu KQ. 2000. Evidence That the Epidermal Targets of Carcinogen Action Are Found in the Interfollicular Epidermis or Infundibulum as well as in the Hair Follicles. *Cancer Res* **60**: 226–229.

Moskalenko S, Henry D, Rosse C, Mirey G, Camonis J, White M. 2002. The exocyst is a Ral effector complex. *Nat Cell Biol* **4**: 66–72.

Mukhopadhyay A, Krishnaswami S, Yu B. 2011. Activated Kras alters epidermal homeostasis of mouse skin, resulting in redundant skin and defective hair cycling. *J Invest Dermatol* **131**: 311–319.

Nakashima S, Morinaka K, Koyama S, Ikeda M, Kishida M, Okawa K, Iwamatsu A, Kishida S, Kikuchi A. 1999. Small G protein Ral and its downstream molecules regulate endocytosis of EGF and insulin receptors. *EMBO J* **18**: 3629–3642.

Neve RM, Chin K, Fridlyand J, Yeh J, Baehner FL, Fevr T, Clark L, Bayani N, Coppe J-P, Tong F, et al. 2006. A collection of breast cancer cell lines for the study of functionally distinct cancer subtypes. *Cancer Cell* **10**: 515–527.

Ng A, Tan S, Singh G, Rizk P, Swathi Y, Tan T, Huang R, Leushacke M, Barker N. 2014. Lgr5 marks stem/progenitor cells in ovary and tubal epithelia. *Nat Cell Biol* **16**: 745–757.

Nicolas M, Wolfer A, Raj K, Kummer JA, Mill P, van Noort M, Hui C, Clevers H, Dotto GP, Radtke F. 2003. Notch1 functions as a tumor suppressor in mouse skin. *Nat Genet* **33**: 416–21.

Nijhof J, Braun K, Giangreco A, van Pelt C, Kawamoto H, Boyd R, Willemze R, Mullenders L, Watt F, de Gruijl F, et al. 2006. The cell-surface marker MTS24 identifies a novel population of follicular keratinocytes with characteristics of progenitor cells. *Development* **133**: 3027–3037.

Nishimura E, Jordan S, Oshima H, Yoshida H, Osawa M, Moriyama M, Jackson I, Barrandon Y, Miyachi Y, Nishikawa S. 2002. Dominant role of the niche in melanocyte stem-cell fate determination. *Nature* **416**: 854–860.

Nishimura EK, Suzuki M, Igras V, Du J, Lonning S, Miyachi Y, Roes J, Beermann F, Fisher DE. 2010. Key roles for transforming growth factor beta in melanocyte stem cell maintenance. *Cell Stem Cell* **6**: 130–40.

Oft M, Akhurst RJ, Balmain A. 2002. Metastasis is driven by sequential elevation of H-ras and Smad2 levels. *Nat Cell Biol* **4**: 487–94.

Olson M, Ashworth A, Hall A. 1995. An essential role for Rho, Rac, and Cdc42 GTPases in cell cycle progression through G1. *Science* **269**: 1270–1272.

Olson M, Paterson H, Marshall C. 1998. Signals from Ras and Rho GTPases interact to regulate expression of p21Waf1/Cip1. *Nature* **394**: 295–299.

Oskarsson T, Acharyya S, Zhang XH-F, Vanharanta S, Tavazoie SF, Morris PG, Downey RJ, Manova-Todorova K, Brogi E, Massagué J. 2011. Breast cancer cells produce tenascin C as a metastatic niche component to colonize the lungs. *Nat Med* **17**: 867–74.

Page ME, Lombard P, Ng F, Göttgens B, Jensen KB. 2013. The Epidermis Comprises Autonomous Compartments Maintained by Distinct Stem Cell Populations. *Cell Stem Cell* **13**: 471–482.

Palmiter RD, Brinster RL. 1986. Germ-line transformation of mice. *Annu Rev Genet* **20**: 465–99.

Parma P, Radi O, Vidal V, Chaboissier MC, Dellambra E, Valentini S, Guerra L, Schedl A, Camerino G. 2006. R-spondin1 is essential in sex determination, skin differentiation and malignancy. *Nat Genet* **38**: 1304–1309.

Peng WC, Lau W De, Forneris F, Granneman JCM, Huch M, Clevers H. 2013. Structure of Stem Cell Growth Factor R-spondin 1 in Complex with the Ectodomain of Its Receptor LGR5. *Cell Rep* **3**: 1885–1892.

Perez-Losada J, Balmain A. 2003. Stem-cell hierarchy in skin cancer. *Nat Rev Cancer* **3**: 434–43.

Petersson M, Brylka H, Kraus A, John S, Rappl G, Schettina P, Niemann C. 2011. TCF/Lef1 activity controls establishment of diverse stem and progenitor cell compartments in mouse epidermis. *EMBO J* **30**: 3004–3018.

Plaks V, Brenot A, Lawson D a, Linnemann JR, Van Kappel EC, Wong KC, de Sauvage F, Klein OD, Werb Z. 2013. Lgr5-expressing cells are sufficient and necessary for postnatal mammary gland organogenesis. *Cell Rep* **3**: 70–8.

Pott P. 1775. *Cancer Scroti. In Chirurgical Observations*. L. Hawes, W. Clarke and R. Collins, London.

Potten C. 1981. Cell replacement in epidermis (keratopoiesis) via discrete units of proliferation. *Int Rev Cytol* **69**: 271–318.

Potten C, Wichmann H, Loeffler M, Dobek K, Major D. 1982. Evidence for discrete cell kinetic subpopulations in mouse epidermis based on mathematical analysis. *Cell Tissue Kinet* **15**: 305–329.

Powell AE, Wang Y, Li Y, Poulin EJ, Means AL, Washington MK, Higginbotham JN, Juchheim A, Prasad N, Levy SE, et al. 2012. The Pan-ErbB Negative Regulator Lrig1 Is an Intestinal Stem Cell Marker that Functions as a Tumor Suppressor. *Cell* **149**: 146–158.

Price J, Turner D, Cepko C. 1987. Lineage analysis in the vertebrate nervous system by retrovirus-mediated gene transfer. *Proc Natl Acad Sci* **84**: 156–160.

Proweller A, Tu L, Lepore JJ, Cheng L, Lu MM, Seykora J, Millar SE, Pear WS, Parmacek MS. 2006. Impaired notch signaling promotes de novo squamous cell carcinoma formation. *Cancer Res* **66**: 7438–44.

Purton L, Scadden D. 2007. Limiting factors in murine hematopoietic stem cell assays. *Cell Stem Cell* **1**: 263–270.

Quigley DA, To MD, Pérez-Losada J, Pelorosso FG, Mao J-H, Nagase H, Ginzinger DG, Balmain A. 2009. Genetic architecture of mouse skin inflammation and tumour susceptibility. *Nature* **458**: 505–508.

Quintana E, Shackleton M, Sabel M, Fullen D, Johnson T, Morrison S. 2008. Efficient tumour formation by single human melanoma cells. *Nature* **456**: 593–598.

Quintanilla M, Brown K, Ramsden M, Balmain A. 1986. Carcinogen-specific mutation and amplification of Ha-ras during mouse skin carcinogenesis. *Nature* **322**: 78–80.

Rabbani P, Takeo M, Chou W, Myung P, Bosenberg M, Chin L, Taketo MM, Ito M. 2011. Coordinated Activation of Wnt in Epithelial and Melanocyte Stem Cells Initiates Pigmented Hair Regeneration. *Cell* **145**: 941–955.

Rangarajan a, Talora C, Okuyama R, Nicolas M, Mammucari C, Oh H, Aster JC, Krishna S, Metzger D, Chambon P, et al. 2001. Notch signaling is a direct determinant of keratinocyte growth arrest and entry into differentiation. *EMBO J* **20**: 3427–36.

Rao G, Liu H, Li B, Hao J, Yang Y, Wang M, Wang X, Wang J, Jin H, Du L, et al. 2013. Establishment of a human colorectal cancer cell line P6C with stem cell properties and resistance to chemotherapeutic drugs. *Acta Pharmacol Sin* **34**: 793–804.

Ren Z, Hedrum A, Pontén F, Nistér M, Ahmadian A, Lundeberg J, Uhlén M, Pontén J. 1996. Human epidermal cancer and accompanying precursors have identical p53 mutations different from p53 mutations in adjacent areas of clonally expanded non-neoplastic keratinocytes. *Oncogene* **12**: 765–773.

Ro S, Rannala B. 2004. A stop-EGFP transgenic mouse to detect clonal cell lineages generated by mutation. *EMBO Rep* **5**: 914–920.

Rogers HW, Weinstock M a, Harris AR, Hinckley MR, Feldman SR, Fleischer AB, Coldiron BM. 2010. Incidence estimate of nonmelanoma skin cancer in the United States, 2006. *Arch Dermatol* **146**: 283–7.

Rowehl RA, Burke S, Bialkowska AB, Pettet III DW, Rowehl L, Li E, Antoniou E, Zhang Y, Bergamaschi R, Shroyer KR, et al. 2014. Establishment of Highly Tumorigenic Human Colorectal Cancer Cell Line (CR4) with Properties of Putative Cancer Stem Cells. *PLoS One* **9**: e99091.

De Ruiter N, Wolthuis R, van Dam H, Burgering B, Bos J. 2000. Ras-dependent regulation of c-Jun phosphorylation is mediated by the Ral guanine nucleotide exchange factor-Ral pathway. *Mol Cell Biol* **20**: 8480–8488.

Sato T, van Es JH, Snippert HJ, Stange DE, Vries RG, van den Born M, Barker N, Shroyer NF, van de Wetering M, Clevers H. 2010. Paneth cells constitute the niche for Lgr5 stem cells in intestinal crypts. *Nature* **469**: 415–418.

Schepers AG, Snippert HJ, Stange DE, van den Born M, van Es JH, van de Wetering M, Clevers H. 2012. Lineage Tracing Reveals Lgr5+ Stem Cell Activity in Mouse Intestinal Adenomas. *Science* **730**.

Schramek D, Leibbrandt A, Sigl V, Kenner L, Pospisilik J a, Lee HJ, Hanada R, Joshi P a, Aliprantis A, Glimcher L, et al. 2010. Osteoclast differentiation factor RANKL controls development of progestin-driven mammary cancer. *Nature* **468**: 98–102.

Schweizer J, Marks F. 1977. Induction of the Formation of New Hair Follicles in Mouse Tail Epidermis by the Tumor Promoter 12-O-Tetradecanoylphorbol-13-acetate. *Cancer Res* **37**: 4195–4201.

Serbedzija G, Bronner-Fraser M, Fraser S. 1989. A vital dye analysis of the timing and pathways of avian trunk neural crest cell migration. *Development* **106**: 809–816.

Shannon P, Markiel A, Ozier O, Baliga NS, Wang JT, Ramage D, Amin N, Schwikowski B, Ideker T. 2003. Cytoscape: a software environment for integrated models of biomolecular interaction networks. *Genome Res* **13**: 2498–504.

Sibilia M, Fleischmann A, Behrens A, Stingl L, Carroll J, Watt FM, Schlessinger J, Wagner EF. 2000. The EGF Receptor Provides an Essential Survival Signal for SOS-Dependent Skin Tumor Development. *Cell* **102**: 211–220.

Da Silva-Diz V, Solé-Sánchez S, Valdés-Gutiérrez a, Urpí M, Riba-Artés D, Penin RM, Pascual G, González-Suárez E, Casanovas O, Viñals F, et al. 2012. Progeny of Lgr5-expressing hair follicle stem cell contributes to papillomavirus-induced tumor development in epidermis. *Oncogene* 1–12.

Sjölund J, Pelorosso F, Quigley D, DelRosario R, Balmain A. 2014. Identification of Hipk2 as an essential regulator of white fat development. *Proc Natl Acad Sci* **111**: 7373–7378.

Snippert HJ, Haegebarth A, Kasper M, Jaks V, van Es JH, Barker N, van de Wetering M, van den Born M, Begthel H, Vries RG, et al. 2010. Lgr6 marks stem cells in the hair follicle that generate all cell lineages of the skin. *Science* **327**: 1385–1389.

Song I, Balmain A. 2014. Cellular reprogramming in skin cancer. *Semin Cancer Biol*.

Soriano P. 1999. Generalized lacZ expression with the ROSA26 Cre reporter strain. *Nat Genet* **21**: 70–71.

Steck P, Pershouse M, Jasser S, Yung W, Lin H, Ligon A, Langford L, Baumgard M, Hattier T, Davis T, et al. 1997. Identification of a candidate tumour suppressor gene, MMAC1, at chromosome 10q23.3 that is mutated in multiple advanced cancers. *Nat Genet* **15**: 356–362.

Stoker M, Shearer M, O'Neill C. 1966. Growth inhibition of polyoma-transformed cells by contact with static normal fibroblasts. *J Cell Sci* **1**: 297–310.

Stransky N, Egloff AM, Tward AD, Kostic AD, Cibulskis K, Sivachenko A, Kryukov G V, Lawrence MS, Sougnez C, McKenna A, et al. 2011. The mutational landscape of head and neck squamous cell carcinoma. *Science* **333**: 1157–60.

Styrkarsdottir U, Thorleifsson G, Sulem P, Gudbjartsson DF, Sigurdsson A, Jonasdottir A, Jonasdottir A, Oddsson A, Helgason A, Magnusson OT, et al. 2013. Nonsense mutation in the LGR4 gene is associated with several human diseases and other traits. *Nature* 4–7.

Sulston J, Schierenberg E, White J, Thomson J. 1983. The embryonic cell lineage of the nematode Caenorhabditis elegans. *Dev Biol* **100**: 64–119.

Suzuki A, Itami S, Ohishi M. 2003. Keratinocyte-specific Pten Deficiency Results in Epidermal Hyperplasia , Accelerated Hair Follicle Morphogenesis and Tumor Formation. *Cancer Res* **63**: 674–681.

Suzuki Y, Miura H, Tanemura A, Kobayashi K, Kondoh G, Sano S, Ozawa K, Inui S, Nakata A, Takagi T, et al. 2002. Targeted disruption of LIG-1 gene results in psoriasiform epidermal hyperplasia. *FEBS Lett* **521**: 67–71.

Tanese K, Fukuma M, Yamada T, Mori T, Yoshikawa T, Watanabe W, Ishiko A, Amagai M, Nishikawa T, Sakamoto M. 2008. G-Protein-Coupled Receptor GPR49 is Up-regulated in Basal Cell Carcinoma and Promotes Cell Proliferation and Tumor Formation. *Am J Pathol* **173**: 835–843.

Tanimura S, Tadokoro Y, Inomata K, Binh NT, Nishie W, Yamazaki S, Nakauchi H, Tanaka Y, McMillan JR, Sawamura D, et al. 2011. Hair follicle stem cells provide a functional niche for melanocyte stem cells. *Cell Stem Cell* **8**: 177–87.

The Cancer Genome Atlas Research Network. 2012. Comprehensive genomic characterization of squamous cell lung cancers. *Nature* **489**: 519–25.

Trempus CS, Morris RJ, Bortner CD, Cotsarelis G, Faircloth RS, Reece JM, Tennant RW. 2003. Enrichment for living murine keratinocytes from the hair follicle bulge with the cell surface marker CD34. *J Invest Dermatol* **120**: 501–11.

Vassar R, Hutton ME, Fuchs E. 1992. Transgenic Overexpression of Transforming Growth Factor Bypasses the Need for c-Ha-ras Mutations in Mouse Skin Tumorigenesis. *Mol Cell Biol* **12**: 4643–4653.

Vassar R, Rosenberg M, Ross S, Tyner a, Fuchs E. 1989. Tissue-specific and differentiation-specific expression of a human K14 keratin gene in transgenic mice. *Proc Natl Acad Sci U S A* **86**: 1563–7.

Veniaminova N a, Vagnozzi AN, Kopinke D, Do TT, Murtaugh LC, Maillard I, Dlugosz A a, Reiter JF, Wong SY. 2013. Keratin 79 identifies a novel population of migratory epithelial cells that initiates hair canal morphogenesis and regeneration. *Development* **140**: 4870–80.

Vermeulen L, Morrissey E, van der Heijden M, Nicholson a. M, Sottoriva A, Buczacki S, Kemp R, Tavare S, Winton DJ. 2013. Defining Stem Cell Dynamics in Models of Intestinal Tumor Initiation. *Science* **342**: 995–998.

Wakabayashi Y, Mao J-H, Brown K, Girardi M, Balmain A. 2007. Promotion of Hras-induced squamous carcinomas by a polymorphic variant of the Patched gene in FVB mice. *Nature* **445**: 761–5.

Wang D, Huang B, Zhang S, Yu X, Wu W, Wang X. 2013. Structural basis for R-spondin recognition by LGR4/5/6 receptors. *Genes Dev* **27**: 1339–44.

Wang NJ, Sanborn Z, Arnett KL, Bayston LJ, Liao W, Proby CM, Leigh IM, Collisson EA, Gordon PB, Jakkula L, et al. 2011. Loss-of-function mutations in Notch receptors in cutaneous and lung squamous cell carcinoma. *Proc Natl Acad Sci U S A* **108**: 17761–6.

Weisblat D, Sawyer R, Stent G. 1978. Cell lineage analysis by intracellular injection of a tracer enzyme. *Science* **202**: 1295–1298.

White a. C, Khuu JK, Dang CY, Hu J, Tran K V., Liu a., Gomez S, Zhang Z, Yi R, Scumpia P, et al. 2013. Stem cell quiescence acts as a tumour suppressor in squamous tumours. *Nat Cell Biol* **16**: 99–107.

White AC, Tran K, Khuu J, Dang C, Cui Y, Binder SW, Lowry WE. 2011. Defining the origins of Ras/p53-mediated squamous cell carcinoma. *Proc Natl Acad Sci* **108**: 7425–7430.

Winton DJ, Blount M a, Ponder B a. 1989. Polyclonal origin of mouse skin papillomas. *Br J Cancer* **60**: 59–63.

Wong C, Yu J, Quigley D, To M, Jen K, Huang P, Del Rosario R, Balmain A. 2013. Inflammation and Hras signaling control epithelial-mesenchymal transition during skin tumor progression. *Genes Dev* **27**: 670–682.

Wu C, Qiu S, Lu L, Zou J, Li W-F, Wang O, Zhao H, Wang H, Tang J, Chen L, et al. 2014. RSPO2-LGR5 signaling has tumour-suppressive activity in colorectal cancer. *Nat Commun* **5**: 3149.

Xu K, Xu Y, Rajashankar KR, Robev D, Nikolov DB. 2013. Crystal Structures of Lgr4 and Its Complex with R-Spondin1. *Structure* 1–7.

Xu Q, Mellitzer G, Wilkinson D. 2000. Roles of Eph receptors and ephrins in segmental patterning. *Philos Trans R Soc* **355**: 993–1002.

Yamamoto Y, Sakamoto M, Fujii G, Tsuiji H, Kanetaka K, Asaka M, Hirohashi S. 2003. Overexpression of orphan G-protein–coupled receptor, Gpr49, in human hepatocellular carcinomas with β-catenin mutations. *Hepatology* **37**: 528–533.

Yann Barrandon and HG. 1987. Three clonal types of keratinocyte with different capacities for multiplication. *Proc Natl Acad Sci* **84**: 2302–2306.

Ye P, Popken GJ, Kemper A, McCarthy K, Popko B, D'Ercole AJ. 2004. Astrocyte-specific overexpression of insulin-like growth factor-I promotes brain overgrowth and glial fibrillary acidic protein expression. *J Neurosci Res* **78**: 472–84.

Youssef KK, Van Keymeulen A, Lapouge G, Beck B, Michaux C, Achouri Y, Sotiropoulou PA, Blanpain C. 2010. Identification of the cell lineage at the origin of basal cell carcinoma. *Nat Cell Biol*.

Yuspa SH. 2000. Overview of carcinogenesis: past, present and future. *Carcinogenesis* **21**: 341–4.

Zagouras P, Stifani S, Blaumueller C, Carcangiu M, Artavanis-Tsakonas S. 1995. Alterations in Notch signaling in neoplastic lesions of the human cervix. *Proc Natl Acad Sci* **92**: 6414–6418.

Zhu L, Gibson P, Currle D, Tong Y, Richardson R, Bayazitov I, Poppleton H, Zakharenko S, Ellison D, Gilbertson R. 2009. Prominin 1 marks intestinal stem cells that are susceptible to neoplastic transformation. *Nature* **457**: 603–607.

Publishing Agreement

It is the policy of the University to encourage the distribution of all theses, dissertations, and manuscripts. Copies of all UCSF theses, dissertations, and manuscripts will be routed to the library via the Graduate Division. The library will make all theses, dissertations, and manuscripts accessible to the public and will preserve these to the best of their abilities, in perpetuity.

Please sign the following statement:

I hereby grant permission to the Graduate Division of the University of California, San Francisco to release copies of my thesis, dissertation, or manuscript to the Campus Library to provide access and preservation, in whole or in part, in perpetuity.

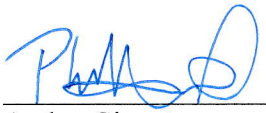

Author Signature

09/16/2014

Date